CHALMERS
UNIVERSITY OF TECHNOLOGY

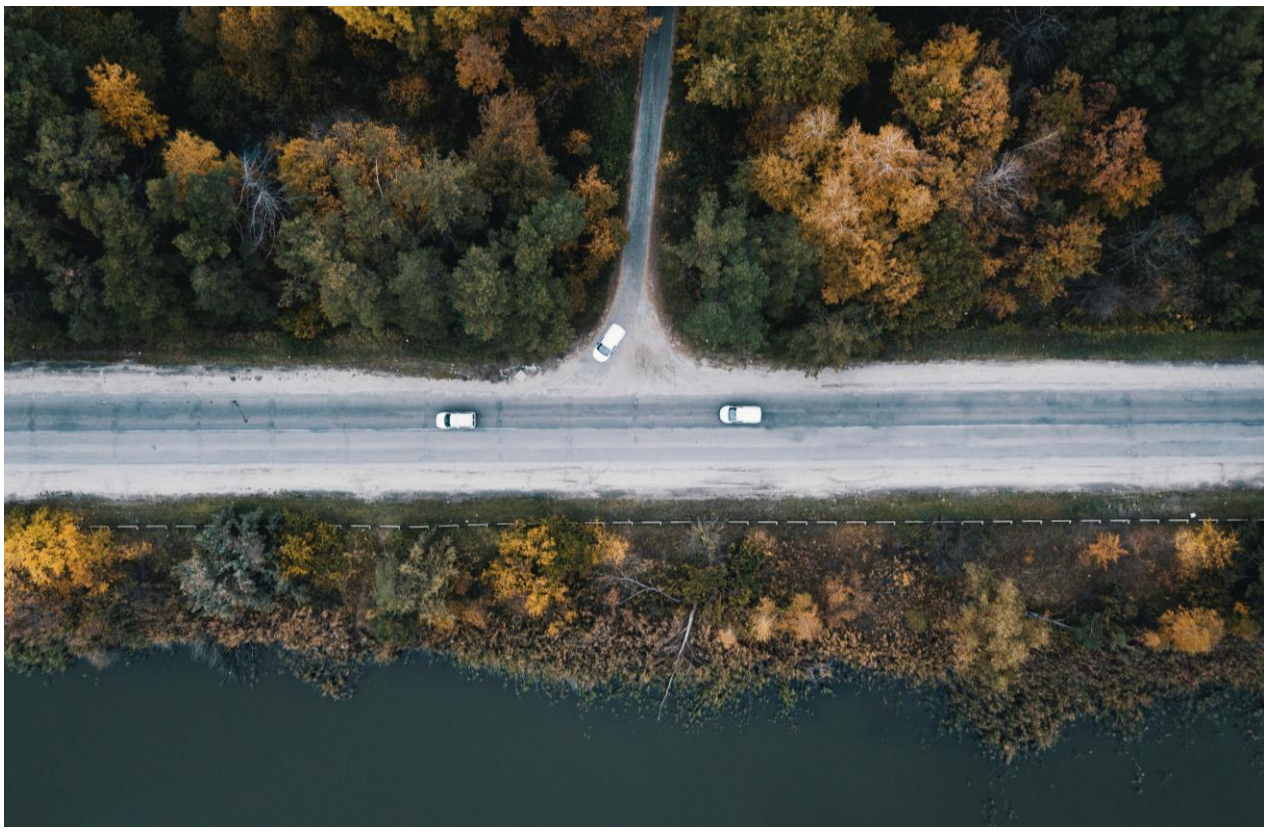

Drivers' response in an intersection scenario during manual and automated driving

Master's thesis in Mechanical Engineering

Andrea Floreano, Alessandro Niro

Department of Mechanics and Maritime Sciences
CHALMERS UNIVERSITY OF TECHNOLOGY
Gothenburg, Sweden 2018

MASTER'S THESIS IN MECHANICAL ENGINEERING

Drivers' response in an intersection scenario during manual and automated driving

Andrea Floreano, Alessandro Niro

Department of Mechanics and Maritime Sciences
Division of Vehicle Safety
Accident Prevention Group
CHALMERS UNIVERSITY OF TECHNOLOGY
Göteborg, Sweden 2018

Drivers' response in an intersection scenario during manual and automated driving

Andrea Floreano, Alessandro Niro

Master's Thesis 2018:07
Department of Mechanics and Maritime Sciences
Division of Vehicle Safety
Accident Prevention Group
Chalmers University of Technology
SE-412 96 Göteborg
Sweden
Telephone: + 46 (0)31-772 1000

Cover:
Up view of a T-intersection [1]

Chalmers / Department of Mechanics and Maritime Sciences
Göteborg, Sweden 2018-03-07

Drivers' response in an intersection scenario during manual and automated driving

Master's thesis in Mechanical Engineering
Andrea Floreano, Alessandro Niro
Department of Mechanics and Maritime Sciences
Division of Vehicle Safety
Accident Prevention Group
Chalmers University of Technology

Abstract

The role of automation is becoming increasingly important in the design of modern vehicles. This is reflected by a large development of advanced driver assistance systems, which are ever more affecting driving behaviour. This work is focused on the analysis and the modelling of driver's response to a critical T-intersection scenario, considering different levels of automation. In this scenario, the subject vehicle is travelling on the main road, and a turning car coming from the perpendicular leg of the T-intersection, cuts in the subject vehicle path. The analysed data was collected during an experiment performed with a moving based driving simulator located at the Swedish National Road and Transport Research Institute (VTI) in Linköping (Sweden). The participants drove in four different experimental conditions: manual driving, intentional car following and two semi-automated driving conditions concerning the use of the adaptive cruise control and the traffic jam assist. The findings of this thesis showed that the main response to the turning car entrance was braking. The steering reaction was negligible since only small and occasional corrective steering were found. In this scenario, drivers reacted with a brake reaction time independently from the driving condition. However, a significant correlation between the brake reaction time and the time to intersection in the moment the turning car enters was found during manual driving, resulting in faster drivers' reaction to an increase of risk.

The braking behaviour was analysed taking into account the maximum deceleration reached, the jerk at the brake onset and the mean brake pedal force. The results of our analysis indicate that drivers react with a higher mean brake force in semi-automated driving modes comparing to manual driving. Consequently, this results in higher values for both brake jerk and maximum deceleration. Additionally, hard braking was correlated with both driver's age and driver's experience in the use of adaptive cruise control. This study analysed driver's behaviour also concerning the gaze direction before approaching the intersection. Results highlighted that, during intentional car following mode, drivers noticed the presence of the turning car later in respect to the other driving conditions.

The results found were used to develop a model able to reproduce and predict the driver's reactions referred to the critical scenario analysed. The model was designed as a feedforward back-propagating artificial neural network. It is capable of computing outputs represented by brake reaction time, maximum deceleration and mean brake pedal force, depending on driving condition, time to intersection, perception time and driver's profile. The obtained results, both in the analysis and in the modelling, aim to contribute to the development of advanced driving assistance systems. In particular, the present study could support the design of emergency vehicle warning systems in order to improve driving safety during critical scenarios.

Keywords: braking response, critical intersection scenario, driving simulator, semi-automated driving, driver behaviour modelling, artificial neural networks.

Contents

Abstract I
Contents IV
Preface VI
Notations VII
List of figures VIII
List of Tables XI
1 Introduction 1
1.1 State of the art 2
1.2 The experiment 6
1.2.1 Simulator 6
1.2.2 Participants 8
1.2.3 Study design 8
1.3 Aim and research questions 12
2 Variables and scenario 13
3 Analyses 20
3.1 Method 20
3.1.1 What drivers do 20
3.1.2 Time to intersection 23
3.1.3 Gaze behaviour 25
3.1.4 Statistical tests and correlation coefficients 28
3.2 Results 29
3.2.1 What drivers do 29
3.2.2 MAN and ICF: leaving throttle vs braking 33
3.2.3 Brake reaction times 34
3.2.4 Drivers without reactions in semi-automated modes 39
3.2.5 Brake jerk 41
3.2.6 Maximum longitudinal deceleration 44
3.2.7 Mean brake pedal force 49
3.2.8 Gaze behaviour 51
3.2.9 Brake reaction time vs perception time 55
4 Modelling driver's behaviour 58
4.1 Method 58
4.1.1 Description of the model's typology 58
4.1.2 Driver model configuration and architecture 72

4.2 Results 77
4.2.1 Capability of reproducing the results analysed 78
4.2.2 Most influential inputs 85
4.2.3 Validation of the model 86
4.2.4 Application 101
5 Discussion 103
5.1 Analyses 103
5.2 Modelling 107
6 Conclusions and future research 113
7 References 115

Preface

This thesis is part of our Master of Science in Mechanical Engineering at Politecnico di Milano. The work has been performed at Autoliv research department and at SAFER.

The thesis is based on a data set, collected with a moving based driving simulator from VTI in Linköping in 2012. The work developed is part of the project Quantitative Driver Behaviour Modelling for Active Safety Assessment Expansion (QUADRAE), started in January 2016 by the Swedish automotive industry (AB Volvo, Volvo Car Corporation, Autoliv) in collaboration with Chalmers University of Technology and VTI.

We would really like to thank our supervisors from Chalmers University, Thomas Streubel and from Autoliv, Annika Larsson; our examiner, Giulio Bianchi Piccinini, that gave us the opportunity to be part of QUADRAE project; our supervisors from Politecnico di Milano: professor Federico Cheli and Stefano Arrigoni. We would like to thank also Marco Dozza and Jonas Bärgman from Chalmers University and Andreas Jansson and Bruno Augusto from VTI. Finally, we would like to thank our families that supported us in this great experience.

Göteborg, 2018-03-07

Andrea Floreano, Alessandro Niro

Notations

ABS	Anti-lock Braking System
ACC	Adaptive Cruise Control
ADAS	Advanced Driver Assistance Systems
AEB	Autonomous Emergency Braking
ANN	Artificial Neural Network
AS	Active Steering
BRT	Brake Reaction Time
DLP	Digital Light Processing
ESC	Electronic Stability Control
FCW	Forward Collision Warning
HMI	Human Machine Interface
ICF	Intentional Car Following
LDW	Lane Departure Warning
LKA	Lane Keep Assist
MAN	Manual
MLD	Maximum Vehicle Longitudinal Deceleration
MPF	Mean Brake Pedal Force
POV	Principal Other Vehicle
PT	Perception Time
SAE	Society of Automotive Engineering
TC	Turning Car
THW	Time Headway
TJA	Traffic Jam Assist
TTI	Time To Intersection
r	Pearson correlation coefficient
R	Regression coefficient
ρ	Spearman's rho

List of figures

Figure 1 - SAE automation levels [10]....2
Figure 2 - VTI Sim III....7
Figure 3 - Interior of Saab 9-3 in the simulator....7
Figure 4 - Interior of the car during the experiment....7
Figure 5 - VTI Sim IV....8
Figure 6 - Sharp curve event....10
Figure 7 - Cut-in event....10
Figure 8 - Broken down car event....11
Figure 9 - Exit event....11
Figure 10 - T-intersection event....11
Figure 11 - Crossing event 4441....15
Figure 12 - Crossing event 4442....15
Figure 13 - T-intersection: event inizialization....16
Figure 14 - T-intersection: TC (blue car) starts to approach the intersection....16
Figure 15 - T-intersection: TC (blue car) reaches the stop line....17
Figure 16 - T-intersection: TC (blue car) gets the intersection....17
Figure 17 - T-intersection: TC (blue car) has the same speed of the leading vehicle (yellow car)....18
Figure 18 - T-intersection: end of the event....18
Figure 19 –Matlab video frames: a) TC approaches the intersection. b) TC waits at the stop of the intersection. c) TC starts to get the intersection. d) Ego vehicle brakes because of the TC. e) Ego vehicle continues its brake. f) The two vehicles are now driving at the same speed.....19
Figure 20 – Example of time histories of throttle gain, brake pedal force, steering wheel angle (driver 13 – manual mode)....21
Figure 21 - Example of a throttle gain time history (driver 69 – manual mode)....22
Figure 22 - Lateral view of the ego vehicle (Saab 9-3)....23
Figure 23 - Front view of the ego vehicle (Saab 9-3)....23
Figure 24 - a) Time to intersection at TC entry. b) Time to intersection at first braking instant....24
Figure 25 - Alfa function graph for driver 1 in manual mode....26
Figure 26 - Beam of considered angles in a single time step....27
Figure 27 - Pie graphs of drivers' actions in different driving modes....29
Figure 28 - Drivers actions sequences in MAN and ICF modes....30
Figure 29 - Drivers actions sequences in ACC and TJA modes....31
Figure 30 - Minimum longitudinal acceleration during the scenario in all driving modes....31
Figure 31 - Maximum lateral acceleration during the scenario in all driving modes....32
Figure 32 - Box plots of brake reaction times for all driving modes....34
Figure 33 - Brake reaction times' box plots of drivers novice (left) and used to (right) ACC system....35
Figure 34 - Correlation between brake reaction time and time to intersection in manual mode....36
Figure 35 - Correlation between brake reaction time and time to intersection in ICF mode....37
Figure 36 - Correlation between brake reaction time and time to intersection in ACC (left) and TJA (right) modes....37
Figure 37 - Brake jerk box plots for all driving modes....41
Figure 38 - Brake jerk box plots of drivers novice (left) and used to (right) ACC system....42
Figure 39 - Correlation between brake jerk and riskiness in manual mode....43
Figure 40 - Correlation between brake jerk and riskiness in ICF mode....43
Figure 41 - Correlation between brake jerk and riskiness in ACC mode: red points correspond to brake jerk higher than 9 m/s^3, blue points correspond to brake jerk lower than 9 m/s^3....44
Figure 42 - Correlation between brake jerk and riskiness in TJA mode: red points correspond to brake jerk higher than 9 m/s^3, blue points correspond to brake jerk lower than 9 m/s^3....44
Figure 43 - Maximum longitudinal deceleration box plots of all driving modes....45
Figure 44 - Max deceleration box plots of drivers novice (left) and used to (right) ACC system....46
Figure 45 - Correlation between maximum longitudinal deceleration and riskiness in MAN mode....47
Figure 46 - Correlation between maximum longitudinal deceleration and riskiness in ICF mode....47
Figure 47 - Correlation between maximum longitudinal deceleration and riskiness in ACC mode: red points correspond to maximum deceleration higher than 6 m/s^2, blue points correspond to maximum deceleration lower than 6 m/s^2....48

Figure 48 - Correlation between maximum longitudinal deceleration and riskiness in TJA mode: red points correspond to maximum deceleration higher than 6 m/s^2, blue points correspond to maximum deceleration lower than 6 m/s^2 48
Figure 49 - Mean brake pedal force box plots of all driving modes 49
Figure 50 - Mean brake pedal force box plots of drivers novice (left) and used to (right) ACC system 50
Figure 51 - Drivers' gaze representation in the four driving modes 10 s before the TC entry and 1 s after 51
Figure 52 – Gaze percentage values to the right direction 10 s before the TC entry and 1 s after for all driving modes 52
Figure 53 - Four examples of eye tracking data 10 s before the TC entry and 1 s after 53
Figure 54 - % of drivers that perceived the TC at each time instant considered (related to the TC entrance) 54
Figure 55 - Correlation between brake reaction time and driver's perception time of the TC in manual mode 55
Figure 56 - Correlation between brake reaction time and driver's perception time of the TC in ICF mode 56
Figure 57 - Correlation between brake reaction time and driver's perception time of the TC in ACC mode 56
Figure 58 - Correlation between brake reaction time and driver's perception time of the TC in TJA mode 57
Figure 59 - Correlation between brake reaction time and time to intersection in ACC (left) and TJA (right) mode taking into account if drivers perceived the TC before or after its entry 57
Figure 60 - General function of the present driver behaviour model 58
Figure 61 - Artificial neural network's structure 60
Figure 62 - Neural network configured with one hidden layer 61
Figure 63 - Neural network configured with two hidden layers 62
Figure 64 - Underfitting 62
Figure 65 - Overfitting 63
Figure 66 - Appropriate fitting 63
Figure 67 - Neuron's processing function scheme [53] 64
Figure 68 - log-sigmoid transfer function 65
Figure 69 - tan-sigmoid transfer function 65
Figure 70 - purelin transfer function 65
Figure 71 - Sequence's scheme of processing steps between input and output 66
Figure 72 - At the red circle the generalization error starts increasing, this situation could bring to a data overfitting 69
Figure 73 - Overview of the neural network 74
Figure 74 - Neural network's architecture 75
Figure 75 - Results of the training process 77
Figure 76 - Performance of the training process 78
Figure 77 - Brake reaction time: comparison between simulated and target outputs 79
Figure 78 - Manual driving modes, brake reaction times in respect to TTI: simulated and target outputs 79
Figure 79 - Semi-automated driving modes, brake reaction time in respect to TTI: simulated and target outputs 80
Figure 80 - Manual driving modes, brake reaction time in respect to the perception time: simulated and target outputs 80
Figure 81 - Semi-automated driving modes, brake reaction time in respect to the perception time: simulated and target outputs 81
Figure 82 - Mean brake pedal force: comparison between simulated and target outputs 81
Figure 83 - Manual driving modes, mean brake pedal force in respect to TTI: simulated and target outputs 82
Figure 84 - Semi-automated driving modes, mean brake pedal force in respect to TTI: simulated and target outputs 82
Figure 85 - Maximum vehicle's deceleration: comparison between simulated and target outputs 83
Figure 86 - Manual driving modes, maximum vehicle's deceleration in respect to TTI: simulated and target outputs 83
Figure 87 – Semi-automated driving modes, maximum vehicle's deceleration in respect to TTI: simulated and target outputs 84
Figure 88 - Brake reaction time in respect to TTI with noise for MAN mode. $\rho = 0,764$ 87

Figure 89 - Brake reaction time in respect to TTI with noise for ICF mode.
ρ = 0,671 87
Figure 90 - Brake reaction time in respect to TTI with noise for ACC mode.
ρ = 0,298 88
Figure 91 - Brake reaction time in respect to TTI with noise for TJA mode.
ρ = 0,244 88
Figure 92 - Brake reaction time in respect to the perception time with noise for MAN mode.
ρ = 0,550 89
Figure 93 - Brake reaction time in respect to the perception time with noise for ICF mode.
ρ = 0,250 89
Figure 94 - Brake reaction time in respect to the perception time with noise for ACC mode.
ρ = 0,550 90
Figure 95 - Brake reaction time in respect to the perception time with noise for TJA mode.
ρ = 0,657 90
Figure 96 - Mean brake pedal force in respect to TTI with noise for MAN mode.
ρ = -0,568 91
Figure 97 - Mean brake pedal force in respect to TTI with noise for ICF mode.
ρ = -0,553 91
Figure 98 - Mean brake pedal force in respect to TTI with noise for ACC mode.
ρ = -0,242 92
Figure 99 - Mean brake pedal force in respect to TTI with noise for TJA mode.
ρ = -0,518 92
Figure 100 - Maximum vehicle's deceleration in respect to TTI with noise for MAN mode.
ρ = -0,379 93
Figure 101 - Maximum vehicle's deceleration in respect to TTI with noise for ICF mode.
ρ = -0,491 93
Figure 102 - Maximum vehicle's deceleration in respect to TTI with noise for ACC mode.
ρ = -0,220 94
Figure 103 - Maximum vehicle's deceleration in respect to TTI with noise for TJA mode.
ρ = -0,543 94
Figure 104 - Manual modes, brake reaction time in respect to TTI with ±2s of noise 96
Figure 105 - Semi-automated modes, brake reaction time in respect to TTI with ±2s of noise 96
Figure 106 - Manual modes, brake reaction time in respect to the perception time with ±2s of TTI noise 97
Figure 107 - Semi-automated modes, brake reaction time in respect to the perception time with ±2s of TTI noise 97
Figure 108 - Manual modes, mean brake pedal force in respect to TTI with ± 2s of noise 98
Figure 109 - Semi-automated modes, mean brake pedal force in respect to TTI with ±2s of noise 98
Figure 110 - Manual modes, maximum vehicle's deceleration in respect to TTI with ±2s of noise 99
Figure 111 - Semi-automated modes, maximum vehicle's deceleration in respect to TTI with ±2s of noise 99
Figure 112 - Example of input box extracted from the Matlab code 101
Figure 113 - Message box regarding the results of the model 102

List of Tables

Table 1 - Technical specifications of VTI driving simulator III 6
Table 2 - Measurement units 13
Table 3 - Part of the table representing which driver did which event in each mode 14
Table 4 - Drivers actions in each driving mode 29
Table 5 - Data concerning the participants that just left the throttle 33
Table 6 - Data concerning the participants that braked 33
Table 7 - Brake reaction time in each driving mode 34
Table 8 - Brake reaction times of novices and used to ACC drivers 35
Table 9 - Brake reaction times and times to intersections of drivers that braked in the scenario 36
Table 10 - Brake reaction times of drivers that performed the scenario braking in all four driving modes 38
Table 11 - Data of participants that had no actions in ACC mode 39
Table 12 - Data of participants that had no actions in TJA mode 39
Table 13 - Brake jerk in each driving mode 41
Table 14 - Brake jerk of novices and used to ACC drivers 42
Table 15 - Maximum longitudinal deceleration in each driving mode 45
Table 16 - Maximum longitudinal deceleration data of novices and used to ACC drivers 46
Table 17 - Mean brake pedal force in each driving mode 49
Table 18 - Mean brake pedal force data of novices and used to ACC drivers 50
Table 19 - Drivers' perception time of the TC in each driving mode 54
Table 20 - Resultant Spearman coefficients, comparison between analysis and model results 85
Table 21 - Results of the input's influence on the performance of the neural network 85
Table 22 - Spearman coefficients regarding the relationships modelled for the examples considered. Comparison between simulations run with original and noisy input data. 95
Table 23 - Spearman coefficients obtained with new input data (TTI noise: ±2s) 100
Table 24 - Spearman coefficients obtained with new input data (TTI noise: ±0,5s) 100

1 Introduction

Every year millions of road accidents occur all over the world causing the death of about 1.25 million people. According to the World Health Organization, car drivers represent the biggest part of these fatalities, followed by motorcyclist, pedestrians and cyclists. Looking thoroughly at the statistics, road traffic accidents today are the 9th highest cause of death worldwide and they represent the most common way to die for people between the age of 15 and 29 [2].

Assuming that the main cause of these fatalities is mostly related to drunk driving or to speeding would be prematurely. Distracted drivers are the top cause of car accidents [3]. Indeed, as written in [4], "driving is one of the most complex and safety critical everyday tasks in modern society". Nevertheless, people often do something else while driving. Some side-activities are to talk on a cell phone, to send a text message, to smoke and to eat. Each of the listed actions is not complex, but can, in critical situations, affect the drivers' reaction time dramatically [5].

Urban and rural roads are the main scenes where car accidents occur. In USA more than half of all car crashes happen close to the drivers' home [6]. Indeed, in known places, drivers are usually more self-confident and so they are more inclined to pay less attention to the road. In particular, intersections are one of the most relevant zones where drivers make mistakes leading into collisions. In Italy, 37.2% of the recorded car accidents appeared along urban and rural intersections in 2016 [7].

In order to reduce the number of fatalities, a lot of technological improvements regarding road safety have been done through the years among the industrialized countries of the world. The first important improvements concerned the vehicle's passive safety. These types of systems reduce the physical consequences of accidents. Seatbelts and airbags are such systems that have reduced injuries or fatalities in vehicle accidents in the last decades [8]. The other big category related to vehicle's safety is represented by active safety systems. These aim to reduce the risk of an accident to occur. ABS (Anti-lock Braking System) and ESC (Electronic Stability Control) have been the first generation of active safety systems to be commercialized giving a big contribution in avoiding crashes [9]. Nowadays, a new generation of active safety systems called ADAS (Advanced Driver Assistance Systems) are changing in a significant way vehicle safety and so the automotive world. These types of systems support drivers in different aspects of vehicle control and in many different ways. Systems like FCW (Forward Collision Warning) and LDW (Lane Departure Warning) warn the driver that a collision is imminent (FCW) or that s/he is moving out of the lane (LDW) respectively. Other systems such as AEB (Autonomous Emergency Braking) and LKA (Lane Keeping Assist) intervene directly in the vehicle controls avoiding or mitigating collisions or preventing dangerous unintentional lane departures respectively. How? Braking (AEB) or keeping the vehicle in the right lane (LKA). Furthermore, other types of ADAS capable to link safety and driving comfort are already present in current vehicle models: ACC (Adaptive Cruise Control) and TJA (Traffic Jam Assist) systems. The ACC acts on the longitudinal control of the vehicle keeping a set maximum speed and a set minimum distance from the vehicle ahead. In this way the driver doesn't need to use the braking and the throttle pedals even if the leading vehicle is decelerating or accelerating. The TJA acts as the ACC system but has in addition an Active Steering (AS) system that permits to follow the leading vehicle also in the lateral movements. In this setup, the system has also the control of the steering wheel, but driver still has to hold it and monitor the environment at all times.

Due to the existence of many different types of ADAS and due to the confusion that is present around the autonomous vehicles' topic, the scale of automation drew up by the SAE (Society of Automotive Engineers) has been reported in *Figure 1*.

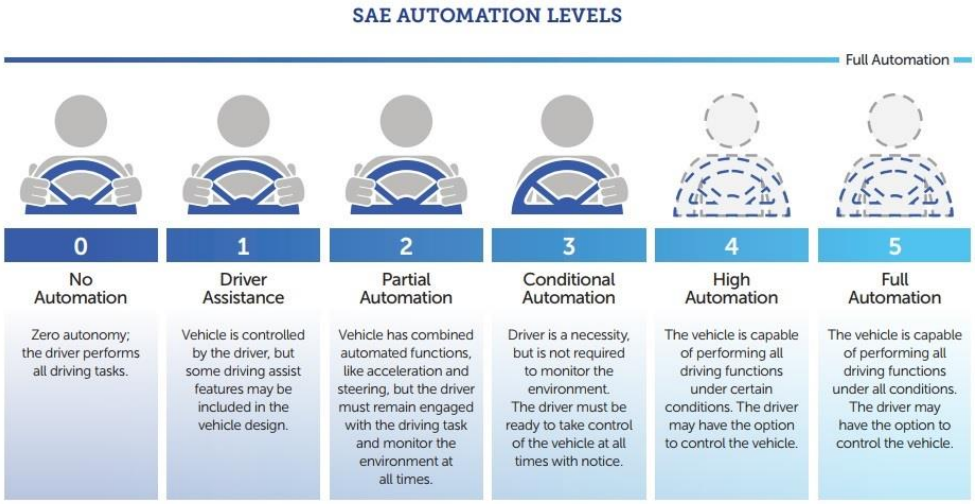

Figure 1 - SAE automation levels [10]

Referring to the scale of automation, warning systems as FCW and LDW still belong to level 0. Indeed, they just alert the driver of a danger, but they do not have any control on the vehicle. On the contrary, ADAS as ACC, AEB and LKA belong to level 1, they can control the vehicle in longitudinal or in lateral direction. TJA belongs to level 2 of the automation scale: it can have the vehicle's control both in lateral and longitudinal directions. Nowadays, in the vehicle's market only the first three levels (0-2) are concretely present.

1.1 State of the art

Driver behaviour has been ascertained to be the main cause of road traffic accidents by the time. Because of this, drivers' reactions have been studied for more than 50 years and hundreds of articles were published in Human Factors journals [11]. Furthermore, during recent years, with the concrete arrival of automation in the vehicles' market, research in this field has been intensified [11], [12] also to realize human interactions with that.

One of the main goals of driver behaviour research is to find reasonable phenomenological relations between different types of factors in order to understand and represent human's decisions and reactions. Most of these relations regard brake and steering reaction times as a function of speed, distances, times to collisions, obstacles or riskiness for example. In order to obtain this kind of information, many types of experiments have been done through the years.

Naturalistic tests and driving simulator experiments are two ways to obtain drivers' behaviour data. Reliability of simulator data has been discussed for years: both from technological and psychological point of view. Concerning the technology of driving simulators, the main issue is the resolution. This is not referred to the simulator display's resolution, but to the capability in recreating reliable driving feelings and perceptions through all the simulator's movements.

Nowadays, this point does not seem to be a big problem anymore: high resolution levels have been reached by the main research institutes (e.g. VTI [13]). From a psychological perspective, the problem of simulator's reliability still remains. Besides technology, studies confirmed that people during simulations can behave as in reality or in a different way, depending on the task they receive and on the scenario in which they are (for further details please refer to [14]). It would be better to have naturalistic tests but these are not always possible because of economical, safety and organization issues. In driving simulations, on the contrary, everything can be created and changed for a precise scenario, without endangering the lives of study participants.

Reaction time is usually defined as the time interval between the appearance of a potential hazard and the instant in which the driver starts to react [15]. In particular, for brake reaction time, it has been confirmed through many studies that it is affected by several factors: driver age, gender, experience, situation urgency, physical state, mental state, cognitive load, automation, warnings, knowledge of the place, and so on [16]–[22]. Computing and analysing brake reaction times for each driving condition, a factor was found that changed these times in a relevant way: the expectancy. It was determined that for fully anticipated events the brake reaction times are around 0.70 - 0.75 seconds; for unexpected but common events 1.25 seconds; whilst for totally surprising events 1.5 seconds [23]. On the contrary another study [24] stated that, for totally surprising events but sufficiently urgent, brake reaction times can decrease to 1 second or lower. Similar outcomes were detected also in other test tracks and simulator studies [20], [22], [25].

Taking into account also driving modes, drivers' behaviour can change in a significant way. The 'intentional car following' mode has been analysed in several studies [26]–[28], revealing always similar results. People driving in this modality are more used to spend time looking at the vehicle ahead, noticeably decreasing the number of glances to the sides of the streets and to the rear-view mirrors. It has been seen that this comportment lead drivers to be less aware of pedestrians, to perpetrate more give-way road violations and to be involved in more give-way accidents. This type of behaviour has been related to the increase of cognitive load on drivers and to the craving to stay connected to the vehicle ahead, as close as possible [28]. Furthermore, studies [26] proved that the biggest difference in glance directions are in the horizontal way and not in the vertical one. However, it has to be reported that gaze durations on the speedometer decrease in this driving modality, meaning again that drivers care less about the speed at which they are going [26].
Here and in most of the experiments, car following mode is considered as a passive activity, as a sub-task. For instance, drivers have to go from point A to point B following a leading vehicle. But it can be seen also in an active way: this is the case of police's pursuits. So, following the car ahead is the main goal. In these cases, same behaviours have been found but in an even more accentuated way [26].

Systems as the Adaptive Cruise Control and the Traffic Jam Assist have been developed to reduce the possibility of human errors, to increase comfort and to improve transport's efficiency [29]. But with the integration of automation in vehicles, drivers' behaviours change in several different ways. The level of automation and the level of trust that drivers allocate into the systems, are the fundamental factors that affect the reaction times in these driving modes. Parasuraman in [30] defined automation as the "execution by a machine agent (usually computer)

of a function that was previously carried out by a human". Hence, we cannot expect the same behaviour by the drivers.
Several studies have discovered that people driving with the ACC system enabled have higher reaction times of about 1.0 – 1.5 seconds in respect to drivers without any longitudinal support. These slower drivers' reactions have been attributed to the cognitive underload, to the cognitive delegation of responsibility for a task and to the cost of switching from automated to manual control [27]. Indeed, drivers think that the system can perform in any situation. This way of thinking leads to postponing an intervention. They act only when they really feel unsafe. Therefore, drivers driving with these kinds of systems often do not have their feet on the pedals. This time, spent to retake the control of the vehicle, is further delaying any driver's actions. Increasing the level of automation by adding lateral support (TJA) should pronounce this inefficiency [31]. Drivers tend usually to give more and more trust to systems [30] and to assume the supervisor's role [27]. However, no significant differences were found between ACC (level 1) and TJA (level 2) systems in several studies [27], [32]. These behaviours were analysed through different scenarios, in particular in those situations in which the system fails and an intervention by the driver is required. It has to be pointed out that these systems still have many limitations. They can work only above a certain speed range. Even in these scenarios, in which they are supposed to work properly, they still have some problems [33]. For instance, they can lose the contact with the car ahead or they can do not care in time about other vehicles. Due to these kinds of phenomena, in [27] was taken into account the experience of drivers with the ACC system. This system is in fact on the market by the time. It was found out that drivers that are used to drive with ACC react in a faster way to failure scenarios, respect to drivers that are novices to this kind of system. This phenomenon has to be imputed to the fact that experienced drivers know the limits of the system better and trust it less. This lack of trust leads to faster reactions for drivers with ACC experience than for those that are novice to ACC.

Intersections represent one of those critical scenarios in which systems as ACC and TJA can fail. It is confirmed that junctions are tricky for drivers and even more for automated systems [34]. The complexity of intersections is due to the fact that the systems, as humans, have to take into account not only vehicles in the same directions but also those ones coming from a perpendicular way. The presence of these vehicles, coming for instance from a perpendicular way, is not always detected in time by the systems. These delays can be dramatically fundamental, causing the concrete possibility of crashes. Hence a prompt intervention of the driver becomes essential in these types of situations. As explained in [35] the interactions human – system in driving are really different in respect to the aviation field or to the process control sector. As a matter of fact, we have to deal with much shorter times while driving: half a second can be fundamental to avoid a crash.

The growing use of automation in vehicles, brought to an increase of the research regarding drivers' behaviour, which has been intensified both by industries and universities. As written before, people driving with automated vehicles react in several different ways, depending on the level of such automation and on the trust they place in the system. As Vicente wrote in [36]: "The key to a successful technology isn't the technology itself, but rather its affinity with its users", the interaction between driver and vehicle is of fundamental importance for the whole driving performance, and in particular for its safety. For these reasons, ever more

researchers focused their attention on the way in which a driver interacts with the vehicle he's driving. The results of these efforts resulted in the creation of models describing driver's behaviour. Even if real experiments provide more detailed and reliable measurements, computer simulations resulted more controllable, fast, repeatable, cheap and safe [37].

The modelling of drivers' reactions aims to represent driving behaviour both in routine and in near-accident scenarios. In this way, depending on the level of accuracy of such models, the resulting information can be used to simulate and predict new different situations and driving conditions. For instance, a proper model application could allow to study and test the same scenario changing easily some desired conditions, such as the environment or the vehicle settings. This allows to understand the effects of such changes on the simulation outcome. The application of driver's models is nowadays very useful for several aspects, including the improvement of safety systems and the virtual testing of new ones.

Many types of driver models have been developed through the years, approaching the topic from different points of view. Considering near-collision scenarios, a large number of driver's behaviour models have been recently developed [37]. Some of them are based on human factors, neuroscience and cognitive loads (e.g., [38]–[40]). Other approaches are utilizing computational algorithms, such as machine learning techniques (e.g., [41]–[44]). The latter represent the typology on which the modelling activity described in this study is based. Machine learning is a field of computer science that is developing and advancing especially in the last decades. It allows the creation of algorithms capable of learning and acting starting from sample data, without being explicitly programmed. Machine learning techniques are nowadays implemented and adopted for many different purposes, including the design of self-driving vehicles. The present work aims to model the driver's behaviour with the usage of artificial neural networks (ANN), which are a branch of machine learning techniques. These computing systems are inspired by the human brain. They are featured by particular processing units, called neurons, which have the function to process the input data in order to provide the corresponding outputs. The last part of this thesis is focused on creating a useful tool for the prediction of driver's reactions, referred to the critical scenario under consideration.

1.2 The experiment

The experiment took place at the Swedish National Road and Transport Research Institute (VTI) in Linköping (Sweden) in 2012.

1.2.1 Simulator

The experiment was performed with the VTI driving simulator III. It is an advanced high-fidelity moving-base driving simulator that allows motion in four degrees of freedom. It can realize the vertical and the longitudinal motions as well as roll and pitch.
In *Table 1* the technical specifications of VTI simulator III are shown [45].

Table 1 - Technical specifications of VTI driving simulator III

	VTI Sim III
Motion system	
Pitch (degrees)	-9 till +14
Roll (degrees)	± 24
Linear system	
Amplitude (m)	± 3.75
Velocity (m/s)	± 3.75
Acceleration (m/s^2)	± 8.0
Vibration table	
Vertical motion (cm)	± 6.0
Longitudinal motion (cm)	± 6.0
Roll (degrees)	± 6
Pitch (degrees)	± 3
Visual system	
Forward view (degrees)	115
Rear view mirrors (LCD screens)	3
Average resolution on screen* (arc minute per line pair)	2.8 (horizontal) 2.7 (vertical)
Cabin (exchangeable)	Saab 9-3

*The human eye has 0.59 arc minute per line pair

This setup permits to simulate and study the effects of lateral and longitudinal forces on drivers during normal everyday driving and also during critical maneuvers. This is made possible on the one hand side by rails that allow big linear movements in one direction and on the other hand side by a vibration table to which the cabin is connected. This vibration table can simulate little displacements of the vehicle in lateral and vertical direction including bumps and road roughness by changing the roll and the pitch angle. Having only a single rail that permits big movements, the Sim III has a platform that can be rotated 90 degrees: in this way big longitudinal accelerations and decelerations can be studied instead of lateral ones, but still one direction at a time.

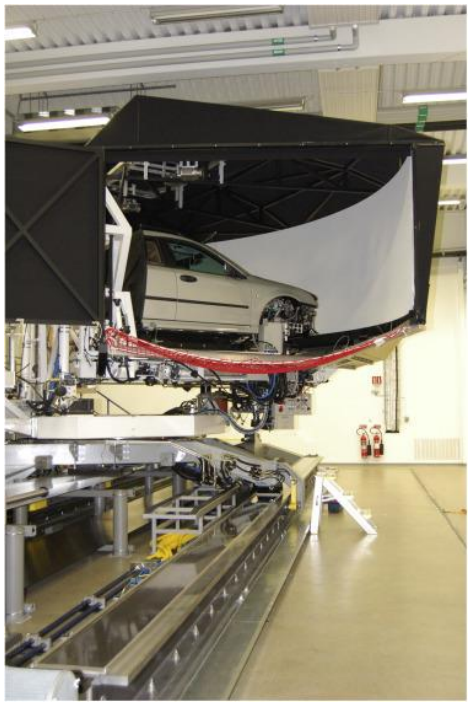

Figure 2 - VTI Sim III

Figure 3 - Interior of Saab 9-3 in the simulator

In *Figure 2*, you can see inside the cabin, where a front body of a Saab 9-3 and a setup with three DLP (Digital Light Processing) projectors are installed. This system can display the environment in a natural way to drivers during simulation. It is providing a field of view of 115 degrees in horizontal and 30 degrees in vertical direction. Moreover, inside the car, there are three LCD screens of 6-inch representing the rear mirrors for an even more realistic simulation. Sometimes, small lags in the displays or projectors can cause nausea problems and simulator sickness. Trying to avoid this kind of problems the VTI simulator was used with the highest possible resolution.

Concerning the analysed experiment ([27], [28]), every data from the simulator was logged at a frequency of 50 Hz. Four cameras of the remote eye-tracking system Smart Eye Pro were installed inside the car in order to track the eye movements of the drivers. On the steering column in front of the instrument cluster a Human Machine Interface (HMI) was placed. This consisted of a 7-inch LCD screen that showed the simulated speed of the vehicle to the participant.
Figure 4 represents the instruments and one of the scenarios analysed in the experiment.

Figure 4 - Interior of the car during the experiment

Unfortunately, it was not possible to access the VTI Driving Simulator III in Linköping and set the experiment because it was done in 2012. Instead, it was possible to take part in another experiment in Gothenburg and experience another VTI simulator (Sim IV). This one is similar to the Sim III with some differences as it is showed in the table of the technical specifications. Having an additional linear axis, the Sim IV permits large movements both in longitudinal and lateral directions. This way, it can simulate simultaneously both large longitudinal and lateral accelerations. Thanks to a system of nine projectors, it can provide drivers with a 210-degree field of view. That makes it the first Sim choice for gaze studies where a wide range is required. Aside, VTI uses the same software for all simulators. In this way, it is possible to move the experiments from one simulator to another.
Below, in *Figure 5*, the VTI Driving Simulator IV in Gothenburg is showed.

Figure 5 - VTI Sim IV

1.2.2 Participants

There were thirty-one participants taking part in the experiment. Twenty-four were male and seven female. Unfortunately, not all participants could complete the experiment because of technical problems (one) or because they got sick (one). Since the experiment included semi-automated driving participants were screened for experience with Adaptive Cruise Control (ACC) in order to have a wider field of study. In this experiment, twenty-one of the participants were used to ACC while the other ten were novices.
The youngest participant was 25 years old while the oldest was 71. The average age of the participants was 50 years (with a standard deviation of 13 years) and they got a driving license for 31 years on average. Another attribute for taking part in the experiment was the time that usually spent driving. On average, their mean annual mileage was 27000 km (with a standard deviation of 13000 km), excluding a tester that was used to do 120000 km per year. It was possible to find the participants with the help of Volvo Car Corporation and with a database of interested members of the public.

1.2.3 Study design

The whole experiment was organized by Annika Larsson (employee at the automotive supplier Autoliv) with the help of VTI. The aim was to study drivers' behaviour during semi critical scenarios. Particularly situations were of interest in which the

Adaptive Cruise Control system malfunctioned and a driver's intervention was required.
First, all participants were asked to complete a questionnaire at home. It asked for their demographic data and their experience with an ACC system. Once arrived at the simulator, they had to read the instructions of the experiment and the supervisors explained how to properly operate the simulator and how the setup of the security systems worked.
When they got in the car, their gaze was calibrated with the four cameras on the dashboard. After that, the participants had some time for a training phase in order to familiarize with the simulator. Once the supervisor and the participants were sure that everything was clear the simulation started.
The participants drove for approximately 15-20 minutes over a distance of 18 km. Most of the time, they drove on a single carriageway (two lane road in opposite direction) with oncoming traffic which made it impossible for the drivers to overtake. However, some scenarios were designed with a 2+1 road configuration. The extra lane was either in the same direction of traveling or on the opposite direction. This was alternating every few kilometers.
The participants had to drive through five different scenarios for each of the four driving modes. Two modes were manual whilst the other two were semi-automated. Every time the mode was changed the drivers were asked to stop the vehicle and follow the experimenter's instructions. The order of driving modes was balanced for each singular participant to avoid order effects. The two semi-automated modes were never performed consecutively in order to avoid confusion for the participants.

Here is a brief explanation of the four driving modes:

- Manual Mode (MAN): The participant had to drive without any automated system and without any subtask.
- Intentional Car Following Mode (ICF): The participant had to drive without any automated system but with the subtask of following a leading vehicle in front of them.
- Adaptive Cruise Control Mode (ACC): The participant had to drive with the ACC system on. It was set to a maximum speed of 75 km/h and with a pre-set time headway of 2 seconds in respect to the leading vehicle.
- Traffic Jam Assist Mode (TJA): The participant had to drive with the TJA system activated in the same setup like the ACC. TJA system combines an ACC system with an Active Steering system (AS) that follows the lead vehicle also laterally.

For the two semi-automated modes, the participants received the instruction to reactivate the system as soon as possible after a switch off. It could be disarmed by overriding the system, braking or using an on-off switch on the left indicator lever in the simulator. There were no buttons on the steering wheel. The distance and the speed were set automatically according to the setup mentioned above and could not be changed. Regarding the active steering, in case the participant decided to take the control of the steering wheel a warning "inactivated steering system" appeared on the screen of the simulator but ACC system resumed its functionality. The active steering implemented in the simulation did not consider the lane markings. It was able to cross them if the leading vehicle did so and it could sustain a turn rate till 45°/sec. Above this value, the system couldn't steer and a warning appeared. Furthermore, the participants were asked to remain at least one hand on the steering wheel in order to

avoid unnecessarily dangerous situations. Past studies confirmed that drivers can react faster and in a proper way when they hold their hands on the steering wheel during semi-automated mode [46]. Additionally, no accidents were possible in order to avoid stress into participants and prejudice the simulation. When an accident was about to happen, the simulator software took the control of the situation throwing far away the other car.

Here a brief explanation of the five scenarios of the experiment is given:

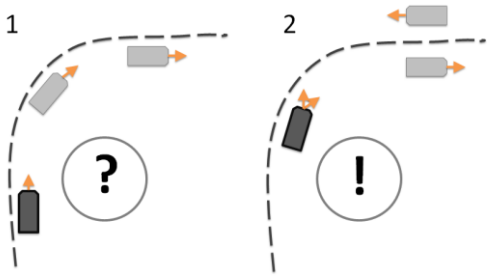

Figure 6 - Sharp curve event

Sharp curve event: The participant had to drive through a sharp curve, while there were two different problems with the automated systems. In ACC mode, the ego vehicle lost the lead vehicle and the system accelerated up to the set speed (75 km/h). In TJA mode the driver had the same problem with the ACC mode and moreover, the active steering was disabled. Thus, the ego vehicle went straight into the oncoming lane.

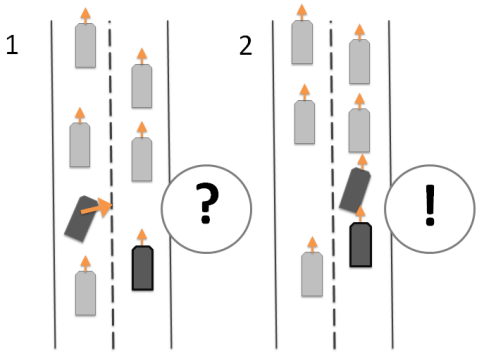

Figure 7 - Cut-in event

Cut-in event: The participant was driving in the right lane of a 2+1 road in a traffic situation and suddenly a car from the next lane cut his trajectory. Driving in both semi-automated modes, the participants had to brake. Otherwise, the system started to accelerate because it couldn't recognize in time its presence.

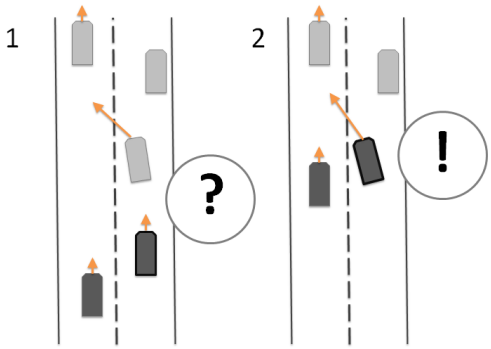

Figure 8 - Broken down car event

Broken down car event: the participant drove in the right lane of a 2+1 road in a traffic situation and suddenly the leading vehicle changed lane because of a broken car. The participants in ACC mode had the problem that the system lost the contact with the leading vehicle and so accelerated to the set speed (75 km/h). This failure would have led them into a collision. In TJA mode on the contrary, the system followed the leading vehicle into the other lane but there was another vehicle on the left of the ego vehicle. So, in order to avoid a possible collision, the driver had to decide to accelerate or to brake letting the left vehicle pass.

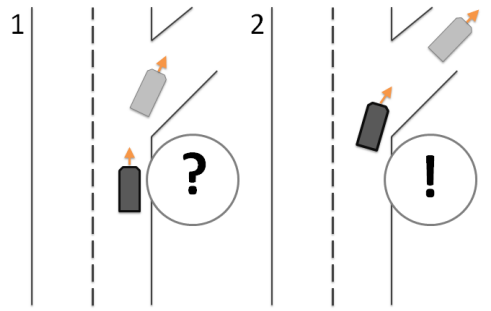

Figure 9 - Exit event

Exit event: The participant had to drive in the right lane of a single carriageway and the leading vehicle took the next exit. In ACC mode, there were no problems: The system of the ego vehicle lost the contact and accelerated till the set speed (75 km/h). In TJA mode, the system kept the contact with the lead vehicle taking the driver out of the main road due to the active steering.

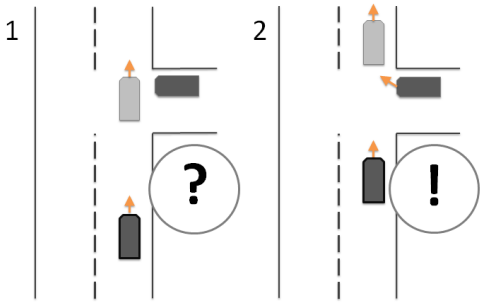

Figure 10 - T-intersection event

T-intersection event: The participant had to drive through an intersection with a T-shape and immediately after the leading vehicle crossed the intersection, another vehicle waiting on the right leg enters promptly in front of the ego vehicle. Driving in both semi-automated modes, the participant had the same issue: the system couldn't recognize in time the second vehicle and so braking was necessary.

1.3 Aim and research questions

The aim of this Master thesis was to analyse driving simulator data in order to assess and model drivers' reaction in a critical T-intersection, during driving with different level of automation and manually. In particular, the analysis focused on the research of significant behavioural differences depending on the experimental driving conditions. The results obtained from the analysis had to be subsequently used in order to build a model capable of both reproducing the results found and predicting the drivers' reaction depending on new input data. This work is part of the project Quantitative Driver Behaviour Modelling for Active Safety Assessment Expansion (QUADRAE), which aims to develop and validate models for driver behaviour that are needed in current and future simulation tools for virtual testing of active safety and automation.

Research questions:

- How do drivers behave to the entry of the turning car into the intersection?
- How do the different driving modes affect the brake reaction time?
- How does the drivers' experience with ACC system affect the brake reaction time?
- How do the different driving modes affect the braking severity?
- How do the different driving modes affect drivers' gaze behaviour?
- How to model drivers' reactions taking into account the data analysed?
- Is the model able to properly predict drivers' reactions?

2 Variables and scenario

The first phase of the project is presented in this chapter. It corresponded to understanding the scenario of interest and all the variables logged in the experiment.

At the beginning of the project, 31 MAT-files (one for each participant) were provided including a Matlab script, that could extract all the variables logged during the experiment. An Excel-file with the most relevant characteristics of the participants was also given. This included:

- the age
- the gender
- years of driving license
- how many km / year driven
- if they were novices or used to the ACC system
- how often they used the ACC system privately

Since there were no video recordings of the simulation, it was necessary to do demanding reverse engineering. Each MAT-file included the whole data of the experiment from a single driver. It was required to study, analyse and model only one scenario of the experiment: the T-intersection. So, the first task was to extract this scenario from the complete dataset. In a first step, we tried to understand the meaning of all present variables that were recorded during the simulation. Overall, each file contained 108 variables over a time period of about 20 minutes with a frequency of 50 Hz. Some variables referred to simulation environment (the road structure), while others described the dynamic of the ego vehicle and also part of the dynamics of the principal other vehicle (POV) that changed in every scenario. In the T-intersection the POV is identified as a turning car (TC). Data regarding the drivers' gaze direction and the head rotation were recorded with an eye-tracker and provided as well. Unfortunately, many variables were not specified in the Matlab script and the measurement units were unknown. In order to understand what they were representing, it was necessary to plot them over the time looking at their ranges and at the shapes of the curves that came out.
Concerning the units of measurement, VTI specified them during the project:

Table 2 - Measurement units

Time	[s]
Length	[m]
Speed	[m/s]
Acceleration	[m/s^2]
Jerk	[m/s^3]
Angle	[rad]
Force	[N]
Pressure	[KPa]

The first variable of interest was the *output.event.eventID*. It identified the present scenario. After having clarified the meaning of each value that the variable assumed, it was possible to detect the T-intersection scenario and to extract the relevant time frame from the MAT-files. Thus, the time-series were shortened to at most 3 minutes. This was due to the fact that every T-intersection scenario lasted about 40 seconds and

that the participants were used to perform that four times each: every time in a different driving mode.

The T-intersection was identified by two different numbers: *4441* for crossing event (*1st*), *4442* for crossing event (*2nd*) as specified in the Matlab script. It wasn't clear why two different values were used to identify the same scenario. Eventually, it was confirmed that both refer to the same scenario. In particular, two checks were fundamental to prove this equality:

- The computation to identify which driver did which event (*4441* or *4442*) in each mode.
- The plots of the trajectories of each participant using the *X* and *Y* global coordinates of the ego vehicle.

From the first check, it was possible to see that none of the drivers completed each intersection (*4441* and *4442*) in every driving mode for a total of eight times. They were performed both without any relation to the driving modes for a total of four times. This indicated that both intersections were representing the same scenario.
Below is reported part of the table that was computed for the first check.

Table 3 - Part of the table representing which driver did which event in each mode

	Crossing event *4441*				Crossing event *4442*			
Drivers	MAN	ICF	ACC	TJA	MAN	ICF	ACC	TJA
1	✓	✓					✓	✓
2	✓	✓		✓			✓	
3		✓	✓		✓			✓
4			✓	✓	✓	✓		

The assumption after the first check became more evident with the second check. It was possible to clearly see that the angle of the two streets was 90 degrees in both cases and that the TC was coming always from the right side of the participant point of view. With a deeper analysis it was confirmed that the only difference was in the global coordinates of the vehicles (but holding the same relative geometry) and in a slight change of dimensions of the principal other vehicle.

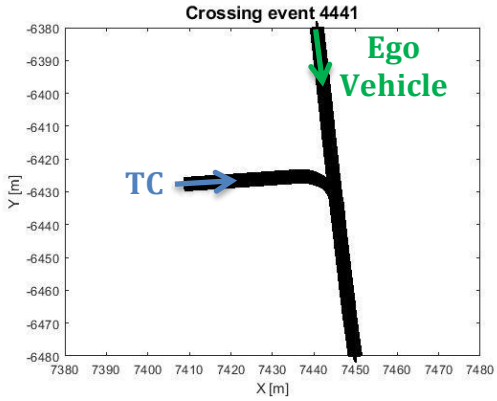

Figure 11 - Crossing event 4441

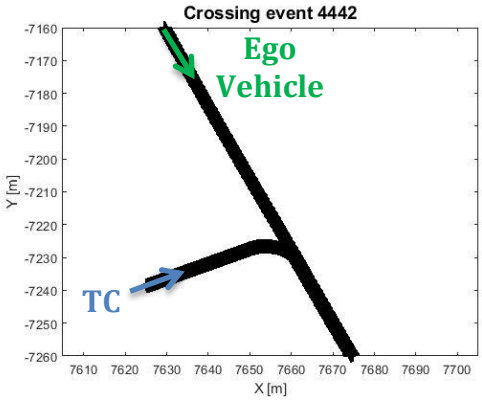

Figure 12 - Crossing event 4442

As written before each intersection was performed in a different driving mode; *output.event.functions* was the variable that identified them:

- *0*: Training mode
- *1*: MAN mode
- *2*: ICF mode
- *3*: ACC mode
- *4*: TJA mode

Unfortunately, not every driver performed the T-intersection in each driving mode.
In order to manage the data a new Matlab script was written. In this way it was possible to plot more drivers at the same time and compare them in a smarter way. Moreover, a clearer distinction between each driving mode was done in order to compare them separately.

A deep analysis of the structure of the scenario was developed necessarily: in particular on the synchronization of the events and on the triggers that ruled the movement of the principal other vehicle.
In the Matlab script four different variables that described the succession of the events were found:

- *output.event.eventID*
- *output.event.event_state*
- *output.event.crossing_event_active*
- *output.event_car.status*

In the simulator's software the environment of the scenario was built as in a track of remote-controlled cars. Therefore, parts of street were identified by a number (*output.road.id*). Moreover, two different reference systems were used: a global one, that identified where the participants were located in the whole experiment (*X, Y, Z*), and a relative one, that identified at which point of that precise piece of street they were located (*s, r*). This means that every time that a participant entered in a new road.id the longitudinal coordinate of that street (*s*) restarted from 0. The beginning or the end of an event was decreed by position triggers, usually located in correspondence of the beginning of a new road.id.

For crossing event *4441* the succession of the events and the respective variables looked like this:

When the participant reached *output.road.id = 7001* and *output.road.s = 0*:
the event was initialized, so *output.event.eventID* changed from *0* to *4441*, the TC was positioned in the perpendicular street far away from the intersection (*output.event_car.road_id = 7005* and *output.event_car.s = 478*). Its velocity was set to 0 km/h and its path was set (the road it should follow).

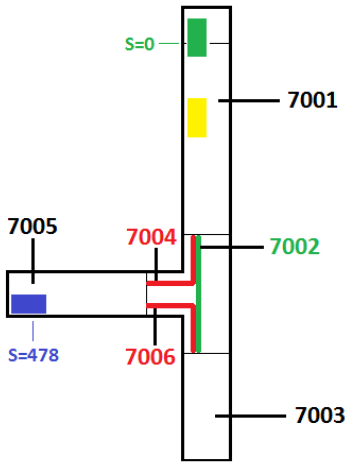

Figure 13 - T-intersection: event inizialization

As it is showed in *Figure 13*, every section of straight road has one path, and so one identification number (*7001*, *7003*, *7005*). On the contrary, the intersection has got three possible paths, and so three different identification numbers appear (*7002*, *7004*, *7006*), one for each path. The lead vehicle (yellow car) and the ego vehicle (green car) could follow two different paths: *7002* or *7004*. The TC (blue car) could follow only the path *7006* as can be seen in the figure. In this scenario the leading vehicle and the ego vehicle followed the path *7002*.

When the driver reached the position *road.id = 7001*, *s = 300* as it is showed in *Figure 14*:
output.event.event_state went from *0* to *1* and the TC started to drive at 10 km/h in the perpendicular street still far away from the intersection.

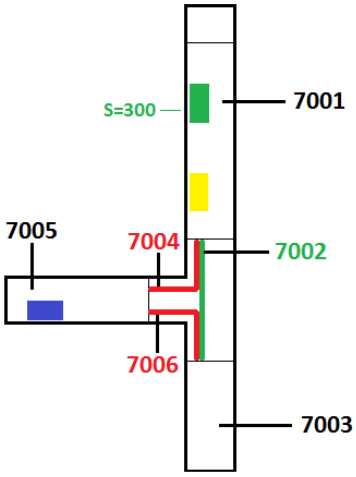

Figure 14 - T-intersection: TC (blue car) starts to approach the intersection

When TC reached its stop position at the intersection (*Figure 15*) precisely at *output.event_car.road_id = 7006*, *s = 15*:
output.event.crossing_event_active went from *0* to *1*.

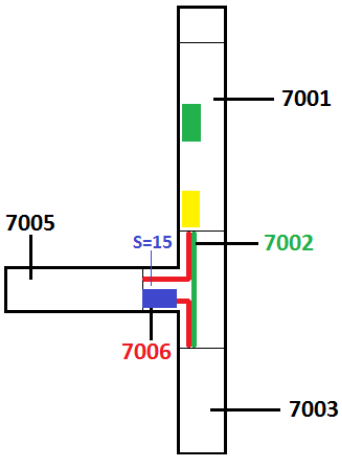

Figure 15 - T-intersection: TC (blue car) reaches the stop line

At this point of the scenario the participant was driving on the main street at a certain distance from the lead vehicle, while TC was waiting at the stop line of the intersection in the perpendicular street.

As soon as the lead vehicle reached the position *road.id = 7002*, *s = 15* (*Figure 16*), i.e. it is in the middle of the intersection:
output.event_car.status assumed a value equal to *7* and TC started to accelerate and to get the intersection, putting itself between the lead vehicle and the participant.

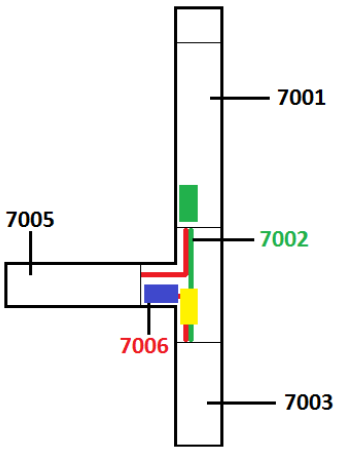

Figure 16 - T-intersection: TC (blue car) gets the intersection

Hence, the precise instant in which TC got the intersection was not depending on the participant vehicle but on the leading vehicle. So, during the manual modes (MAN and ICF) the distance of the drivers from the intersection at the moment in which the TC enters the intersection was different because it was depending on how close the participants were driving respect to the leading vehicle. Meanwhile, in semi-automated modes (ACC and TJA) this distance was always the same because the THW was fixed by the system.
It has to be stated that the TC entered the intersection with an unrealistic acceleration of 12.8 m/s^2, indeed after one second from time zero it reached the intersection point with a speed of 46.2 km/h. This setup was chosen to analyse the first reactions of the participants without any possibility of crashes.

When TC reached the same speed of the vehicle in front (*Figure 17*):
output.event.crossing_event_active went from *1* to *0*.

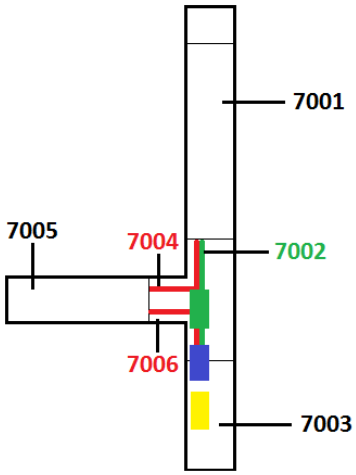

Figure 17 - T-intersection: TC (blue car) has the same speed of the leading vehicle (yellow car)

When TC reached the position *road.id = 7003*, *s = 50* (*Figure 18*):
output.event.event_state went from *1* to *0* and *output.event.eventID* went from *4441* to *0*, the event was over.

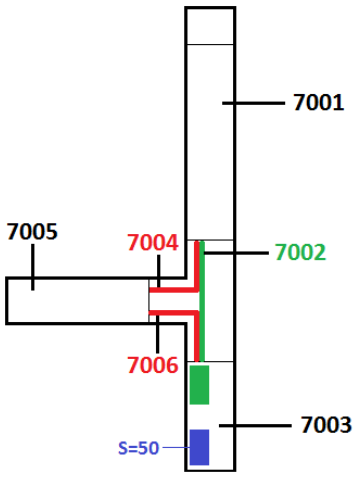

Figure 18 - T-intersection: end of the event

The figures and the explanation of the event are valid also for the crossing event *4442*. It had the same structure but with different *road.id* numbers (*8001* instead of *7001*).

The scenario was plotted on Matlab using the global coordinates of the ego vehicle and of TC, and implementing two functions that could represent them with the shape of a car. This was done in order to have a graphical representation of the scenario. Indeed, as written before, no videos of the experiment were available. Unfortunately, the trajectory of the leading vehicle couldn't be plotted, due to the fact that the global coordinates of that were not registered during the experiment.
The most significant frames of the Matlab graphical representation are reported in *Figure 19*. TC is always represented in blue whilst the ego vehicle is represented in green and in red. Green means that the participant was going straight without braking, while red means that was braking. The enforcement of changing the colour of the ego vehicle in the Matlab video was fundamental to recognize what was really happening

during the simulation. It has been a visual proof that they were truly braking due to the presence of TC. The Matlab frames shows exactly the same scenario described between *Figure 13* and *Figure 18*.

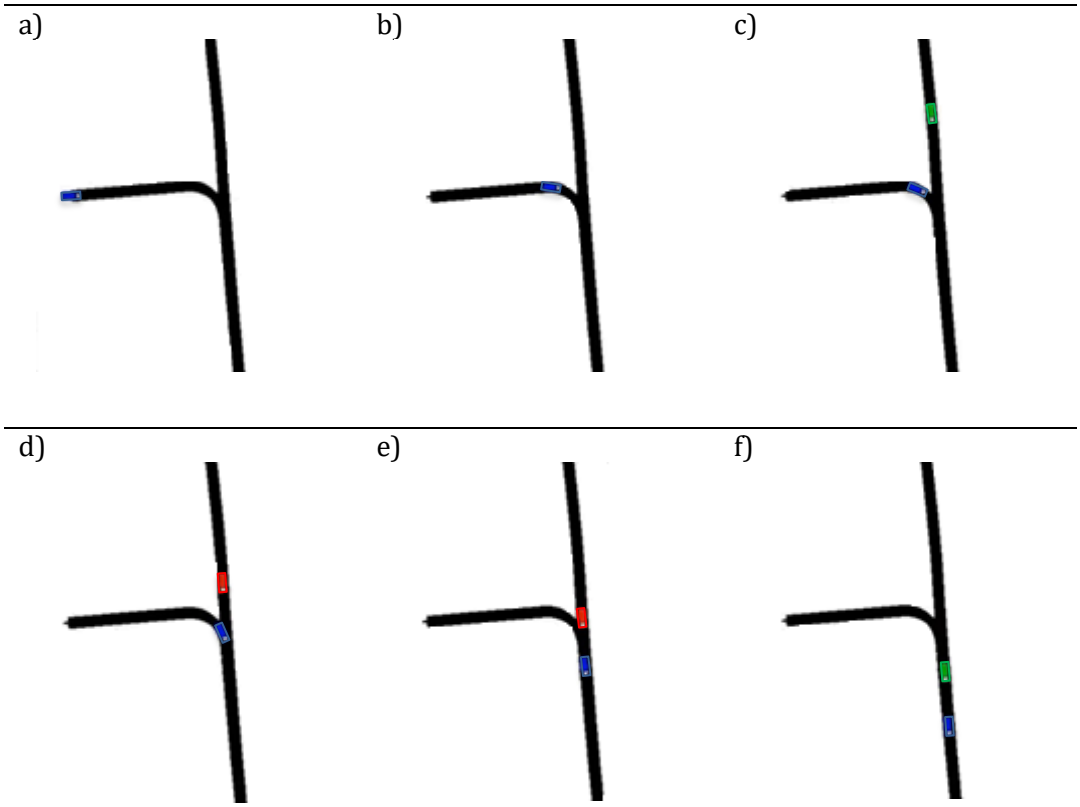

Figure 19 –Matlab video frames: a) TC approaches the intersection. b) TC waits at the stop of the intersection. c) TC starts to get the intersection. d) Ego vehicle brakes because of the TC. e) Ego vehicle continues its brake. f) The two vehicles are now driving at the same speed.

3 Analyses

All the analyses performed during the project are represented in this chapter. They have been done after having realized thoroughly the scenario and its variables. The chapter is divided in two main sections: method and results.

3.1 Method

Proceedings, techniques and formulas carried out to perform analyses of drivers' behaviour are described in detail in this section.

3.1.1 What drivers do

The main purpose of the project was to analyse and to represent drivers' reactions to the sudden entering of TC into the intersection. The moment in which the TC was at the stop line and started to accelerate, was taken as the time zero of the scenario. This instant was identified when the variable *output.event_car.status* was equal to *7*. This way, it could be possible to have an instant that was meaningful for every participant. Indeed, as it was explained in the previous chapter, the boundary conditions of the experiment were not always the same in the two manual modes: the distance from the intersection of the ego vehicle (the participant's vehicle) at the moment of TC's entrance were dependent on how close to the leading vehicle they were driving.
One mode per time was analysed, looking at what drivers were used to do after the time zero. Concerning the manual modes, the time-series of the throttle and the brake pedal, and those of the steering wheel angle were plotted simultaneously for each driver. In this way, every action of each participant was noticed with its respective time.
The throttle pedal was identified by a variable (*output.ove.throttle*), that could go continuously from *0* to *1*, representing the throttle gain and so having no unit measure. The brake pedal force was instead measured in Newton (*output.ove.brake_force*), while the steering wheel angle was expressed in radiant (*output.ove.stwa*).
In *Figure 20* an example of the three time histories is reported (driver 13 – MAN mode). The red vertical lines indicate the instant in which the TC started to get the intersection.

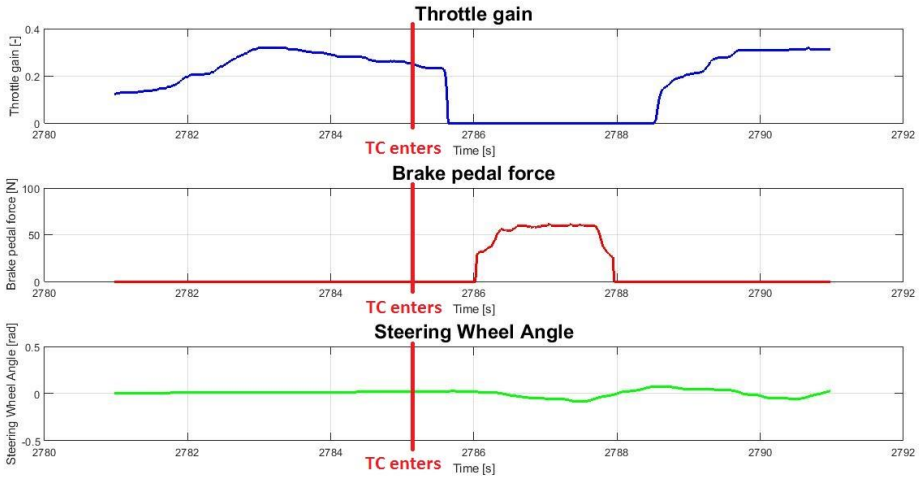

Figure 20 – Example of time histories of throttle gain, brake pedal force, steering wheel angle (driver 13 – manual mode)

As it was written before, only the actions that they did immediately after the time zero were taken into account. According to this, all the simulations in which the participants were used to brake or leaving the throttle before any movement of the TC were cut. It was assumed that the participants that did it were afraid of the intersection in general and not of TC's movement.
The same studies were computed for both the semi-automated modes but taking into account also the activation of the automated braking system, that was represented by a Boolean variable called *output.event.tja_braking*.
An excel file was done, representing in each row every intersection performed by every participant, whilst in each column every analysed variable. So, every participant had four rows, one for each driving mode. The file was updated every time that a new variable was computed.
The reaction times of each driver were computed taking the difference between the moment in which they had a reaction and the moment in which the TC started to get the intersection. It was considered as a reaction: the leaving throttle, the braking and the movement of the steering wheel. In this way, it could be possible to understand what drivers did and when they did it.

Leaving throttle. This action concerned only the two manual modes, due to the fact that in ACC and TJA no force on the throttle pedal is required to drive. It was analysed why some participants could just leave the throttle instead of braking and where they were located when they did it. This action was analysed also for drivers that decided to brake after leaving the throttle. This was done in order to see if they left the throttle because of the intersection or because of the TC movement and to compute the mean time to pass from the throttle pedal to the brake pedal. Due to the fact the throttle pedal has to be released and not pushed it was not immediate to decide what time to take. Indeed, as can be seen in *Figure 21*, the variable representing the throttle didn't go never to zero in an instant. So, it was possible to take three different moments looking at its time history:

1. The moment in which the decreasing of the throttle's gain was starting.
2. The moment in which the throttle's gain was completely equal to zero.
3. The average of the two moments.

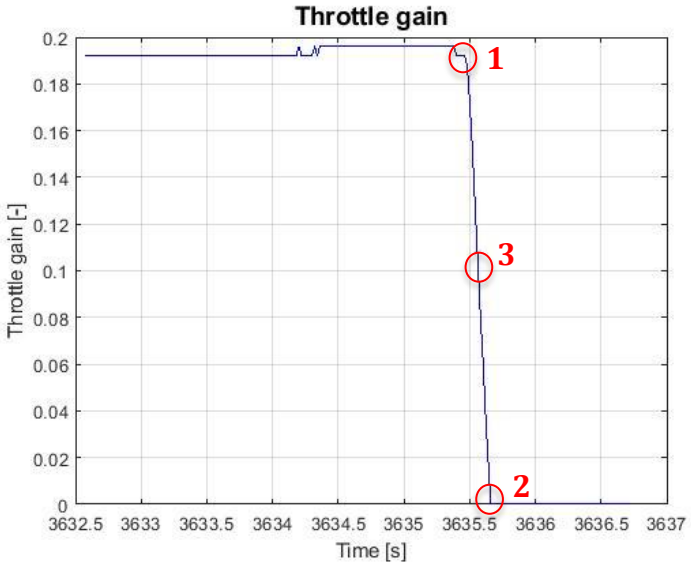

Figure 21 - Example of a throttle gain time history (driver 69 – manual mode)

The first moment, so the first reaction of the drivers was taken into account. The other two moments instead represented not only the drivers' reactions but also the mechanical delay that a gas pedal usually has. And this was not the purpose of the project.

Braking. Most part of the analysis was focused on the braking. In particular on the brake reaction times that participants had, driving with the four different modes. They were computed as the differences of time between the moment in which the driver pushed the brake pedal and the time in which TC started to get the intersection.
In order to quantify how drivers braked, the most significant values of the deceleration, jerk and brake pedal force were taken. In particular, a friction coefficient equal to 0.8 was assumed, due to the fact that the simulation environment was composed by a dry paved road. According to [23], looking at the braking time history, it was considered for each participant the maximum value for the deceleration, whilst for the jerk the value at the beginning of the braking. For what concern the jerk, it was noted that most of the time it reached values that were physically unfeasible with peaks of -80 m/s^3. According to [47] the minimum values that could be reached during braking are around -15 m/s^3. So it was decided to compute the jerk time histories deriving them from the acceleration in several different ways on Matlab. The results were always equal and they corresponded to the jerk received from the VTI simulator. A test on the acceleration was computed too in order to verify if it was correct. It was derived from the speed time histories but also in this case the same results of the VTI simulator data were found. These strange peaks of the jerk and sometimes also of the deceleration were attributed to the data acquisition frequency (50 Hz). Concerning the maximum pedal force, reliable values were found, always under 400 N. Instead, the maximum force that a driver could put on the brake pedal is around 400 N [48].
Concerning the brake reaction time, the initial jerk, the maximum deceleration and the mean force on the brake pedal, a comparison between each driving mode was done. All the accelerations and the jerks were reported in absolute values in order to make it clear. Therefore, they were called "maximum deceleration" and "brake jerk". All the averages and standard deviations were calculated for each driving mode. Moreover, box plots and statistical tests were computed, in order to see if any significant

difference was present. All these analyses were also performed taking into account if the participants were used to the ACC system or not. In particular, looking at the averages of the variables just described, it could be possible to understand which type of driver trusted more the ACC and TJA systems and which one not.

Corrective steering. The movement of the steering wheel was taken into account looking at the steering wheel angle variable. This was defined in radiant and assumed both negative and positive values. Negative values meant turning to the right, whilst positive to the left. The structure of the scenario consisted in one lane per direction and frequent cars from the opposite lane. Therefore, no changes of lane and no avoidances of the TC were allowed. For this reason, it was decided to call and represent this action not like a real steering but as a correction.

3.1.2 Time to intersection

Knowing the paths and the dimensions of the two vehicles (ego vehicle and TC), it was possible to compute a collision point in the intersection zone for both the crossing events (*4441* and *4442*). For a more accurate calculation, it was necessary to consider that the global coordinates of the vehicles were referred the headrest of the vehicle, that is usually located in the middle of the car. The point used to compute the collision point was referred to the right part of the ego vehicle's front bumper and to the left part of the TC's front bumper.

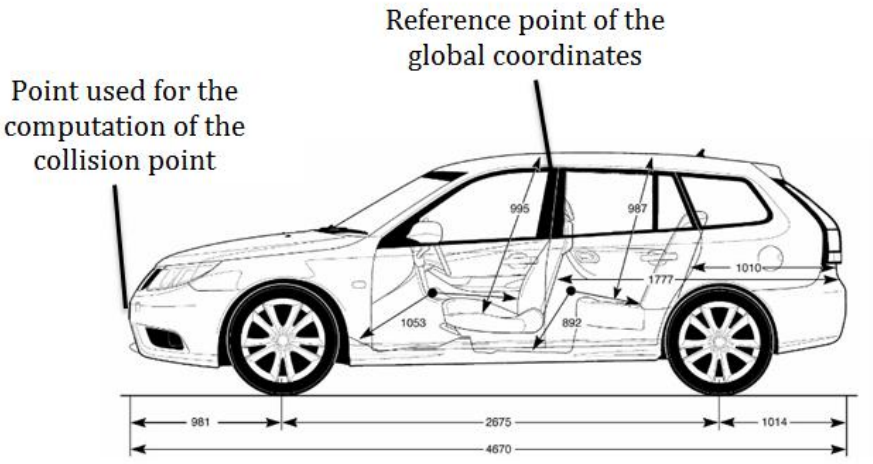

Figure 22 - Lateral view of the ego vehicle (Saab 9-3)

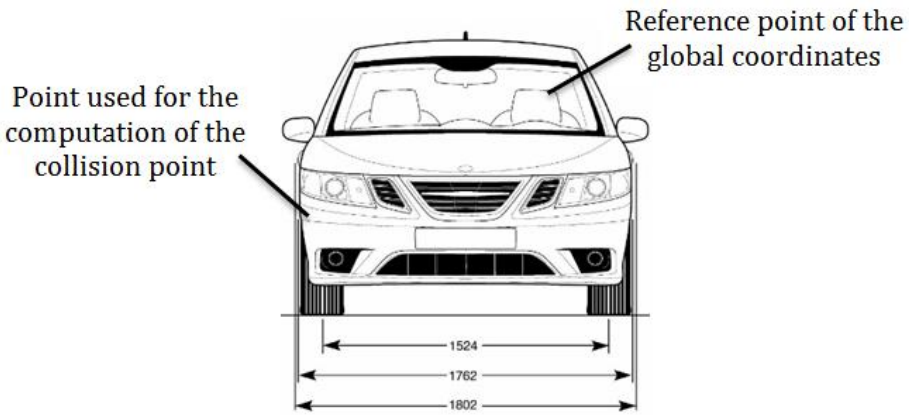

Figure 23 - Front view of the ego vehicle (Saab 9-3)

Moreover, the dimensions of the TC changed between the two crossing events.

Crossing event *4441*:

- Collision point: *X = 7444.5* ; *Y = -6428.3*
- TC dimension: *L = 4.47 m* ; *W = 1.77 m*

Crossing event *4442*:

- Collision point: *X = 7658.5* ; *Y = -7227*
- TC dimension: *L = 3.99 m* ; *W = 1.86 m*

Once computed the collision points, more important physical data could be calculated. Two fundamental moments were considered in each simulation:

- The moment in which the TC entered.
- The moment in which the drivers started to brake.

At these moments, the distances of the ego vehicle from the intersection and the speeds of the same were annotated. In this way, it could be easily possible to compute two different times to intersection (TTI_{enter} and TTI_{brake}), dividing the distance from the intersection with the respective speed annotated. As can be seen in *Figure 24*, one time to intersection was referred to the TC entrance (TTI_{enter}), whilst the other one to the first braking instant of the participant (TTI_{brake}).

a) TC entrance frame **b) Ego vehicle braking frame**

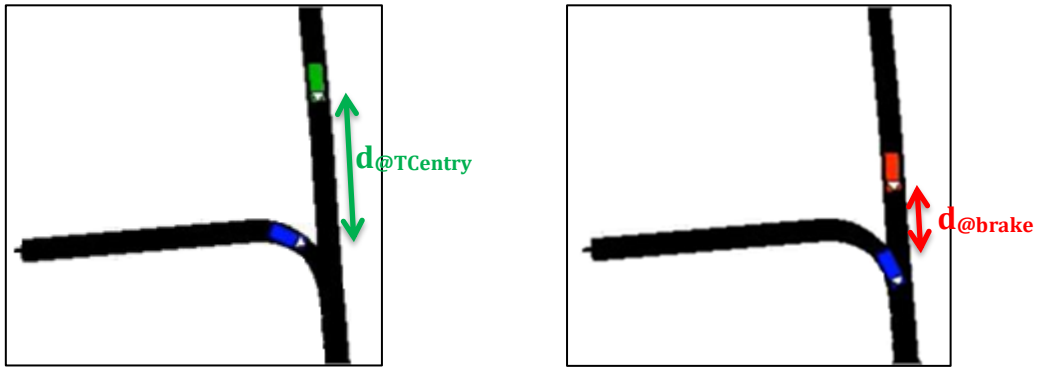

$$TTI_{enter} = \frac{d_{@TCentry}}{V_{@TCentry}} \qquad TTI_{brake} = \frac{d_{@brake}}{V_{@brake}}$$

Figure 24 - a) Time to intersection at TC entry. b) Time to intersection at first braking instant

Both of them were fundamental to understand why drivers decided to react in different ways and also in different moments of the scenario.
According to [23] from the time to intersection at the braking point it was possible to quantify the riskiness of the scenario for each participant. This was represented by the inverse of the TTI_{brake} (1/ TTI_{brake} represented also as $1/\tau_b$) [23].

Most part of the analyses was focused on the dependence of the main variables to both of the times to intersection (TTI_{enter} and TTI_{brake}). In particular, for each driving mode were studied correlations between:

- The brake reaction times and the time to intersection when TC got the intersection (TTI_{enter}).
- The initial brake jerk and the riskiness of the scenario ($1/\tau_{brake}$).
- The maximum deceleration and the riskiness of the scenario ($1/\tau_{brake}$).

3.1.3 Gaze behaviour

Several variables, concerning the movements of the eyes, the head rotation and the eyelid opening, were logged during the simulation. This was realized in order to study and analyse drivers' gaze behaviour.
The gaze in x and y directions (*output.se.gaze_dir_x* and *output.se.gaze.dir_y*) and the gaze quality (*output.se.gaze_dir_quality*) were the most useful variables used for the gaze analyses.
The gaze in the x direction assumed values both positive and negative, and it represented if the drivers were looking to the right or to the left:

- *positive* values meant they were looking to the *left*
- *negative* values meant they were looking to the *right*

In order to have a clearer representation in the Matlab plots this vector (*output.se.gaze_dir_x)* was multiplied for -1.

For what concern the gaze in the y direction:

- *positive* values meant to look *up*
- *negative* values meant to look *down*

The gaze quality variable was fundamental to understand the reliability of the cameras' acquisitions. It assumed values between *0* and *1*:

- *0* meant that the quality was really low
- *1* meant that the quality was really high

Data with a quality higher than 0.6 were considered.

Once that all the gaze variables were defined, a physical reference point was computed in order to perform the analyses in the right way. Knowing the path of the ego vehicle and of the TC, an intersection point was computed similar to the collision point. But in this case the dimensions of the vehicles were not considered, due to the fact that a more theoretical point was needed in order to set a perfect straight point.
The coordinates of the intersection points were:

- *X = 7444.5* ; *Y = -6431* for crossing event *4441*
- *X = 7660*; *Y = -7230* for crossing event *4442*

Knowing the position of the ego vehicle, of TC and of the intersection point it could be possible to implement a function that computed the angle between the two vehicles in each time step (0.02 sec).
Here below the formulas used to compute the angle in each time step:

$$\alpha = \text{atan}\left(\frac{d_{TC}}{d_{EGO}}\right)$$

where

$$d_{TC} = \sqrt{(X_{TC} - X_{INT})^2 + (Y_{TC} - Y_{INT})^2}$$

$$d_{EGO} = \sqrt{(X_{EGO} - X_{INT})^2 + (Y_{EGO} - Y_{INT})^2}$$

X and *Y* where the global coordinates referred to TC, to the ego vehicle (EGO) and to the intersection point (INT); d_{TC} was the distance between TC and the intersection point, whilst d_{EGO} the distance between the ego vehicle and the intersection point.
In *Figure 25* an example of the function is showed:

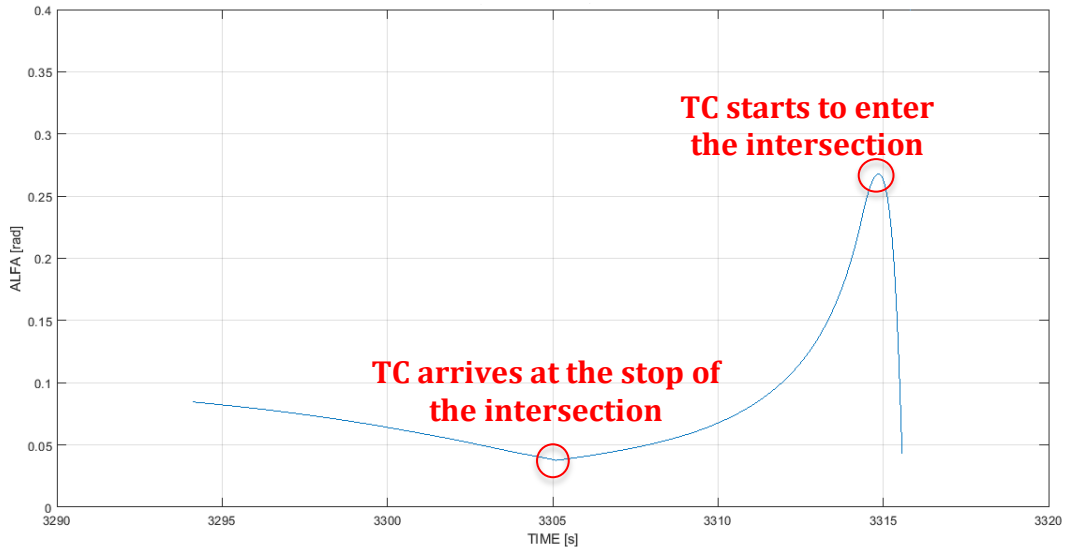

Figure 25 - Alfa function graph for driver 1 in manual mode

In this case, around second *3305*, TC reached the stop line at the intersection, while the participant was going straight. From this moment the function describing the angle between the two vehicles increased, due to the fact that TC was at standstill at the intersection, while the ego vehicle was coming from far away. The function stopped increasing when TC started to get the intersection (here around second *3315*). From this moment the angle decreased again due to TC's movement.

Remembering that the global coordinates of the vehicle were referred to the headrest of the car and not to the front bumper, smaller angles were taken into account. In particular, a correction factor of 0.8 was considered. The correction factor was decided after that the angle between the two vehicles was computed, considering different global coordinates for TC. In particular adding half of its length to the car it could be possible to detect the coordinates related to the front bumper. This angle was

computed only for one time step and compared with the angle calculated with the original global coordinates (referred to the headrest and not to the front bumper) at the same time step. Through simple proportions, it was found out that the new angle (referred to the front bumper of the TC) was smaller than the original angle (referred to the headrest) of a factor of 0.8 – 0.85. So the threshold angles were defined as:

$$\alpha_{threshold} = 0.8 * \alpha$$

Where α was the angle computed before.

This function was used as a dynamic threshold for two analyses:

1. How much the participants looked to the right before the intersection.
2. When they noticed the presence of the TC.

For both the analysis, a time window of eleven seconds was considered: 10 seconds before the TC's entry and one after that. Before the 10 seconds, the values of the angle were too small and so it was not possible to understand if the participants were looking to the TC or somewhere else.
In the first analysis, it was possible to quantify, as a percentage, how much the drivers looked to the right in each second before the intersection. So, every time that an angle was greater than the dynamic threshold, it was taken into account.
Instead, for the second analysis, drivers' perception time of TC was computed. It was not considered simply a threshold angle but a slice. As can be seen in *Figure 26*, this slice was delimited (from the participant point of view): to the left by the previous angle and to the right by a greater angle. In this way it could be possible to detect the entire car from the front bumper to the rear one. All the angles inside this band were considered:

$$0.8 * \alpha < angles\ considered < 1.2 * \alpha$$

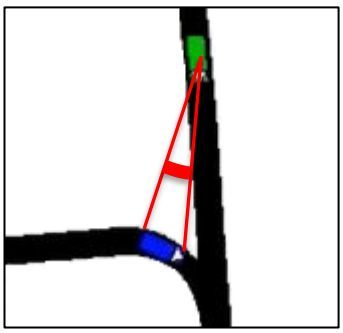

Figure 26 - Beam of considered angles in a single time step

Moreover it was defined that the smaller glance had to be at least 0.25 seconds long [49]. So, every time that a participant looked consecutively to this area for 0.25 seconds, the last time of this interval was considered as the time of perception of TC. It could be possible to detect this information for all those drivers that had a gaze quality greater than 0.6. Moreover, a comparison between all the driving modes was performed in order to detect gaze behavioural differences.
Correlations between drivers' perception time of TC and the brake reaction times were computed.

3.1.4 Statistical tests and correlation coefficients

Averages and standard deviations were computed for all the analysed data in each driving mode. They were also verified using different types of statistical tests [50]. The *One repeated measures Anova* test was computed to compare the braking reaction times of the same participants that drove through all the four different driving modes and braked. It was performed in order to take into account and compare the behaviour of the exactly same drivers. This type of test can be applied only if the same amount of data is present between the factors that had to be compared. If significant differences were found with the *Anova test*, the *T-tests* were computed in order to understand between which factors the significant difference was present. Indeed, the *T-test* can compare two factors at a time. Moreover, it is possible to perform the *T-test* only if the interested data are normally distributed. To verify if a distribution of data was normal or not the *Shapiro test* was computed, giving a *p-value* as result. If the *p-value* was higher than *0.05* the distribution was normal otherwise it wasn't. Every time that the distribution of data was not normal the *Mann-Whitney U test* was performed with the same purpose of the *T-test*. The *Mann-Whitney U test* is a non-parametric test. It compares the corresponding ranks of each value, instead of taking directly the values. The *T-test* and *Mann-Whitney U test* were applied depending on data distribution of the variables analysed. In most of the cases the *Mann-Whitney U test* was applied to compare data from different driving modes. It was decided to use this test, even if the samples (participants) corresponding to the different driving modes were not completely independent. However, it has to be specified that the number of considered participants in semi-automated driving was higher compared to the manual modes. Moreover, the participants considered even within the four driving modes were not always the same. Insight of this and due to the fact that the data were not normally distributed, the *Mann-Whitney U test* was applied.

Concerning the analysed correlations, two different coefficients were applied: the *Pearson* (r) and the *Spearman* (ρ). Both of them are used to define the linear correlation between two variables. The *Pearson correlation coefficient* can be used every time that a normal distribution of data is present. Otherwise, when the data are not normally distributed, the *Spearman correlation coefficient* has to be used [50]. Moreover, the *Spearman coefficient* has the perk that is less subject to the outliers. So, in each analysis carried out in this project, the *Spearman coefficient* was used. When it was possible (when the data were normally distributed) also the *Pearson correlation coefficient* was computed, in order to have a complete view of the correlations.

3.2 Results

All the results of the analysis are showed in detail in this section. They are divided in several sub sections. All the actions by the participants are presented and their correlations with the different scenario conditions.

3.2.1 What drivers do

First, we show in a general way how the drivers reacted to the TC's entry into the intersection in the different driving modes. In *Table 4* and in the pie graphs of *Figure 27*, the actions and the corresponding number of drivers that performed those actions are reported.

Table 4 - Drivers actions in each driving mode

Driving mode	Braking + corr. steering	Only braking	Leaving throttle + corr. steering	Only corr. steering	Only leaving throttle	No actions	Tot n° drivers
MAN	9	6	0	0	5	/	20
ICF	6	10	1	1	5	/	23
ACC	13	7	/	2	/	6	28
TJA	13	8	/	1	/	6	28

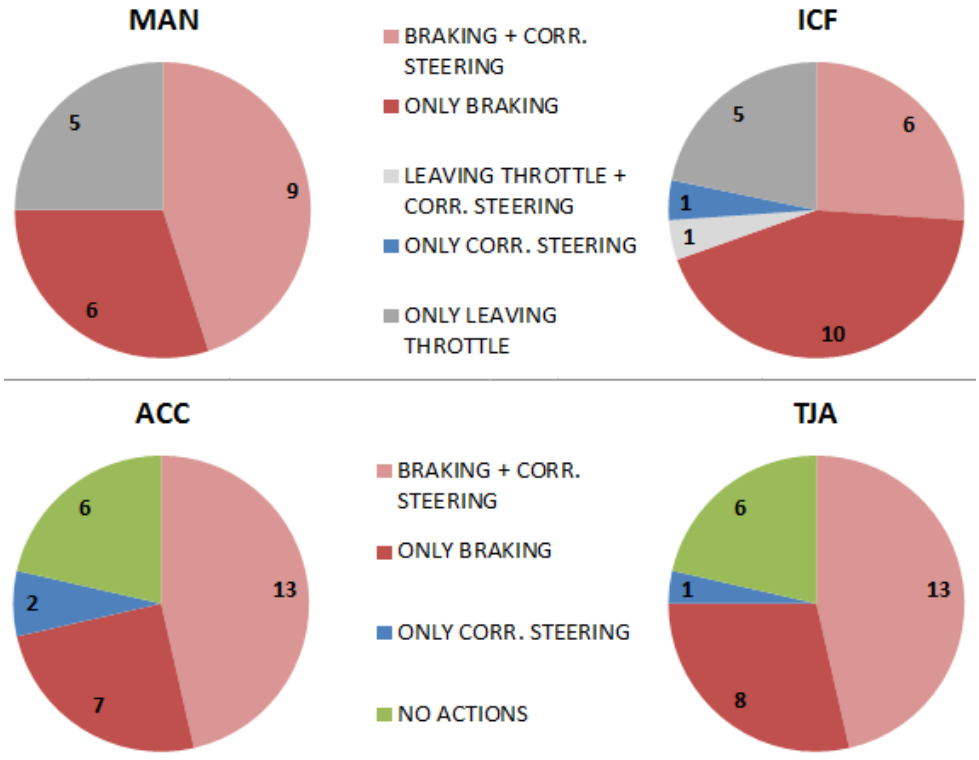

Figure 27 - Pie graphs of drivers' actions in different driving modes

Regarding the actions done by the participants it is necessary to make a distinction between the manual modes (in the upper part of *Figure 27*) and the semi-automated modes (in the lower part). The *leaving throttle* action was unfeasible for the semi-automated modes. On the contrary, it was possible in these modes to decide to do

nothing, leading the vehicle to a near crash. Regarding the two manual modes, the *no action* was not considered, due to the fact that would have been incorrect: all the participants that are not included in the analyses in the manual modes (MAN and ICF) left the throttle or braked far away from the intersection, before TC's movement. So, it was not necessary to brake again or do any other action after that. Therefore, it is not true that they didn't perform any action. Indeed, as explained in 3.1.1, only drivers' reactions to the TC's movement have been taken into account.
The situation for the two semi-automated modes is different. Here, the participants categorized as performing *no actions* did not perform any of the analysed actions for the entire scenario. Also in these two modes, participants braking before the TC's movement and herewith disabling the semi-automated systems, were not considered.
For all these reasons the number of participants considered in each driving mode is always small than 31 (total number of participants in the experiment).

In *Figure 28* and *Figure 29* the temporal sequences of the actions carried out by the participants are showed, for each driving mode. On the right of each sequence, the number of participants that performed that sequence is reported. The sequences are displayed in order of their frequency: from the most common sequence to the least one.

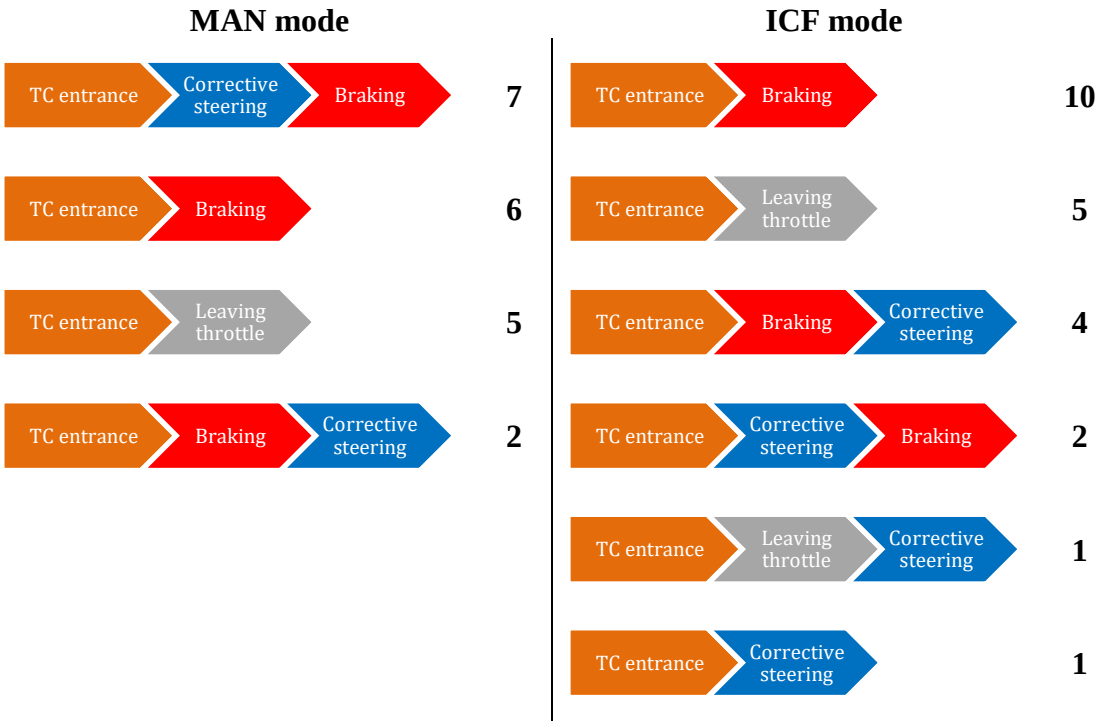

Figure 28 - Drivers actions sequences in MAN and ICF modes

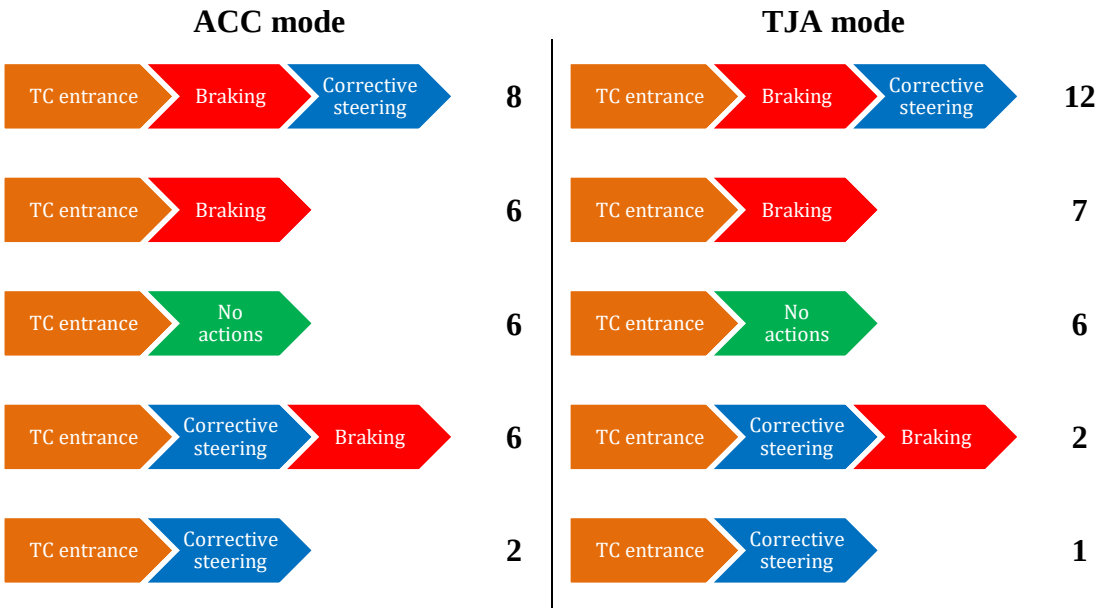

Figure 29 - Drivers actions sequences in ACC and TJA modes

It is clear from the sequences that the main action of participants during the scenario is brake. This is true in all four driving modes: in MAN mode they were 75% of the total, in ICF 70%, in ACC 71% and in TJA 75%. Moreover, only small corrective steering maneuvers were found. This concludes that none of the participants did try to avoid the TC with an evasive steering manoeuvre.

These statements were confirmed by the analyses of the time histories of the brake pedal force and of the steering wheel (3.1.1), but also by the values of longitudinal and lateral acceleration. Two graphs representing respectively the minimum and the maximum values that these two variables reached during the scenario are showed in *Figure 30* and *Figure 31***.** Each blue point represents one participant in one of the two manual modes (MAN and ICF), whilst each orange point represents one participant in one of the two semi-automated modes (ACC and TJA). In the two figures all drivers considered in *Table 4* are present.

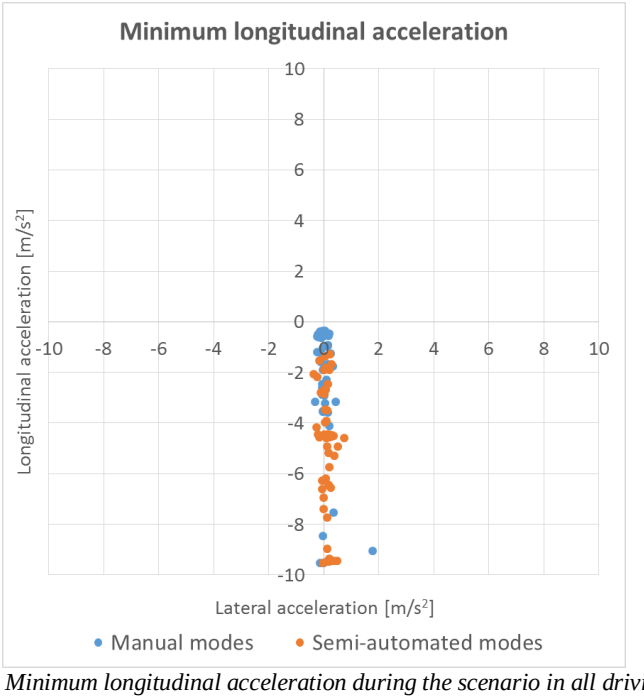

Figure 30 - Minimum longitudinal acceleration during the scenario in all driving modes

For each participant, the minimum value that the longitudinal acceleration reached during the scenario was taken into account to build the graph. A narrow distribution of the longitudinal accelerations along the negative part of the y axis is present. Moreover, it is possible to note that red points (representing the two semi-automated modes), assumed on average lower values than the manual modes (a further analysis is showed in 3.2.6).

The graph representing the maximum lateral accelerations is showed below.

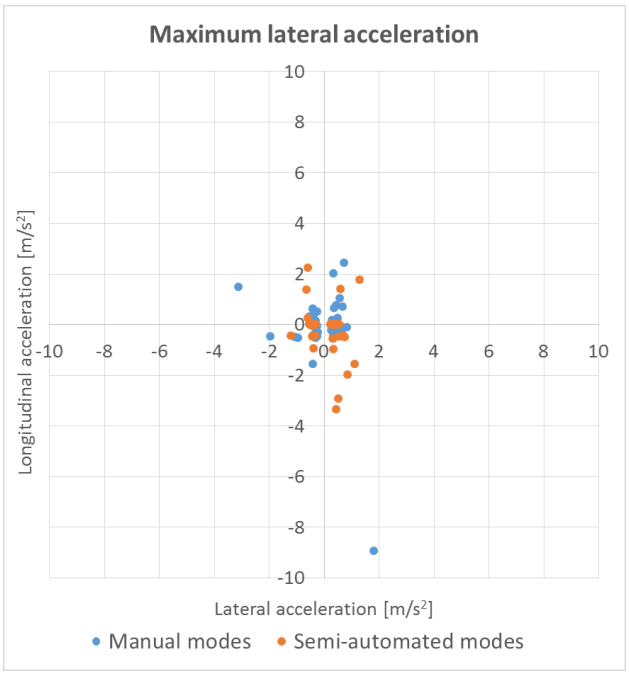

Figure 31 - Maximum lateral acceleration during the scenario in all driving modes

Points in *Figure 31* correspond to the maximum absolute lateral acceleration of the ego vehicle during the scenario. In the graph, the points form a circular spot and no clear distinction can be done between the different driving modes.

Comparing the two acceleration graphs it is possible to detect that higher values (in absolute values) of longitudinal acceleration are present compared to the lateral ones.

3.2.2 MAN and ICF: leaving throttle vs braking

This analysis is referred to the two manual modes: MAN and ICF.
It shows why some participants decided to just leave the throttle pedal while others decided to brake after TC's movement. In order to justify these different behaviours, two meaningful factors were taken into account at the time zero (the instant in which TC started to get the intersection): the distance from the intersection and the speed of the ego vehicle. To show both these factors together, the time to intersection was computed.
In *Table 5* and *Table 6*, the averages and the standard deviations of these three factors are reported. Moreover, for what concern the ICF mode, the sum of the participants that are taken into account in this analysis is not corresponding to the total amount (22 instead of 23) due to the fact that one driver performed only a steering correction.

Table 5 - Data concerning the participants that just left the throttle

Driving mode	Average distance ego vehicle from intersection [m]	Average speed ego vehicle [km/h]	Average time to intersection when TC enters [s]	N° drivers
MAN	70.33 ± 18.88	63.75 ± 4.43	4.02 ± 1.28	5/20
ICF	113.33 ± 52.54	67.00 ± 3.46	6.16 ± 2.96	6/23

Table 6 - Data concerning the participants that braked

Driving mode	Average distance ego vehicle from intersection [m]	Average speed ego vehicle [km/h]	Average time to intersection when TC enters [s]	N° drivers
MAN	59.53 ± 20.31	67.73 ± 4.92	3.15 ± 1.00	15/20
ICF	56.27 ± 17.65	68.02 ± 4.90	3.02 ± 1.05	16/23

Low intersection times correspond to small distances from the intersection and high speeds. On the contrary high intersection times correspond to long distances from the intersection and low speeds. Looking at both driving modes higher values of intersection times can be noted for the participants that just left the throttle.

3.2.3 Brake reaction times

In this sub-section, only the participants that braked during the intersection approach are taken into account. All driving modes are considered.
In particular, different comparisons and correlations are represented:

- Comparison of brake reaction times between different driving modes.
- Comparison of brake reaction times between different driving modes taking into account if the drivers were used to the ACC system or novices.
- Correlations of the brake reaction time with the time to intersection (when the TC gets the intersection) for each driving mode.
- Comparison of brake reaction times for all the drivers that braked in each driving mode.

Table 7 and the box plot in *Figure 32* represent the mean values and the ranges of the brake reaction times for each driving mode. In the last row of the table the numbers of considered drivers for this analysis is shown. It can be noted that these drivers coincide to the sum of those ones that were displayed as '*braking + corr. steering*' and '*only braking*' in *Figure 27*. Furthermore, the red crosses in the box plot represent the average values reported in the table.

Table 7 - Brake reaction time in each driving mode

Brake reaction times [s]				
Driving mode	MAN	ICF	ACC	TJA
Average	1.05 ± 0.33	0.95 ± 0.23	0.84 ± 0.18	0.94 ± 0.28
N° drivers	15	16	20	21

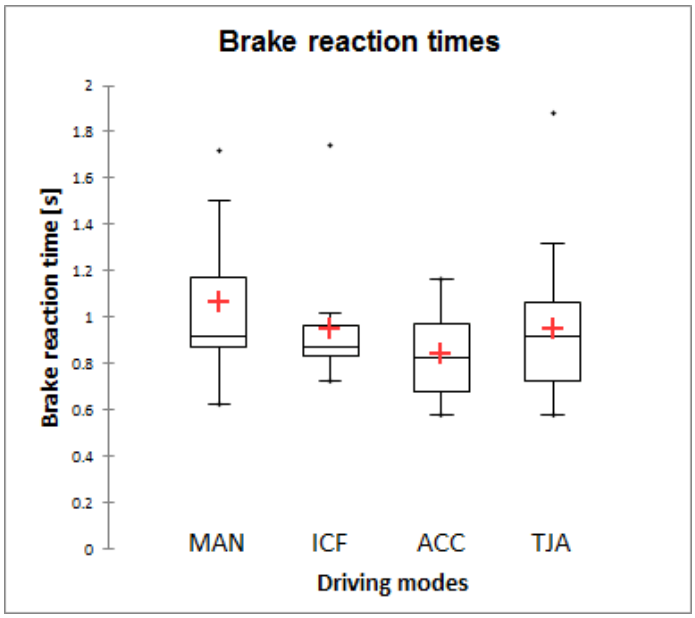

Figure 32 - Box plots of brake reaction times for all driving modes

Looking at the averages of the brake reaction times, a slight difference can be noted between the two manual modes and the two semi-automated modes. Nevertheless, computing the *Mann-Whitney U test* between these two groups, no significant differences were found: $U=502$, $p>0.05$. This test reported no significant difference neither between the manual mode and the ICF one: $U=95$, $p>0.05$. So, drivers reacted

in a very similar way even if they were driving with different automated systems (ACC and TJA) or different task (ICF).
Looking thoroughly the box plot, one outlier around value 1.8 can be noted in each driving mode, except for the ACC. However, it has to be clarified that these outliers are not referred to the same driver.

Table 8 and boxplots of *Figure 33* show again the brake reaction times of the participants but taking into account if they were used to or novices to the Adaptive Cruise Control system. It can be noted that the number of drivers used to ACC is always much higher compared to the novice ones.

Table 8 - Brake reaction times of novices and used to ACC drivers

Brake reaction times [s]			
Driving mode		Novices	Used to
MAN	Average	1.08 ± 0.24	1.05 ± 0.36
	N° drivers	4	11
ICF	Average	0.89 ± 0.05	0.97 ± 0.26
	N° drivers	4	12
ACC	Average	0.86 ± 0.15	0.84 ± 0.19
	N° drivers	5	15
TJA	Average	1.08 ± 0.35	0.86 ± 0.19
	N° drivers	8	13

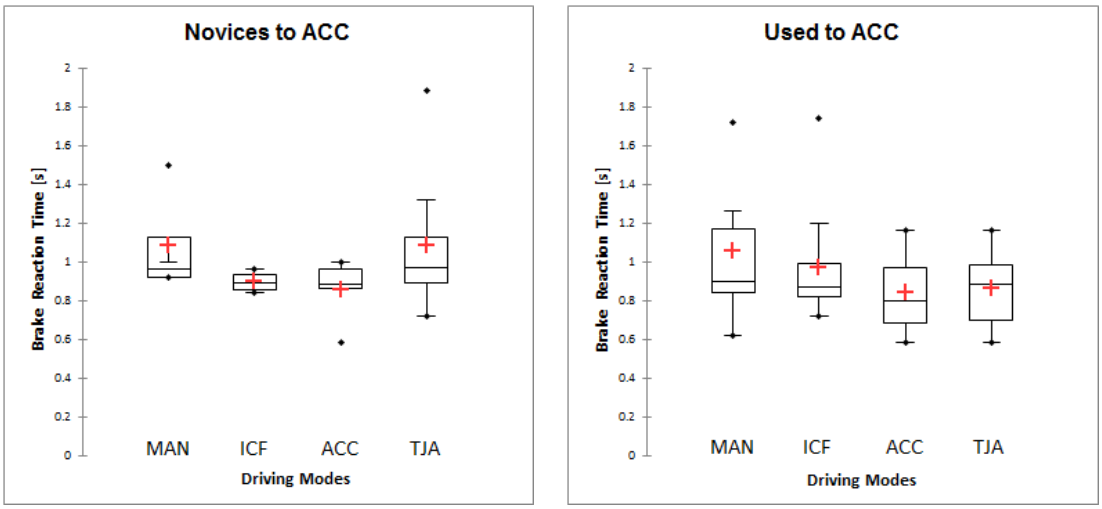

Figure 33 - Brake reaction times' box plots of drivers novice (left) and used to (right) ACC system

No relevant differences can be noted between these two groups of drivers. Unfortunately, statistical tests were not performed due to the low number of novice drivers available. The only slight difference in the averages of the brake reaction times in TJA mode: about 0.2 seconds between novices and used to. But the standard deviation is still high for the novices group.

Now the correlation of the brake reaction time with the time to intersection is taken into account. *Table 9* shows for each driving mode the averages and the standard deviations of the time to intersection, when TC starts, and the related brake reaction times.

Table 9 - Brake reaction times and times to intersections of drivers that braked in the scenario

Driving mode	Average brake reaction times [s]	Average distance ego vehicle from intersection [m]	Average speed ego vehicle [km/h]	Average time to intersection when TC enters [s]	N° drivers
MAN	1.05 ± 0.33	59.53 ± 20.31	67.73 ± 4.92	3.15 ± 1.00	15
ICF	0.95 ± 0.23	56.27 ± 17.65	68.02 ± 4.90	3.02 ± 1.05	16
ACC	0.84 ± 0.18	46.06 ± 0.12	69.99 ± 0.01	2.37 ± 0.01	20
TJA	0.94 ± 0.28	46.09 ± 0.13	69.99 ± 0.01	2.37 ± 0.01	21

Looking at the values in *Table 9* it is confirmed that in the two semi-automated modes TC entered always at the same time (2.37 sec to the intersection). Indeed, the speeds, the distances from the intersection and so to the time to intersection have the same averages and really small standard deviations. Moreover, it is important to note that the times to intersection of the semi-automated modes are smaller about 0.7 seconds than the averages of the manual and intentional car following ones. This factor determined different levels of criticality between the driving modes.

The following graphs show for each driving mode the relation between the brake reaction times and the time to intersection when TC enters.

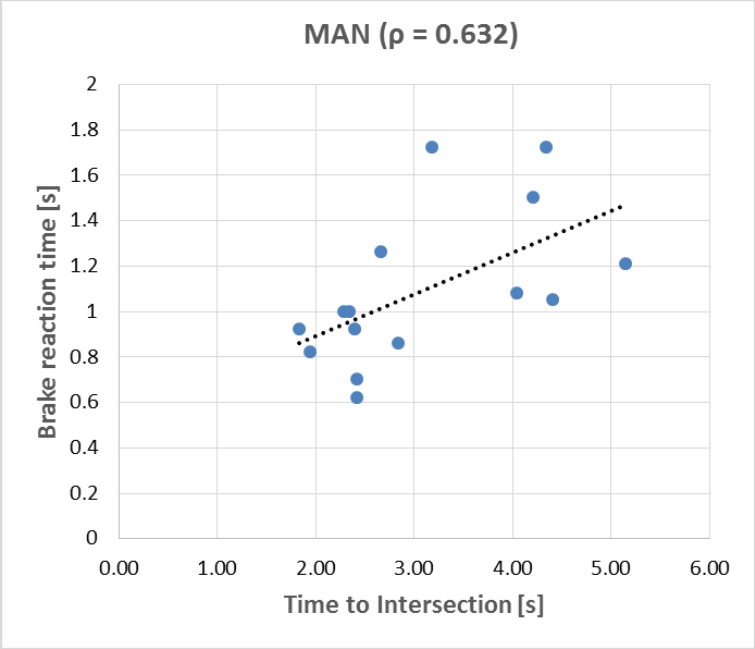

Figure 34 - Correlation between brake reaction time and time to intersection in manual mode

For MAN driving (*Figure 34*) a medium direct correlation between the two factors is present: The *Spearman correlation coefficient (ρ)* is equal to 0.632. Low times to intersection (around 2 s) represent that drivers are closer to that when TC started. On the contrary, higher values (around 4-5 s) represent those that are far away. It is possible to note that drivers closer to the intersection reacted in a faster way.

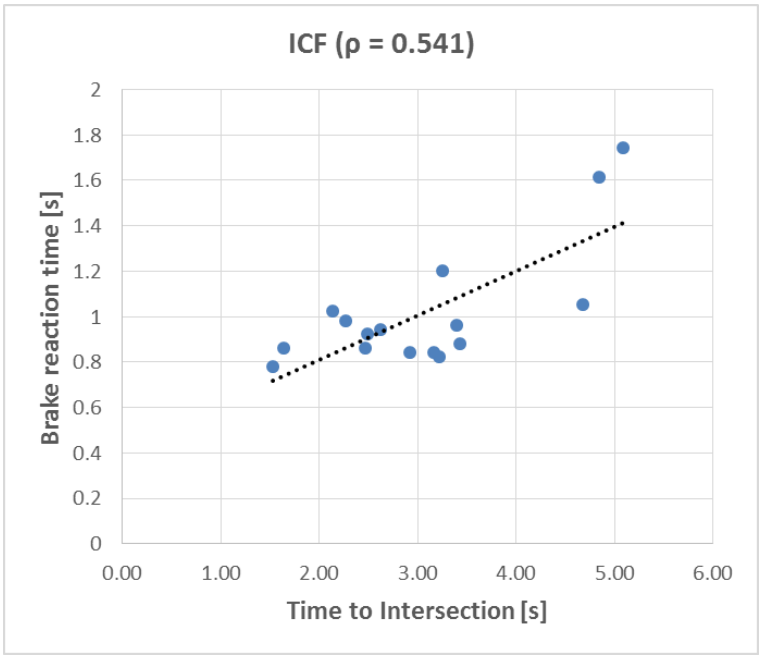

Figure 35 - Correlation between brake reaction time and time to intersection in ICF mode

For ICF mode (*Figure 35*) a medium linear correlation between the two factors is present: the *Spearman correlation coefficient (ρ)* is equal to 0.541. A similar behaviour to the MAN mode can be detected, even if it is possible to see that more drivers reacted in a faster way. Indeed, most of the brake reaction times are in the range of 0.8-1 s. This is confirmed looking at the averages of the MAN and ICF modes in *Table 9*.

Concerning the two semi-automated modes no correlations between the two factors can be computed due to the fact TC entered always at the same time. Indeed, in both graphs of *Figure 36*, the points form a vertical line.

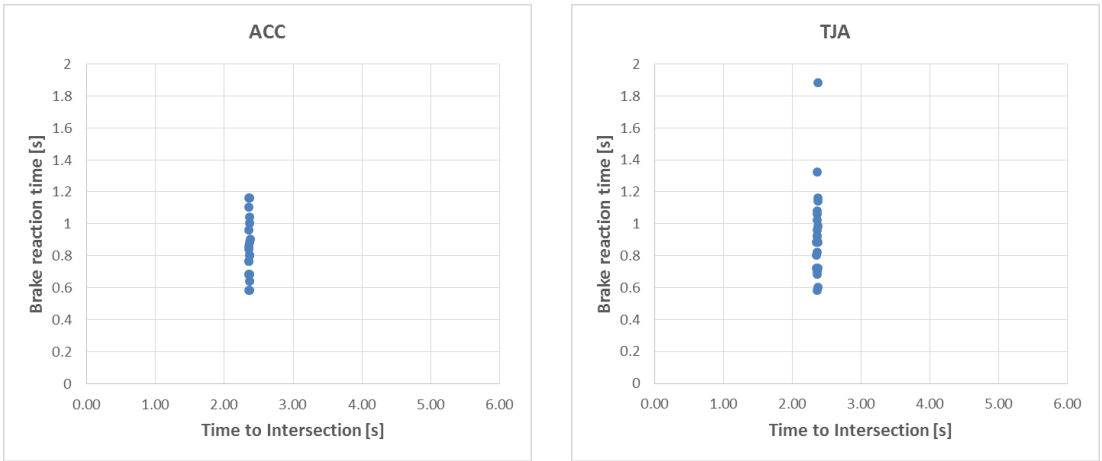

Figure 36 - Correlation between brake reaction time and time to intersection in ACC (left) and TJA (right) modes

In the last comparison for brake reaction time, we selected only participants that were driving in all four modes. In this way, results affected by considering different drivers in different modes are avoided. *Table 10* shows the brake reaction times for all drivers passing the intersection in each mode and using the brake.
For this analysis a *repeated measurement Anova* was performed. The result shows no significant differences between the four driving modes ($F(3,39)=2.36$, $p>0.05$).

Table 10 - Brake reaction times of drivers that performed the scenario braking in all four driving modes

Brake reaction times [s]				
Driver	MAN	ICF	ACC	TJA
1	0.92	0.86	0.84	1.02
6	1.72	0.98	0.76	1.16
7	1.00	0.82	1.10	1.14
8	1.05	1.74	0.64	0.70
10	0.70	0.95	0.68	0.82
13	0.92	0.84	1.00	0.80
14	1.05	0.82	0.68	0.68
19	1.08	0.78	0.84	0.96
20	1.26	1.02	1.04	0.94
27	0.88	0.95	0.76	0.60
28	0.86	1.20	1.16	0.88
29	0.90	0.72	0.68	0.58
32	1.50	0.92	0.58	1.88
69	1.05	0.88	0.58	0.98
Average	1.06 ± 0.26	0.96 ± 0.24	0.81 ± 0.19	0.94 ± 0.31

3.2.4 Drivers without reactions in semi-automated modes

This analysis is aimed to all the participants that in the two semi-automated modes didn't have any reaction to the TC's movement. Because of this decision, they would have crashed, if they would have been in a real situation. Indeed, as written in chapter **Error! Reference source not found.**, the TC was accelerating in unnatural way in the scenario in order to avoid crashes.
In *Table 11* and *Table 12*, participants' age and their experience with ACC system are reported. Furthermore, all data concerning the instant in which the systems of the ego vehicle started to brake are showed. In particular, it is reported the system brake reaction time referred to the TC's entry; the speed and the distance from the intersection when the system started to brake, and finally the time to intersection at that instant. It could be seen that they were really close to the intersection (8-10 m) when the system intervened.

Table 11 - Data of participants that had no actions in ACC mode

Driver	System brake reaction time [s]	Speed at braking point [km/h]	Distance ego vehicle from intersection at braking point [m]	Time to intersection at braking point [s]	Used to ACC	Age
1	1.74	74.16	8.74	0.42	no	27
13	1.66	74.14	10.63	0.52	no	29
11	1.70	74.14	9.79	0.48	no	49
16	1.62	74.17	10.87	0.53	yes	59
24	1.66	74.11	10.19	0.50	yes	56
25	1.70	74.18	9.45	0.46	yes	53
Average	1.68 ± 0.04	74.15 ± 0.02	9.94 ± 0.72	0.48 ± 0.03	/	45.5 ± 12.8

Table 12 - Data of participants that had no actions in TJA mode

Driver	System brake reaction time [s]	Speed at braking point [s]	Distance ego vehicle from intersection at braking point [m]	Time to intersection at braking point [s]	Used to ACC	Age
17	1.68	74.12	9.75	0.47	yes	52
20	1.66	74.13	10.16	0.49	yes	65
22	1.66	74.18	10.03	0.49	no	25
25	1.72	74.17	9.54	0.46	yes	53
26	1.72	74.23	9.55	0.46	yes	65
41	1.66	74.13	10.12	0.49	yes	27
Average	1.68 ± 0.03	74.16 ± 0.04	9.86 ± 0.26	0.48 ± 0.01	/	47.8 ± 16.3

Taking into account the two semi-automated modes together the average age of the participants that didn't react is 46.6 years, slightly below the overall average (49

years). Concerning the experience with the ACC system, 8 out of 12 were used to ACC, whilst 4 out of 12 were novices to the system.
Regarding the brake reaction time of the systems, it can be noticed that the average of ACC and TJA's response times is over the human reactions: *1.68 sec* against *~1 sec*.
It has to be stated that most of the cases (*10/12*), in which drivers had no reactions, happened when participants were exposed to the scenario for the third or the fourth time. It never happened in the first time passing the intersection.

3.2.5 Brake jerk

This analysis is focussed on how the participants braked, considering the values that the longitudinal jerk reached at the beginning of the brake.
Table 13 and the boxplot in *Figure 37* show the averages and the ranges of the brake jerks registered for each driving mode. The red crosses in the box plot represent the average values reported in the table. Unfortunately, three brake jerk values in the TJA mode were not reported. As can be seen, there are 18 in *Table 13* whilst 21 in *Table 7* in the column regarding the TJA mode. This is due to physically unfeasible values in the dataset. In these cases, values higher than 15 m/s^3 were found which is unreasonable high.

Since only the jerk during braking was taken into account, the results are shown in absolute values. For clarification, we call these values *brake jerk*.

Table 13 - Brake jerk in each driving mode

Brake jerk [m/s^3]				
Driving mode	MAN	ICF	ACC	TJA
Average	4.93 ± 3.66	4.70 ± 3.65	6.81 ± 3.88	6.98 ± 4.03
N° drivers	15	16	20	18

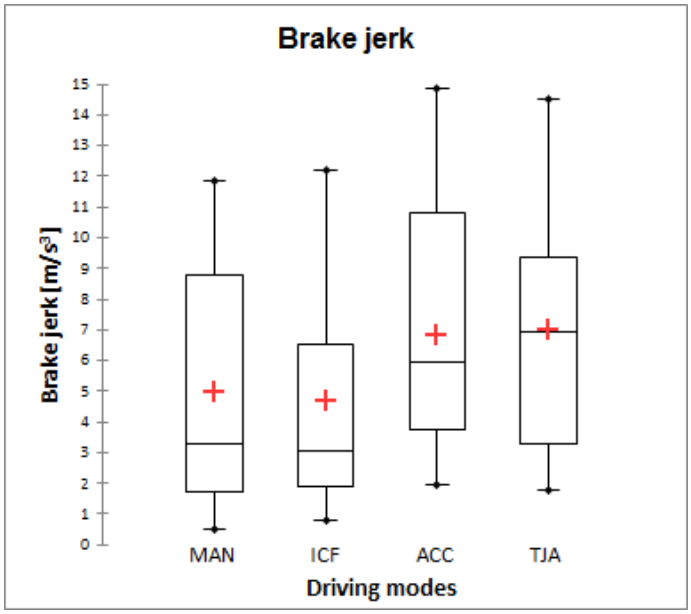

Figure 37 - Brake jerk box plots for all driving modes

The box plot shows that the brake jerk reaches different values between the manual modes and the semi-automated modes. In particular, the brake jerk is higher in the two semi-automated modes comparted to the manual modes, meaning that the drivers were braking in a fast way driving with ACC and TJA systems.
As proof of this statement a significant difference was found between the manual modes and the semi-automated modes computing the *Mann-Whitney U test*: *U=393; p=0.018*. Instead no significant difference is present between the MAN mode and ICF one: *U=116, p>0.05.*

In *Table 14* and in *Figure 38* the brake jerk is examined in relation to the driver's experience with ACC. Indeed, this feature proved to be very important in these kinds

of experiment, sometimes decisively changing the driver's behaviour. As a matter of fact, drivers used to this system know better its perks and limitations. This consciousness can affect their reliance to the system and so the braking severity.

Table 14 - Brake jerk of novices and used to ACC drivers

Brake jerk [m/s^3]			
Driving mode		Novices	Used to
MAN	Average	5.50 ± 3.81	4.73 ± 3.58
	N° drivers	4	11
ICF	Average	5.33 ± 2.86	4.49 ± 3.86
	N° drivers	4	12
ACC	Average	3.99 ± 1.76	7.76 ± 3.94
	N° drivers	5	15
TJA	Average	5.77 ± 4.20	7.94 ± 3.61
	N° drivers	8	10

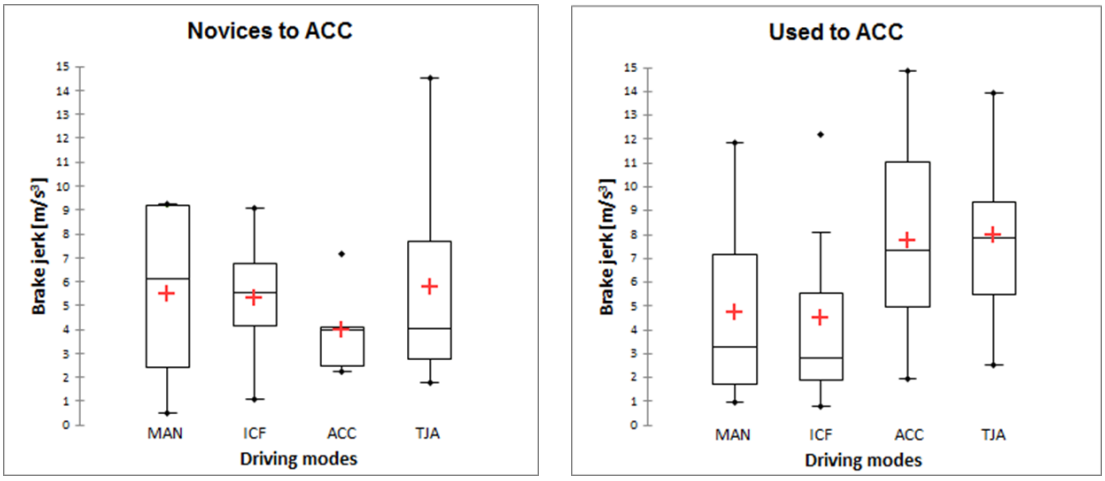

Figure 38 - Brake jerk box plots of drivers novice (left) and used to (right) ACC system

Looking at the two manual modes no relevant differences are present between these two types of drivers. Instead, concerning the two semi-automated modes, it can be noted that the participants that were used to the ACC system braked in a quicker way. This is more evident looking at the ACC driving mode: a mean value equal to 7.76 m/s^3 was detected for drivers used to the system, whilst a mean brake jerk equal to 3.99 m/s^3 for the novice ones.
Unfortunately, statistical tests were not applicable due to the low number of drivers in the different groups in regard to the modes.

The graphs in *Figure 39*, *Figure 40*, *Figure 41* and *Figure 42* show the correlation between the brake jerk and the riskiness of the scenario in each driving mode. This riskiness, is represented by the inverse of the time to intersection referred to the instant in which the driver starts to brake ($1/TTI_{brake}$) [23]. In the graphs this factor is reported on the x-axis as $1/\tau_B$. As a matter of fact, the riskiness ($1/\tau_B$) is high if the time to intersection is low.

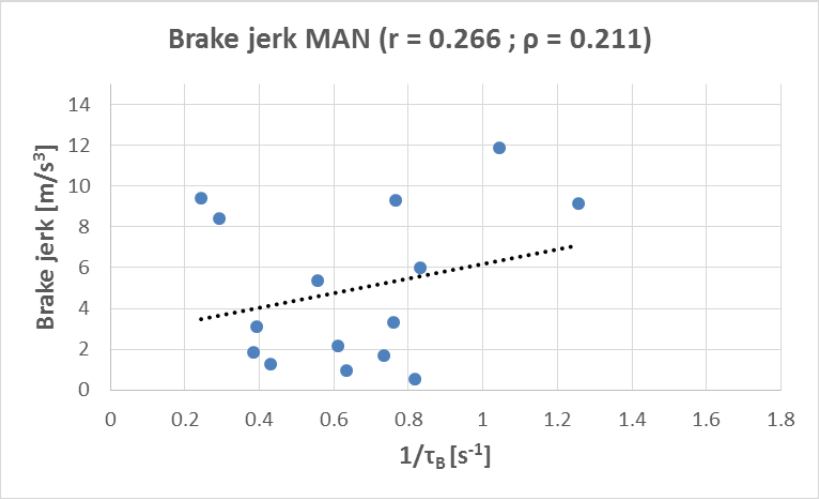

Figure 39 - Correlation between brake jerk and riskiness in manual mode

Concerning the MAN mode in *Figure 39*, a weak direct correlation is present between the two factors. In fact, as reported in the graph, the *Pearson coefficient (r)* is equal to 0.266, whilst the *Spearman coefficient (ρ)* is 0.211. Very different values of brake jerk can be seen for similar riskiness levels.

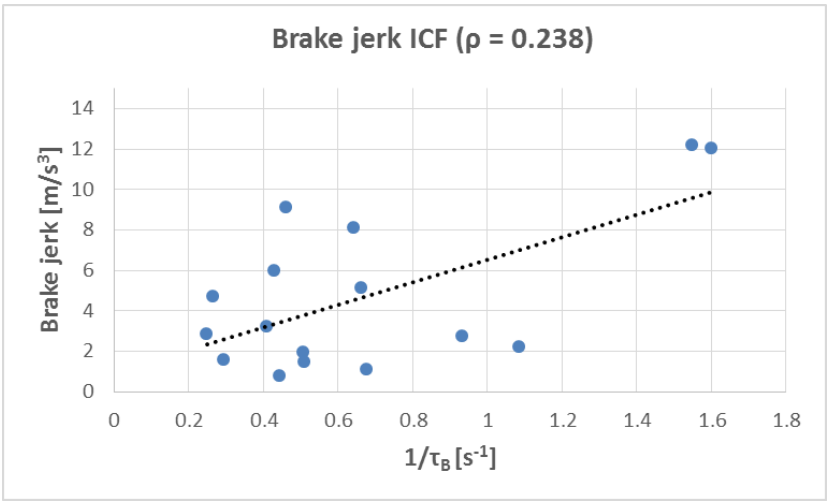

Figure 40 - Correlation between brake jerk and riskiness in ICF mode

Also in ICF mode (*Figure 40*) a weak direct correlations can be seen. Indeed, the *Spearman coefficient (ρ)* is equal to 0.238. The *Pearson coefficient (r)* was not computed due to the fact that the data in the ICF mode were not normally distributed (see 3.1.4). It has to be noted that in this mode two drivers started to brake really close to the intersection, reaching the highest values of brake jerk. These drivers are represented by the two points in the upper-right part of the graph. Concerning the other drives, different brake jerk values can be seen for similar riskiness levels, as was found out in the MAN mode.

Concerning the two semi-automated modes, an additional analysis was performed, due to the fact that they had exactly the same boundary conditions (when the TC was getting the intersection, the drivers were always at the same point of the street and at the same speed). So, driver's age and experience with ACC were taken into account for all those drivers that reached highest values of brake jerk.

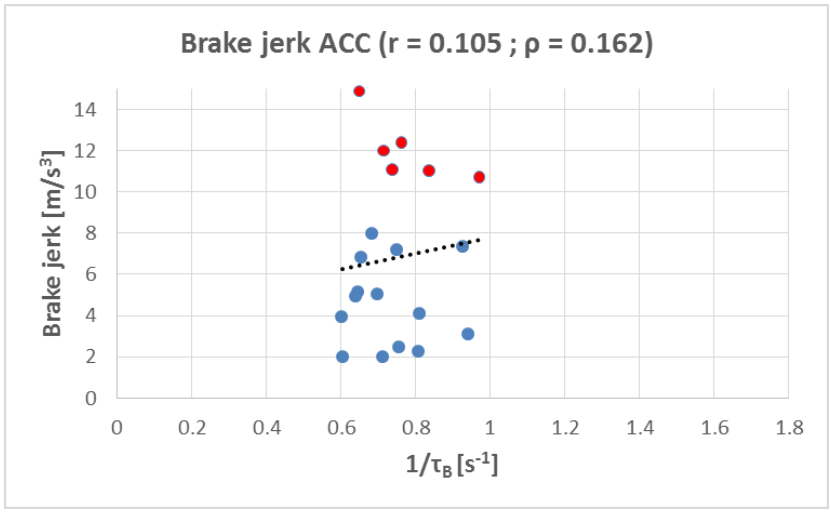

Figure 41 - Correlation between brake jerk and riskiness in ACC mode: red points correspond to brake jerk higher than 9 m/s^3, blue points correspond to brake jerk lower than 9 m/s^3

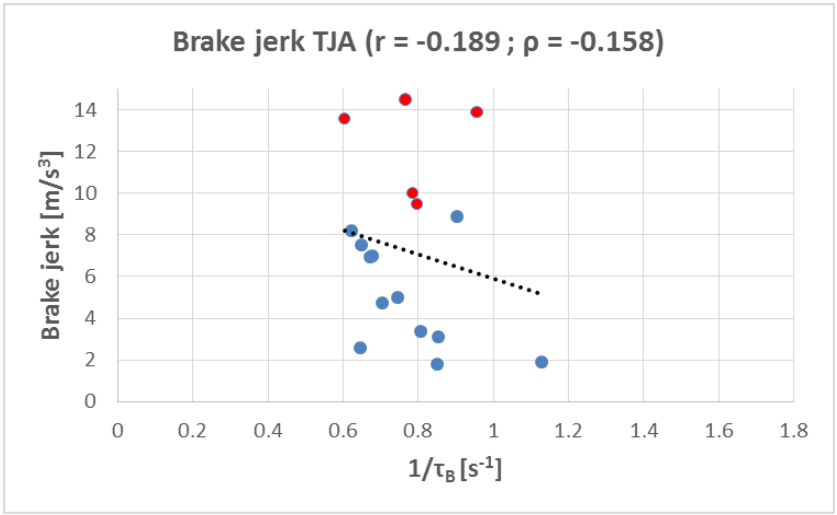

Figure 42 - Correlation between brake jerk and riskiness in TJA mode: red points correspond to brake jerk higher than 9 m/s^3, blue points correspond to brake jerk lower than 9 m/s^3

As can be seen in *Figure 41* and *Figure 42*, there are no correlations between the two factors: in ACC mode a *Spearman coefficient (ρ)* equal to *0.162* was found out, whilst a *ρ=-0.158* in TJA mode. On the other hand, it can be noted that all the points are located rather in a narrower risk zone (0.6 - 1.0 s^{-1}) compared to the two manual modes. This is due to the fact that in the semi-automated modes the boundary conditions of the scenario were always the same. Considering both graphs, a threshold value of 9 m/s^3 can be noted. It was found that participants below this threshold (points in blue) have a mean age of 46.3, while the participants above the threshold (points in red) have a mean age of 56.9. Moreover, all the participants that braked in a quicker way (points in red) are all used to the ACC system except one. Also in automated modes, drivers reached very different values of brake jerk even if they were subjected to similar levels of riskiness.

3.2.6 Maximum longitudinal deceleration

This analysis is focussed on how participants braked, taking into account the maximum values of the longitudinal deceleration of the ego vehicle.

Table 15 and the boxplot in *Figure 43* show the averages and the ranges of the longitudinal decelerations registered for each driving mode. As can be seen in the table, the number of participants took into account in the TJA mode (21) is the same of the brake reaction time's analysis. So, contrary to what happened in the jerk analysis, no participants were put out due to strange values.

Table 15 - Maximum longitudinal deceleration in each driving mode

Maximum longitudinal deceleration [m/s^2]				
Driving mode	MAN	ICF	ACC	TJA
Average	3.01 ± 2.54	3.47 ± 2.71	4.58 ± 2.61	5.54 ± 2.52
N° drivers	15	16	20	21

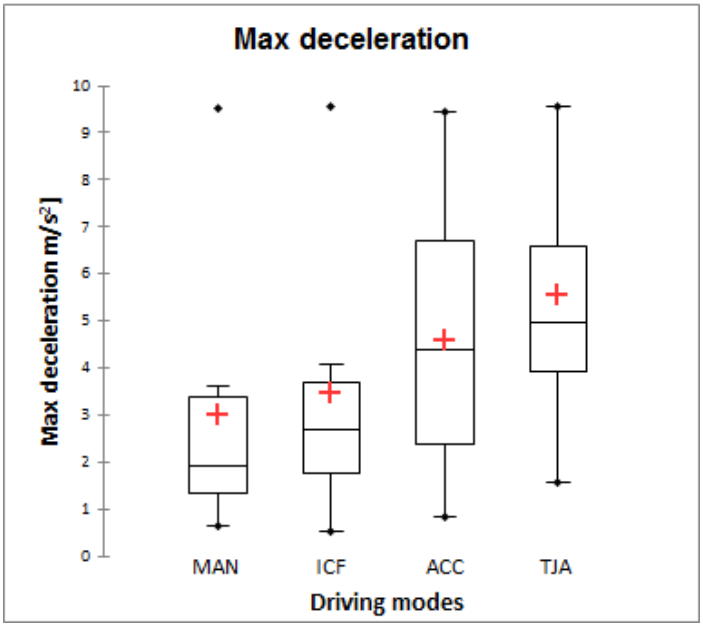

Figure 43 - Maximum longitudinal deceleration box plots of all driving modes

It can be noticed that in the semi-automated modes the participants reached on average higher values of maximum deceleration, in particular in the TJA mode. This statement was confirmed again by the *Mann-Whitney U test*. Indeed, significant difference was found between the manual modes and the semi-automated modes: $U=356$, $p=0.001$. Instead, comparing the two manual modes with each other (MAN – ICF) no significant difference was noticed: $U=117$, $p>0.05$. As previously mentioned, no unnatural values are present. However, it can be noted that in each driving mode there are some really high values of maximum deceleration, almost equal to 1g (9.81m/s^2). It was verified and confirmed that these values through the different driving modes are not referred to same driver. Moreover, it can be noted that in semi-automated modes the values cover a much wider range of maximum decelerations compared to the two manual modes.

In *Table 16* and in *Figure 44* the maximum longitudinal deceleration is again analysed, but taking into account the experience of the participants with the ACC system. As mentioned in 0, this peculiarity turned out to be fundamental in drivers' behaviour analyses. The number of novice and used to drivers is the same of the brake reaction time analysis in *Table 8* but differs from the brake jerk analysis in *Table 14*, concerning the TJA driving mode.

Table 16 - Maximum longitudinal deceleration data of novices and used to ACC drivers

Maximum longitudinal deceleration [m/s^2]			
Driving mode		Novices	Used to
MAN	Average	1.74 ± 0.84	3.47 ± 2.78
	N° drivers	4	11
ICF	Average	2.58 ± 0.50	3.76 ± 3.06
	N° drivers	4	12
ACC	Average	3.84 ± 2.77	4.83 ± 2.50
	N° drivers	5	15
TJA	Average	4.37 ± 2.09	6.26 ± 2.50
	N° drivers	8	13

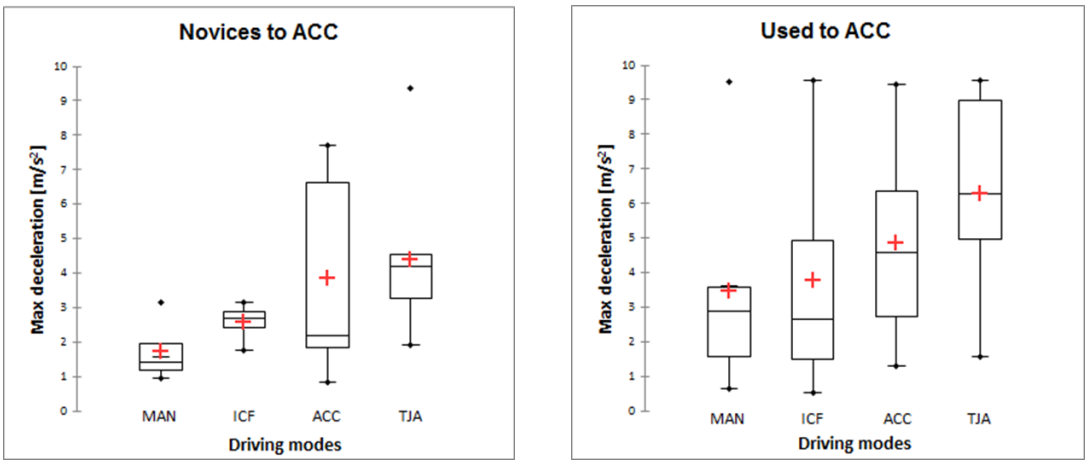

Figure 44 - Max deceleration box plots of drivers novice (left) and used to (right) ACC system

Looking at the averages and at the ranges in the boxplot, it can be stated that in all the driving modes the participants used to the ACC system reached higher values of maximum deceleration compared to the novice to ACC drivers. This trend is particularly evident looking at TJA. Unfortunately, statistical tests couldn't be done due to the low number of novice drivers available respect to the used to. Moreover, it is possible to see same averages' trend between the two groups of drivers. The average maximum deceleration increases going through MAN to TJA mode.

The following graphs, in *Figure 45*, *Figure 46*, *Figure 47* and *Figure 48*, show the correlation between the maximum longitudinal deceleration and the riskiness of the scenario in each driving mode. As written before, the riskiness, is represented by the inverse of the time to intersection referred to the braking moment (1/ TTI_{brake}) [23]. In the graphs this factor is reported on the x-axis as $1/\tau_B$. The riskiness ($1/\tau_B$) is high if the time to intersection is low.

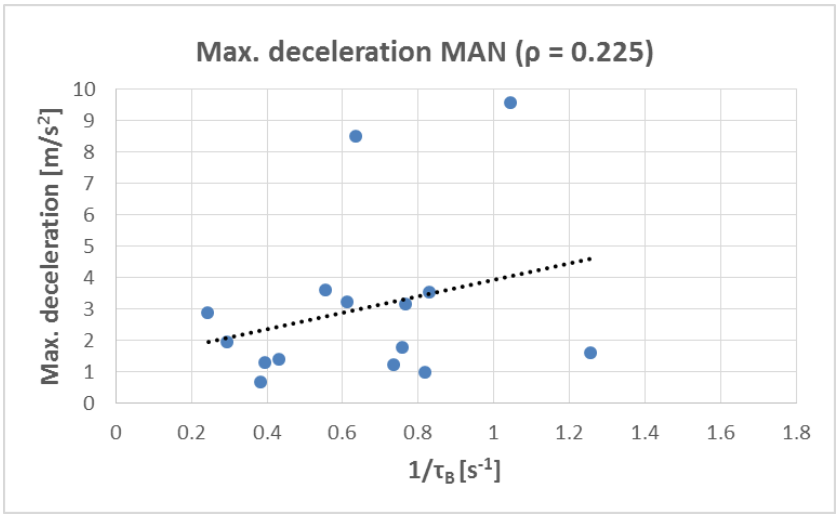

Figure 45 - Correlation between maximum longitudinal deceleration and riskiness in MAN mode

Concerning the MAN mode's data in *Figure 45* a weak direct correlation is present between the two factors. As displayed in the graph, the *Spearman coefficient (ρ)* is equal to 0.225. Moreover, it can be noted that all the values, except two outliers, are in the range 0.5 – 4 m/s^2 of maximum decelerations. The two outliers in the upper part of the graph represent drivers that braked in a really strong way.

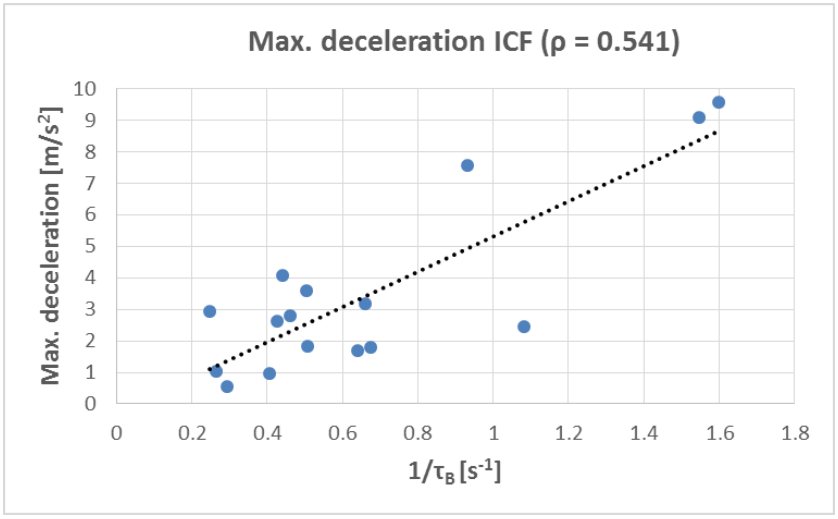

Figure 46 - Correlation between maximum longitudinal deceleration and riskiness in ICF mode

The ICF mode, as can be seen in *Figure 46*, presents a moderate direct correlation between the two factors. As displayed in the graph, the *Spearman correlation coefficient (ρ)* is equal to *0.541*. Furthermore, it has to be stated that, as in MAN mode, there are two really high values of maximum deceleration (around 1g). These values correspond to the highest values of riskiness. However, most of the drivers braked reaching maximum decelerations in the range 0.5 – 4 m/s^2.

Concerning the two semi-automated modes, an additional analysis was performed, as was done in the brake jerk analysis (0). It was reasonable to carry out this analysis due to the fact that they had exactly the same boundary conditions (when the TC was getting the intersection, the drivers were always at the same point of the street and at the same speed). So, driver's age and experience with ACC were taken into account for all those drivers that reached highest values of maximum deceleration.

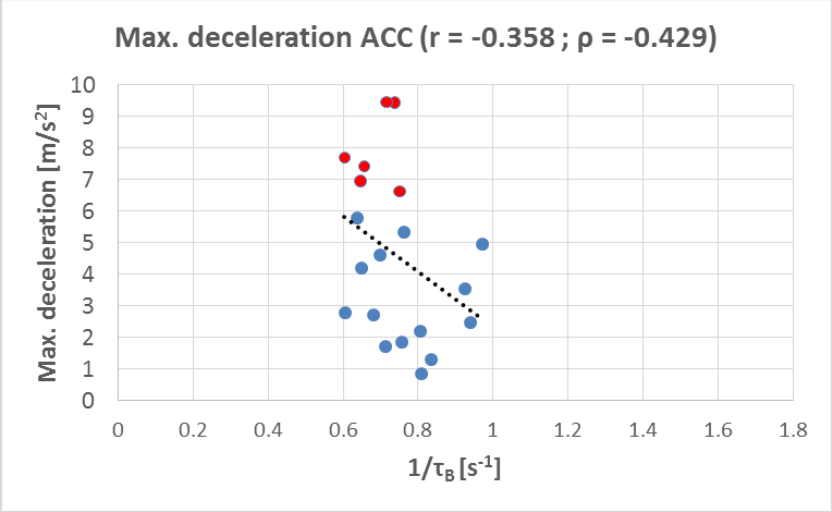

Figure 47 - Correlation between maximum longitudinal deceleration and riskiness in ACC mode: red points correspond to maximum deceleration higher than 6 m/s^2, blue points correspond to maximum deceleration lower than 6 m/s^2

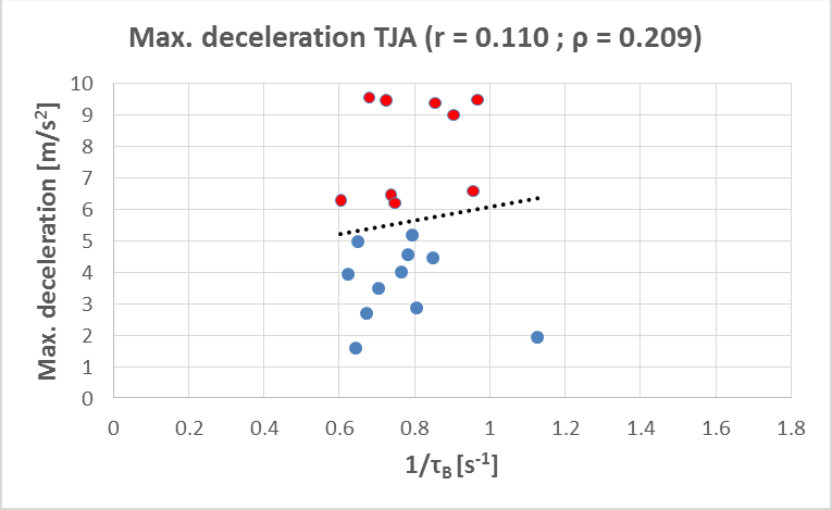

Figure 48 - Correlation between maximum longitudinal deceleration and riskiness in TJA mode: red points correspond to maximum deceleration higher than 6 m/s^2, blue points correspond to maximum deceleration lower than 6 m/s^2

The two graphs in *Figure 47* and *Figure 48* show two different types of trend. It can be seen a weak inverse correlation for ACC mode, represented by a *Spearman coefficient (ρ)* equal to -0.429; whilst a slight direct trend in the TJA mode (*ρ=0.209*). Besides these values, it has to be stated that the riskiness values are in a so narrow range (0.6 – 1 s^{-1}), that no significant correlations can be detected.
Concerning the additional analysis for the two semi-automated modes, a threshold value equal to 6 m/s^2 was defined in order to detect which type of driver were braking in a harder (max dec. > 6 m/s^2) or in a softer way (max dec. < 6 m/s^2). It came up that the participants below this threshold (points in blue) have a mean age of 44.7 years, while the participants above the threshold (points in red) have a mean age of 56.6 years. Furthermore, most of the drivers that braked in a harder way (points in red) are used to the ACC system (12/15). This result is in accordance with what found out in the brake jerk analysis (0), in which drivers used to ACC reached even in this case the highest values.

3.2.7 Mean brake pedal force

In this section the mean force with which participants pressed the brake pedal is taken into account for each driving mode.
The mean force applied in the brake pedal by the driver is closely linked to the maximum deceleration reached by the vehicle. While the maximum deceleration is referred to a single time instant which identifies the braking hardness, the mean brake pedal force gives a further inside of the braking process. It describes, indeed, braking during its whole time of application, from the first to the final instant in which the driver pressed the brake pedal. This allows to describe the driver's behaviour from a different and more general point of view.

Table 17 and the boxplot in *Figure 49* show the averages and the ranges of this force.

Table 17 - Mean brake pedal force in each driving mode

Mean brake pedal force[N]				
Driving mode	MAN	ICF	ACC	TJA
Average	49.43 ± 33.19	62.20 ± 57.41	66.17 ± 32.75	77.67 ± 38.84
N° drivers	15	16	20	21

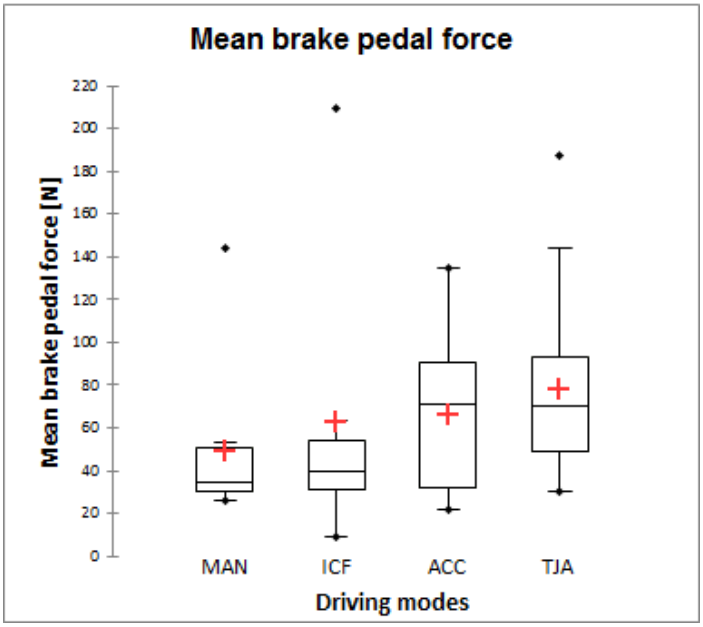

Figure 49 - Mean brake pedal force box plots of all driving modes

It is possible to note that, in the two semi-automated modes, the values representing the mean brake pedal forces are higher compared to the two other modes, in particular compared to the manual mode.
Even in this case, the *Mann-Whitney U test* confirmed that there is significant difference between the manual modes and the semi-automated modes (*U=392*, *p=0.006*), in particular with respect to the TJA one (MAN – TJA: *U=68*, *p=0.004*). Once again, no significant difference was found between the manual mode and ICF one: *U=108*, *p>0.05*.
This means that, on average, drivers during ACC and TJA modes pressed the brake pedal generally with a higher force comparing to the same critical scenario in MAN and ICF modes.

In *Table 18* and in *Figure 50*, the mean brake pedal force is again analysed, but taking into account the experience of the participants with the ACC system.

Table 18 - Mean brake pedal force data of novices and used to ACC drivers

Mean brake pedal force [N]			
Driving mode		Novices	Used to
MAN	Average	34.96 ± 10.29	54.69 ± 36.87
	N° drivers	4	11
ICF	Average	40.16 ± 6.82	69.54 ± 64.52
	N° drivers	4	12
ACC	Average	57.75 ± 36.92	68.98 ± 30.73
	N° drivers	5	15
TJA	Average	56.84 ± 24.79	90.49 ± 40.33
	N° drivers	8	13

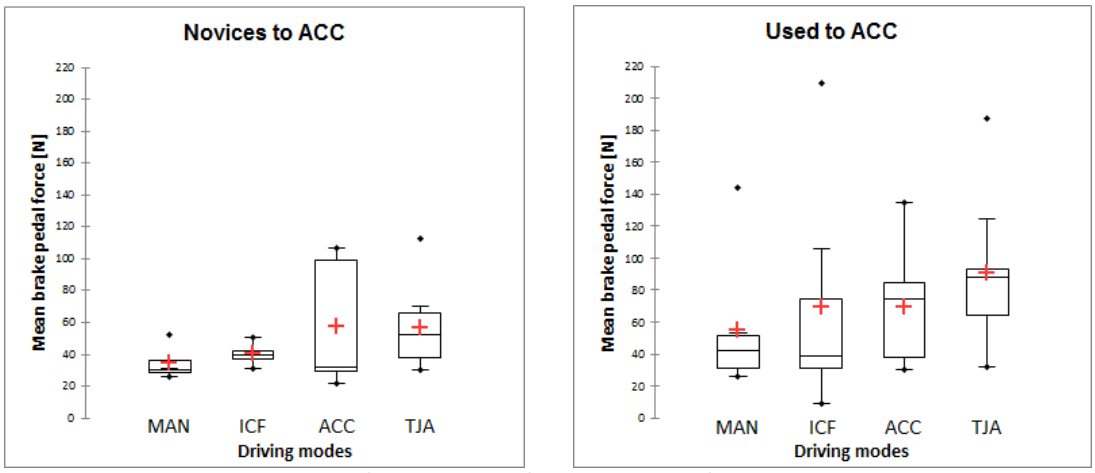

Figure 50 - Mean brake pedal force box plots of drivers novice (left) and used to (right) ACC system

Looking at the averages and at the ranges in the boxplots, it can be stated that in all driving modes the participants used to the ACC system pushed the brake pedal with higher force on average compared to the novice drivers. This trend is particularly evident looking at the TJA mode, but it is not for the ACC boxplots.
Unfortunately, statistical tests couldn't be done due to the low number of novice drivers available respect to the used to.

3.2.8 Gaze behaviour

This section is dedicated to the description of the drivers' gaze behaviour during the critical scenario under study.

Before going into the detail of such analysis, a general overview regarding the gaze behaviour is reported in *Figure 51*. It represents where the overall participants directed their gaze while performing the scenario in different driving modes. A time window of eleven seconds was considered: ten seconds before the movement of the TC and one second after.

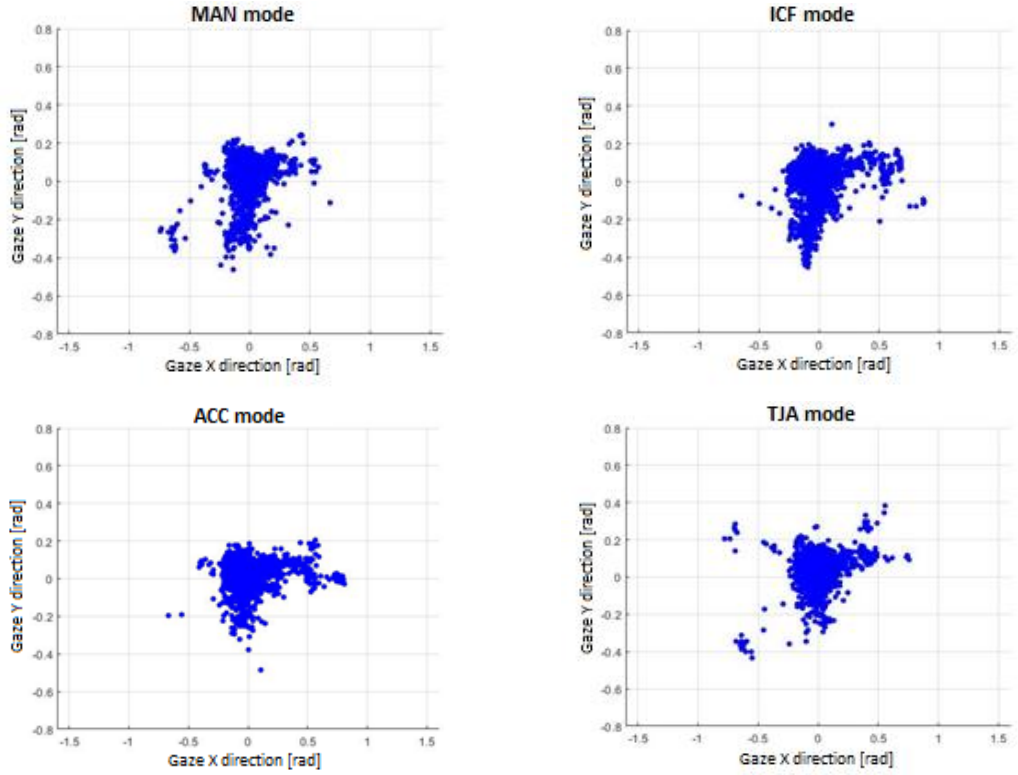

Figure 51 - Drivers' gaze representation in the four driving modes 10 s before the TC entry and 1 s after

The graphs of *Figure 51* are in a radiant scale that goes from -1.57 rad (-90°) to 1.57 rad (+90°) for what concern the horizontal axis, whilst -0.8 / +0.8 rad (-45°/+45°) for the vertical one. Each point in the graphs represents a single glance in a single time step. No qualitative differences between the four driving modes can be identified. The participants looked mainly straight, as can be seen by the high density of points around the origin (0;0). Also based on points' density, it can be seen that they looked more to the right (positive values in x direction) than to the left (negative values in x direction): this is because the TC approached the intersection from a perpendicular road coming from the right side of the drivers' point of view.

Two in-depth analyses regarding the participants gaze data are now presented.

The first gaze analysis shows how much the participants looked to the right before the intersection. As described in 3.1.3, a glance was considered directed to the "right" if it was focused on an angle (on the right side of the lane) greater than the one defined by the position of the TC and the ego vehicle's travelling direction. The time window considered is the same described before.

Taking into account the quality of the gaze's data (3.1.3), it was possible to use for this analysis 19 drivers in manual mode, 21 drivers in ICF mode, 27 drivers in ACC mode and 25 drivers in TJA mode.
The graphs in *Figure 52* show the result obtained, they take into account all the participants, depending on the driving mode considered. Each graph represents an average, between all the participants considered, of how much time they spent looking to the right in one second time spans. As explained in the methods section 3.1.3, a dynamic threshold referred to the TC position was used in order to define when a glance is towards the TC.

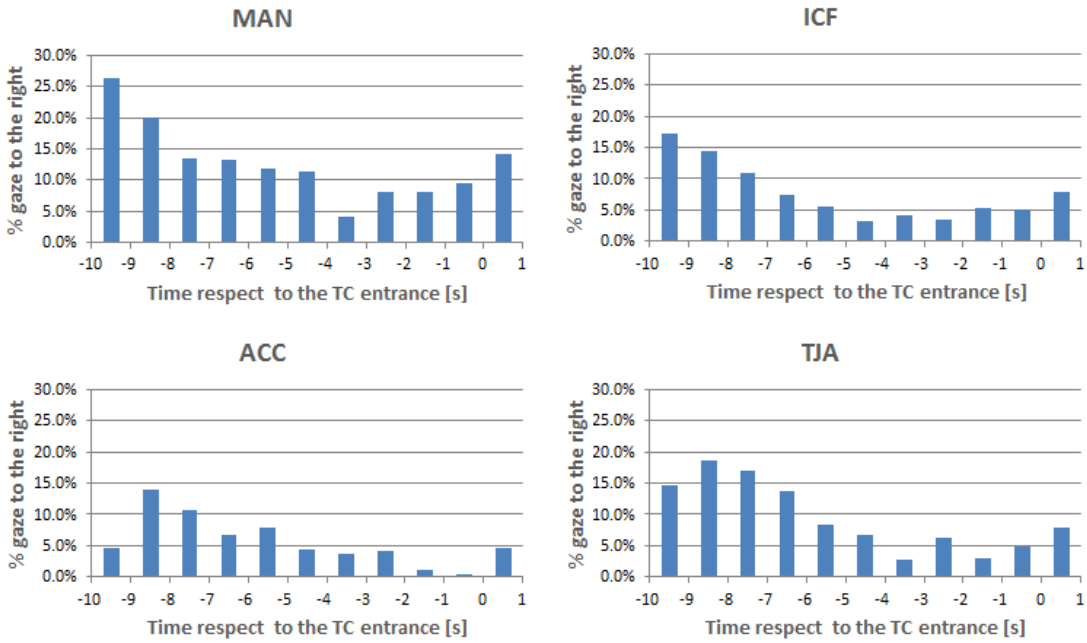

Figure 52 – Gaze percentage values to the right direction 10 s before the TC entry and 1 s after for all driving modes

Looking at the histograms in *Figure 52*, the x-axes represent the time slots. The reference point (zero on scale) is the starting of the movement of the TC. On the y-axes the percentage of time spent on looking to the right (towards the TC) is displayed. The values are averages over the drivers in each mode. It is noted that the trend between both the two manual modes and the TJA mode seems to be similar: higher values at the beginning (9-10 seconds before the TC movement), lower in the middle and then a small increase again close to the intersection. These results help to describe and explain the drivers' gaze behaviour regarding this critical scenario: while the ego vehicle is still far away from the intersection, drivers tended to look to the right more in order to check the situation and looking for possible threats; subsequently, few seconds before the TC entrance, they seemed to be focused mainly on the road; from 2s before the TC entrance forward, drivers focused their glance on the right again due to the TC entrance.
Similar percentage values are present in the ICF and TJA modes graphs, while higher values can be seen in the MAN mode. Concerning the ACC mode, a trend similar to the others could be seen if the first band is not considered. However, in ACC lower overall values are shown compared to the other driving modes.

The second analysis regarding the gaze of the participants shows the instant in which drivers perceived the presence of the TC. As explained in the methods section 3.1.3, for this analysis two dynamic thresholds referred to the TC's position and dimensions were used: the angles between the front and the rear bumper of the TC. As for the previous gaze analysis, a time window of eleven seconds was taken into account: ten seconds before the TC entrance in the intersection zone and one second after.

In *Figure 53* four examples of gaze behaviour of different participants are reported (one per driving mode).

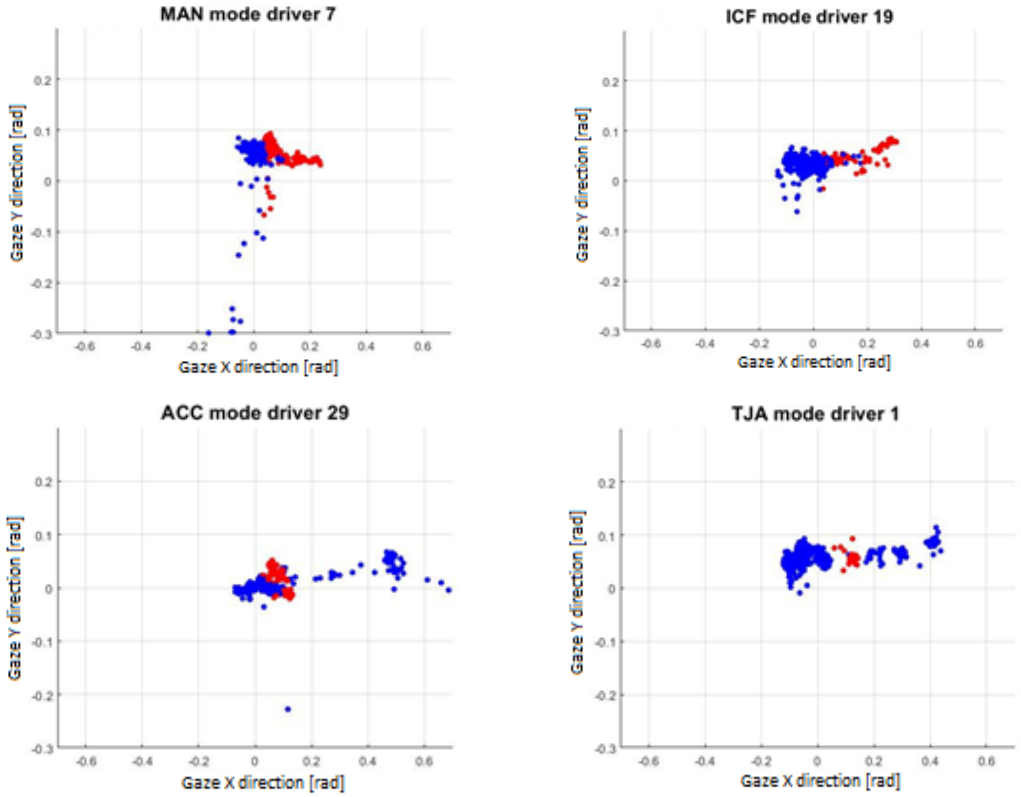

Figure 53 - Four examples of eye tracking data 10 s before the TC entry and 1 s after

As stated before, each point in the graphs represents a single glance in a single time step. The red points correspond to the glances facing inside the zone delimited by the two dynamic thresholds, so facing to the TC. The blue points correspond to all the other directions. The axes of the graphs refer to radiant values. Taking into account the x direction, the 0 is referred to the intersection point (looking straight). Positive values refer to looks toward the right, whilst negative to the left. The red points, indeed, are in the range of 0-0.3 rad. With these graphs a visual confirmation of the functionality of dynamic thresholds was obtained, but no time relations could be deducted. Indeed, no time axis is present in the charts.

On the contrary, the graph in *Figure 54* takes into account the time, satisfying the goal of the second gaze analysis. As a matter of fact, it shows for each driving mode how many drivers (in percentage values) looked towards the TC in respect to the time instant considered (related to the TC entrance). As described in 3.1.3, the TC was considered as perceived by a driver when the gaze remained focused on the TC direction for at least 0,25s.

Obviously, all the curves reached the maximum value (100% of drivers that noted the TC) 1s after the entrance of the TC. This is because, from that time on, the TC is exactly in front of them.

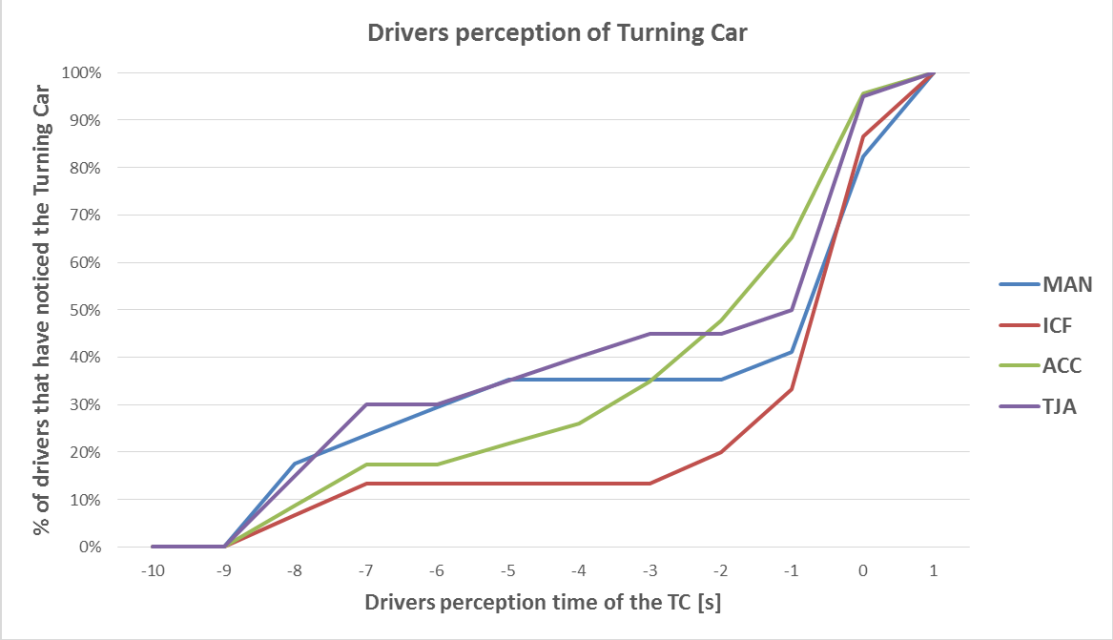

Figure 54 - % of drivers that perceived the TC at each time instant considered (related to the TC entrance)

Looking at the graph, it can be noted that the most of the participants driving in ICF mode (red line) perceived the TC later compared to the other driving modes. As can be seen, three seconds before the entrance of the TC only the 13% of the participant driving in ICF mode perceived its presence. On the contrary, looking at the other driving modes' lines at the same time the TC's presence was already perceived by the 35-45% of the participants.

In *Table 19* the average times of TC perception are reported. They are always referred to the time zero (the TC entrance in the intersection zone). The number of drivers reported is different compared to the first gaze analysis (here only glances that lasted at least 0.25s were considered. As a consequence, drivers who didn't look at the TC for such a long time were not considered (see 3.1.3)).

Table 19 - Drivers' perception time of the TC in each driving mode

Driving mode	MAN	ICF	ACC	TJA
Average	-1.91 ± 3.56	-0.63 ± 2.57	-1.71 ± 2.81	-2.30 ± 3.38
N° drivers	17	15	23	20

The average perception times seem similar for all the driving modes, except for the ICF mode: in such situation drivers noted the TC later compared to the other driving modes, thus they stayed more focused on the road, perceiving the TC only in proximity of the intersection.

3.2.9 Brake reaction time vs perception time

This analysis is focused on the relationship between drivers' brake reaction time and perception time of the TC. It aims to assess if drivers started braking before or later depending on the moment in which they noted the presence of the TC. As before, each driving mode is examined separately.
The number of participants in this analysis doesn't correspond to the one in the brake reaction times analysis (0) due to the fact that the gaze data were not always available or reliable. Moreover, the number of drivers considered now is different from the ones in *Table 19* because not all the drivers for which the perception time was collected, braked. As a consequence, 15 drivers were considered in MAN mode, 15 in ICF, 20 in ACC and 20 in TJA.

Below, the graphs related to each driving mode are shown. Drivers' perception times of TC are reported on the x axis, while the brake reaction times can be seen on the y axis. Both the times are referred to the time zero: the TC's entry.
It's important to note that, in each of the following graphs, the dispersion of the points along the x axis is obviously dependent on the results described by *Figure 54*.

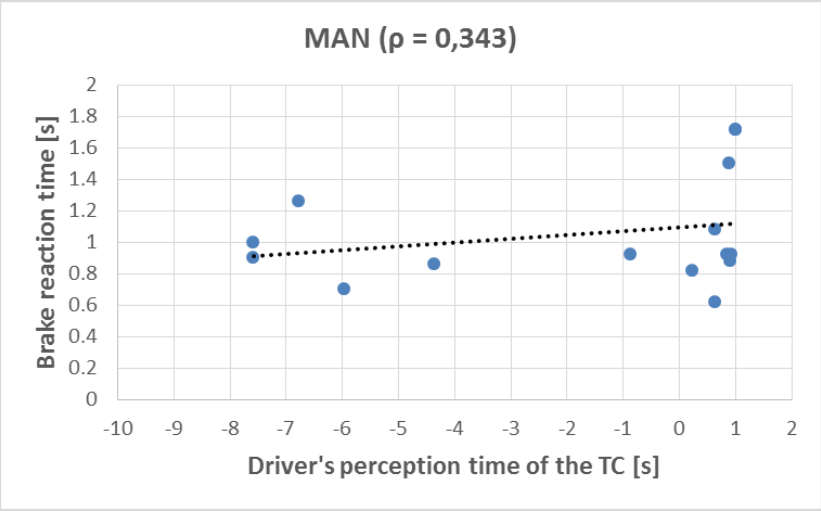

Figure 55 - Correlation between brake reaction time and driver's perception time of the TC in manual mode

In MAN mode (*Figure 55*) a weak direct correlation between the two factors can be noticed. Indeed, the *Spearman* coefficient is equal to *0.343*. It seems that drivers' braking behaviour was slightly affected whether they noticed the TC in advance or not: driver reacted a little faster when the TC was perceived before approaching the intersection zone.

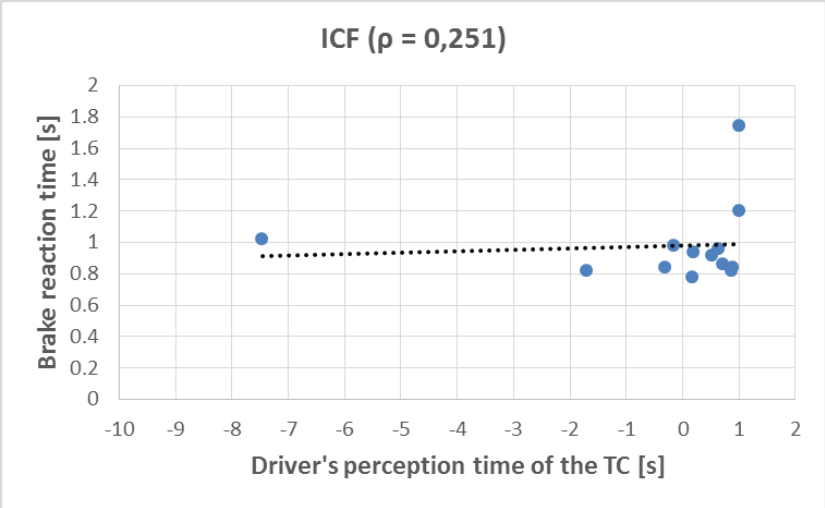

Figure 56 - Correlation between brake reaction time and driver's perception time of the TC in ICF mode

In ICF mode (*Figure 56*), there is a slight direct trend between the two factors, even if lower compared to MAN mode. Most of the points are located in the right part of the graph, due to the fact that the participants perceived TC later, close to the intersection. Removing the outlier in the left part of the graph, a medium positive correlation is found with a *Spearman* coefficient of $\rho = 0.458$.

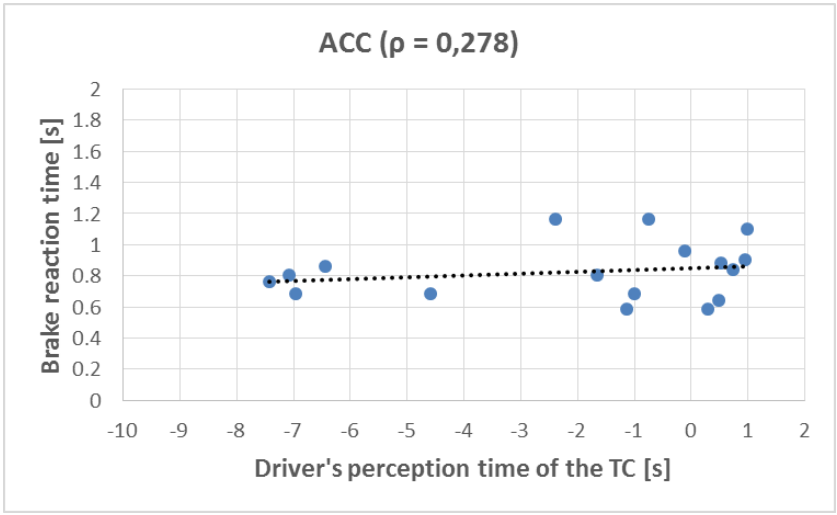

Figure 57 - Correlation between brake reaction time and driver's perception time of the TC in ACC mode

Regarding the ACC mode (*Figure 57*), a weak direct trend was found between the two factors. The points are spread through all the length of the perception time axis (x axis) but in a narrow range of brake reaction times (y axis). This means that the brake reaction times weren't so much affected by the fact that drivers noted the TC in advance or later.

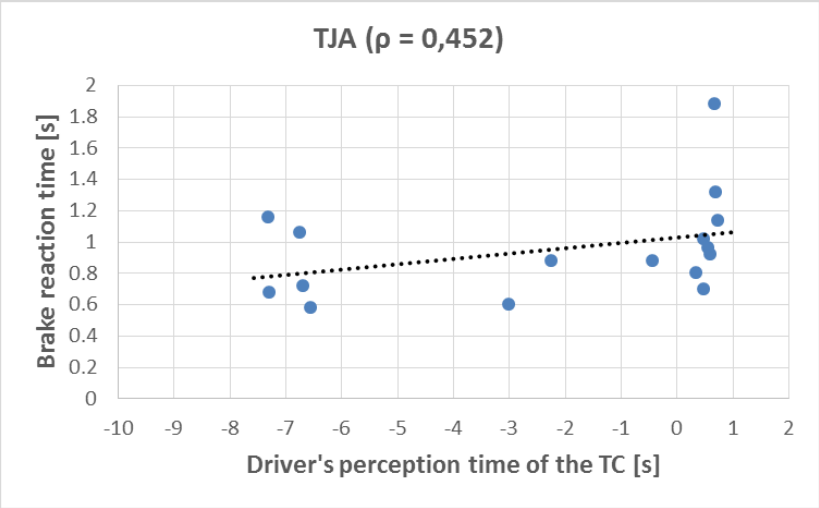

Figure 58 - Correlation between brake reaction time and driver's perception time of the TC in TJA mode

A medium direct correlation was found for the TJA mode (*Figure 58*): *Spearman* correlation coefficient is equal to *0.452*. The points are spread as in the ACC mode for what concern the x axis, but in a wider range of brake reaction times: in this driving mode drivers seem to have reacted slightly faster if they noticed the TC in advance.

In order to complete the overview of the relationship between brake reaction time and perception time, graphs of *Figure 36* were plotted again in *Figure 59*, but this time taking into account if drivers perceived TC before (red crosses) or after (blue circles) its movement. This is done in order to understand if, concerning the semi-automated modes (in which the TTI at TC entrance was the same for all the participants), drivers reacted with brake reaction times which depend on whether they noted the TC or not.

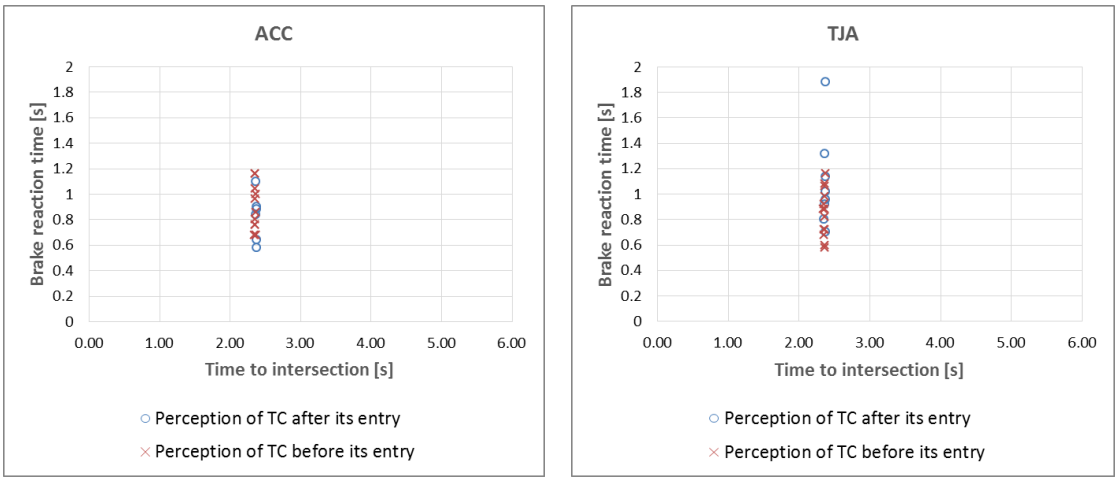

Figure 59 - Correlation between brake reaction time and time to intersection in ACC (left) and TJA (right) mode taking into account if drivers perceived the TC before or after its entry

As can be observed, no defined clusters are present: regarding ACC and TJA mode, there isn't a clear difference of braking behaviour between drivers who perceived the TC before or after its entrance. This confirmed in this way the weak correlations that resulted from the previous graphs (*Figure 57* and *Figure 58*).

4 Modelling driver's behaviour

The second main goal of the overall project was the creation of a model based on the analyses assessed and studied in chapter 3. The aim of this modelling is to describe and to simulate the behaviour of a driver in the critical intersection approach previously introduced.

The prediction of human behaviour plays a fundamental role in order to design and improve safety systems on vehicles, this can be achieved by means of driver models. The importance of having valid models is derived from the fact that they can be used in order to be implemented in computer simulations to assess the potential of future active safety systems. In general, computer simulations allow to collect a large quantity of data in a very fast and repeatable way. Moreover, they allow to study the performances of systems and to make reliable assessments much more safely in respect to real measurements. Therefore, simulations represent an important tool for traffic safety research. It has to be noted that all the previous considerations regarding the benefits of making simulations are true, only if the quantitative models in the simulation are well-established and reliable. This can be accomplished by building models from real driving data or in our case from a driver simulator study.

4.1 Method

This section describes in detail the method applied in order to build a driver's behaviour model for the scenario under study. Such model was designed based on the results obtained in the analysis.

4.1.1 Description of the model's typology

The creation of a well-defined model describing driver behaviour can be performed, as took place in this project, relying on a previous deep analysis of data obtained by real drivers' performances. Based on the experiment, it can be possible to extrapolate meaningful considerations in order to define a general behaviour of the drivers.

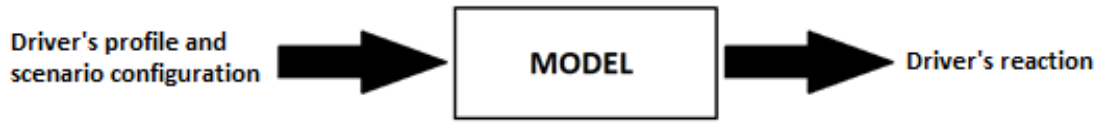

Figure 60 - General function of the present driver behaviour model

The main reaction in our scenario is the braking behaviour of the driver when the turning vehicle enters the intersection. This is made in accordance with the previous analyses, in which it has been found that the most important reaction that a driver performs in such scenario is the braking; the analyses confirm that there is no presence of an evident steering reaction during the critical maneuver. Moreover, the steering corrections analysed didn't impact in a meaningful way the general behaviour of the driver, for this reason not even they were included in the model. In this way the model has been built taking into account the data collected during the analyses performed on the reactions of the participants involved in the experiment at the VTI driving simulator.

The main target of this modelling activity is to build an instrument capable of recreating and generalizing the braking behaviour of a driver in such a critical scenario, without only regarding the participants' reactions analysed during the experiment.
The model has been ideated as to be an *artificial neural network* (ANN). The decision of considering such a model typology allows to utilize properly and in an effective way the data collected during the analyses.

Artificial neural networks are a wide class of flexible non-linear regression models, they find application mainly as a function approximation tool [51]. They are able to provide a mapping between some inputs and outputs with an arbitrary degree of accuracy. Neural networks were inspired by the data processing characteristics that are typical of the human brain. The common approach is to replicate a biological nervous system by combining many simple computing elements (neurons) in a highly interconnected system.

The artificial neural network model regarding this project has been built with a multi-layer perceptron architecture (feedforward, back-propagating neural network), which is widely used.

Back-propagating neural network is able to perform the following main functions:

- ***Learning***: modify behaviour in response to environment
- ***Generalization***: abstract the essence from a given set of inputs

ANN can be used when there is a little knowledge about the form of the relationship between the inputs and dependent outputs. In this case it can fit very well the input data analysed with the output target data.
Essentially, a neural network performs as a "black box" that elaborates the input data in order to obtain the desired output data. This mapping is realized by a *training mechanism*, in which the ANN learns how to behave in order to obtain the outputs data in function of the inputs. After the training phase, the resulting neural network becomes in this way a sort of transfer function *f* able to predict new outputs *Y* starting from new inputs *X:*

$$f : X \rightarrow Y$$

Basically, the artificial neural network algorithm's target is to find a reliable function that maps in the best possible way the inputs with the correspondent outputs data [51].
The main steps required to design efficiently a neural network are the following:

1. Input and output datasets collection
2. Input and output datasets pre-processing
3. Creation of the network
4. Choice and configuration of the network's architecture
5. Initialization of weights and biases
6. Training process
7. Validation of the neural network
8. Application of the trained neural network to new input datasets

In order to obtain a neural network able to provide sufficiently good results it is very important that all the steps listed above are correctly applied.
The multi-layer perceptron neural network architecture is made of a set of processing units called neurons.
These are connected with each other over a large number of lines which are "weighted" basically in function of the importance of the respective input on which it is connected.
The higher the weight the more the strength of the signal transferred in the connection becomes. Each neuron receives an input signal from previous neurons or external sources.
Afterwards, its internal state is changed (in a process called "*activation of the neuron*"). Finally, it computes an output signal. A neuron activates only if the signal to be transferred overcomes a threshold value. The functions that determine the activation of the neuron and the weights could change during the training process of the network. In the training the parameters of the ANN, such as the weights are modified in order to best match the input to the given output data. It's important to remind that generally each training session is initialized with starting weights and biases chosen randomly.

These different starting conditions have influence on the results. The number of iterations to reach a certain optimum also change due to the random starting values. For further details, please see [51], [52].

Main architecture and configuration of a feedforward neural network

A typical structure of an artificial neural network is showed by *Figure 61*:

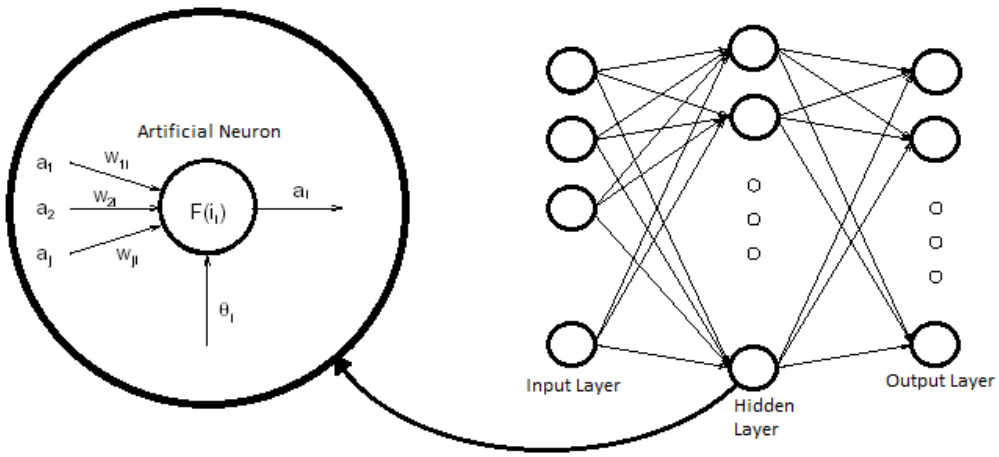

Figure 61 - Artificial neural network's structure

The architecture of the network is configured by three types of layers, each of these is made of several neurons. The first layer is called *input layer*, which has the function of treating and pre-processing the input data in order to be ready to be managed by the next layers. The *hidden layer* is the most important one and has a fundamental influence on the output of the overall model.
It has the function of processing the data coming from the input layers. The signals are in the end transmitted to the *output layer* which plays the role in the collecting of the resulting outputs.

Defining a good architecture of a neural network is not always a straight-forward process. The designer has to make the best decisions in order to configure properly the artificial neural network for the matter in question.
Choices such as the number of hidden layers, the number of neurons in each hidden layer, the training mechanism or the transfer function of the processing layers, are all features that can be adequately chosen in the best way only if the designer's experience is sufficiently high.

Every artificial neural network is made of one input layer, which is composed by one or more input neurons.
The choice regarding how many neurons have to be included in the input layer is uniquely determined by the shape of the training input dataset: each input variable of the neural network corresponds to one input neuron. Some neural network typologies add one additional node for a bias term.
Similarly, to the input layer, every neural network is composed by one output layer. Determining its size (number of neurons) is quite simple since each output variable corresponds to one output neuron. It is thus clear that the shapes of the input and output layers are determined by the chosen model configuration (the number of inputs and outputs on which is made the neural network).

Considering the number of hidden layers, the designer selects the best configuration in respect to the problem that is under consideration. For relatively simple problems, an adequate number of hidden layers is one or two. Since neural networks configured with two hidden layers allow to reproduce functions with whatever shape, there is currently no theoretical reason to utilize models with more than two hidden layers. The decision regarding the number of hidden layers is generally one of the most important steps in order to properly build an artificial neural network [52].

- A neural network without hidden layers permits to represents linear functions or decisions.

- Neural networks having only one hidden layer (*Figure 62*) are very popular and common since they are able to approximate whichever function that contains a continuous mapping from one finite space to another.

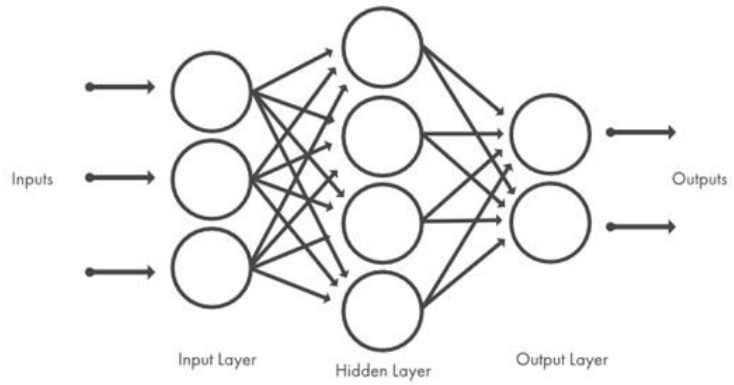

Figure 62 - Neural network configured with one hidden layer

- A neural network configured with two hidden layers (*Figure 63*) is capable as well of representing whatever function and, depending on the problem to be solved, its performances can be even better than with only one hidden layer. As drawback, the network's complexity and the computational time could dramatically increase [52].

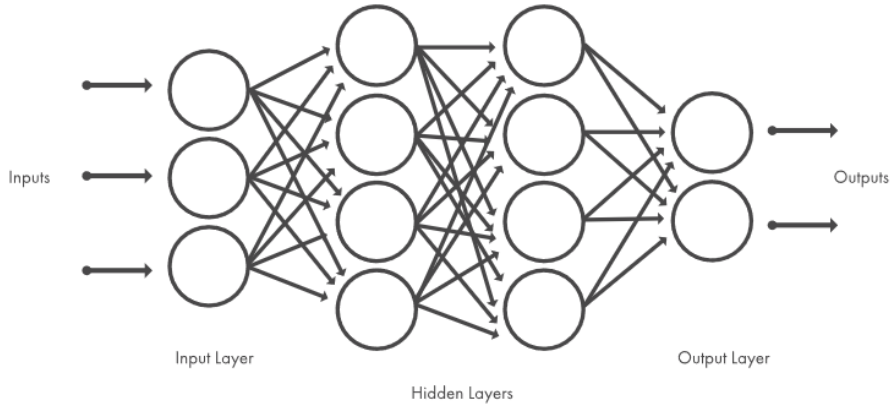

Figure 63 - Neural network configured with two hidden layers

The subsequent step in order to configure a neural network is represented by the choice of the number of neurons in each hidden layer, which could be a tricky decision. The role that these neurons play on the outputs is of fundamental importance. For this reason, deciding a proper number of hidden neurons constitutes a very delicate matter. A small number of hidden neurons could generate an *underfitting*, that occurs in the moment in which there are not enough neurons to properly detect and reproduce the function between the input and the output datasets. This problem is accentuated especially in highly non-linear relationships [52].

Vice versa if the number of hidden neurons is too high, it could result in other problems; the data could easily be *overfitted* by the network since the model reaches a too high level of learning ability with a consequent loss of generalization capability. The second main problem is that the computational time needed by a neural network having an exaggerated number of hidden neurons could increase substantially [52].

The following examples are useful in order to understand the occurrence of an underfitting (*Figure 64*) and overfitting (*Figure 65*) situation:

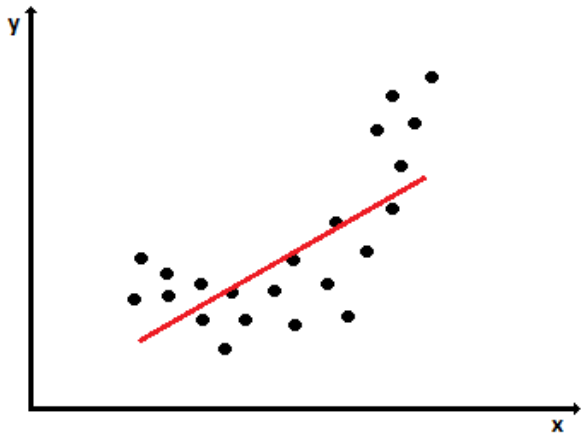

Figure 64 - Underfitting

The red curve doesn't describe properly the trend of the data.

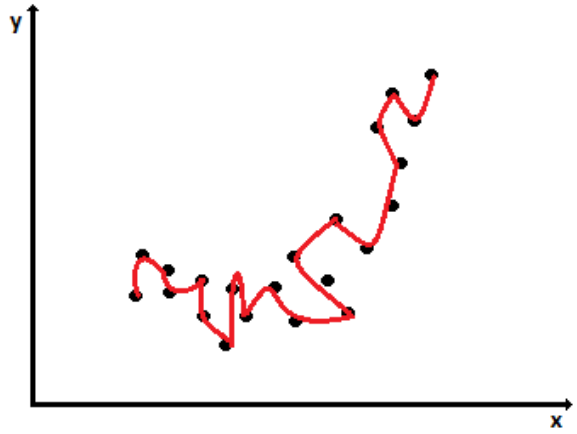

Figure 65 - Overfitting

The red curve follows fits each point, the network has memorized the dataset without extrapolating a general trend.

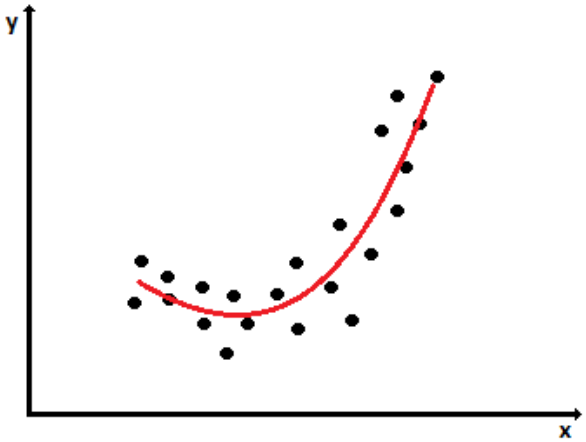

Figure 66 - Appropriate fitting

The red curve is able to describe properly the general trend of the points.

The goal regarding the choice of the number of hidden neurons is to find a good middle ground between too many and too few neurons. Generally, the selection of a proper structure of the neural network comes down to trial and error [52].

Processing units

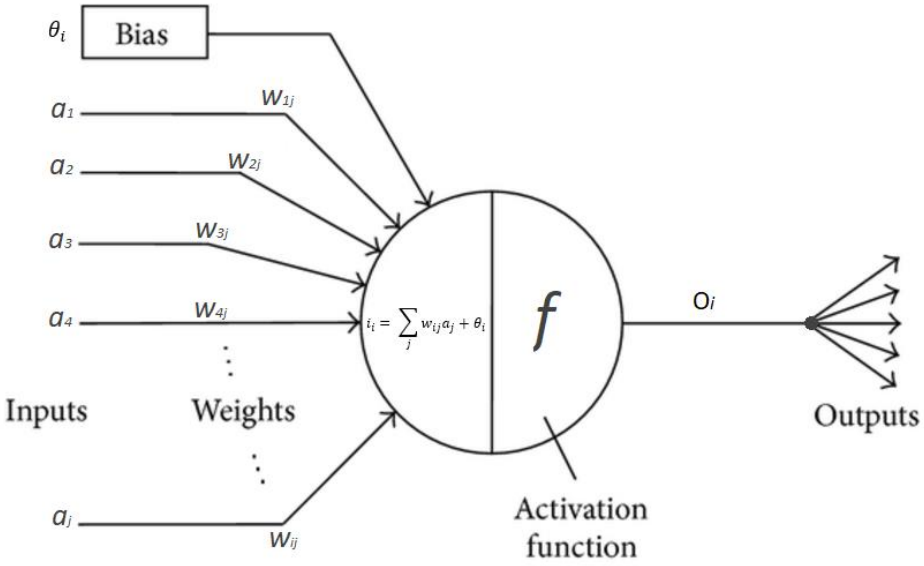

Figure 67 - Neuron's processing function scheme [53]

The following equations are in accordance with [51].
Each neuron i receives some inputs signals from the previous neurons (*Figure 67*). The total input i_i is the weighted sum of the output a_j coming from the units connected plus a bias term (offset ϑ):

$$i_i = \sum_j w_{ij} a_j + \theta_i \tag{1}$$

The term w_{ij} is the weight for the j-th input. The function which gives the effect of the total input i_i on the activation of the neuron is a non-decreasing function of the total input F, which is called *activation function*:

$$o_i = F(i_i) = F\left(\sum_j w_{ij} a_j + \theta_i\right) \tag{2}$$

The choice of the activation function is a matter of the designer of the ANN. It represents a very important task since the nature of the activation function determines how the signals are processed by each neuron. Consequently, it has a strong effect on the output of the network. The main activation functions available can vary between any differentiable transfer function, linear or non-linear.

Multi-layer networks are often designed with neurons having log-sigmoid transfer function *a=logsig(n)*, which is showed by *Figure 68*.

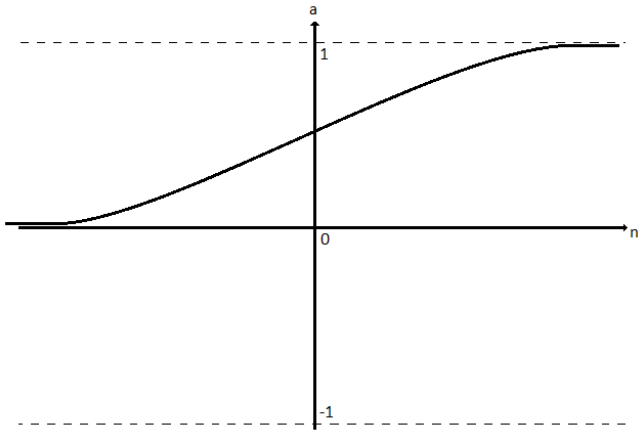

Figure 68 - log-sigmoid transfer function

The outputs of the *logsig* function are included between 0 and 1 as the neuron's net input goes from negative to positive infinity. Another possible choice is represented by the tan-sigmoid transfer function *a=tansig(n)*, which is described by *Figure 69.*

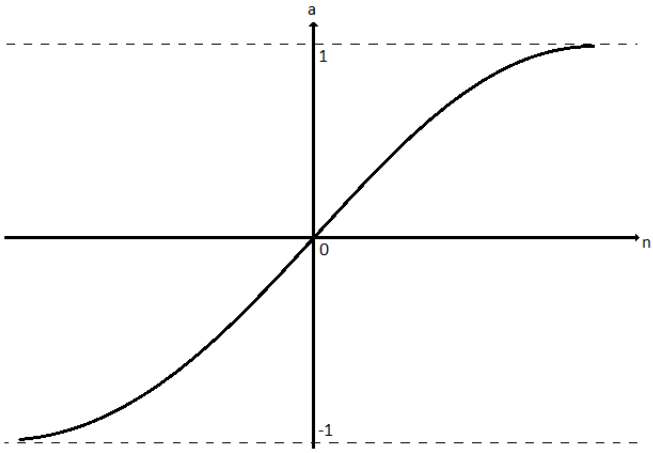

Figure 69 - tan-sigmoid transfer function

Sigmoid output neurons are often used for pattern recognition problems. There is the possibility to choose also a linear transfer function called *purelin* (*Figure 70*), which is mainly utilized in order to configure output neurons with the aim to solve function fitting problems.

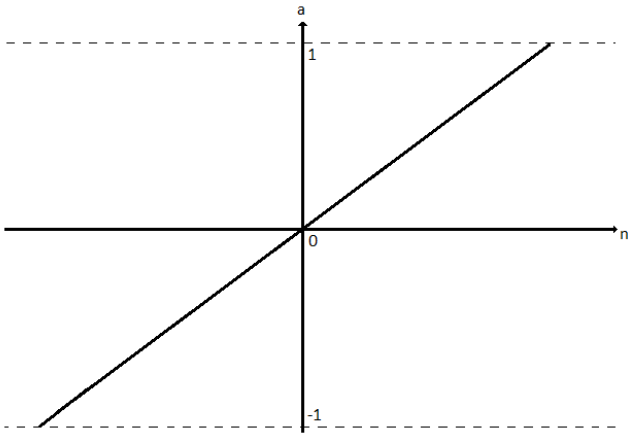

Figure 70 - purelin transfer function

The possible transfer functions showed previously are the most commonly used for multi-layer networks, but other differentiable transfer functions can be created and used if desired [54]–[56].

Preparation of the data

Generally, before beginning the training process, the input and output datasets are prepared in order to fit in the best way the network: it's important to know that the model can only be as precise and reliable as the data used in the training process. First of all, it is very important that the input and output datasets cover the full range of values and situations for which the neural network will be used. Multi-layer neural networks are able to predict outputs and generalize the results regarding inputs included in the range of data used for the training process. As a drawback, this type of neural network is incapable of predicting accurately and extrapolating beyond the input's data range. For this reason, it's very important to choose carefully the data for the training process.

Besides this general rule, it's good that the input and output datasets undergo a pre-processing step in order to build a neural network in the best way possible. The main important pre-processing treatment consists of the normalization of both the input and the output datasets before applying them for the training process. Normalization (scaling) of data within a uniform range is essential to prevent larger numbers from overriding smaller ones, and to prevent premature saturation of hidden nodes, which impedes the training process. This is especially true when actual input data take large values [52]. In this way the training process will be much faster and it will assure trustable outputs.
After the learning phase, the output data can be transformed back into the units of the original target data in order to be ready to be used.

As shown in *Figure 71*, the pre-processing phase occurs before the first layer of the neural network, while the post-processing one happens just before the output of the network.

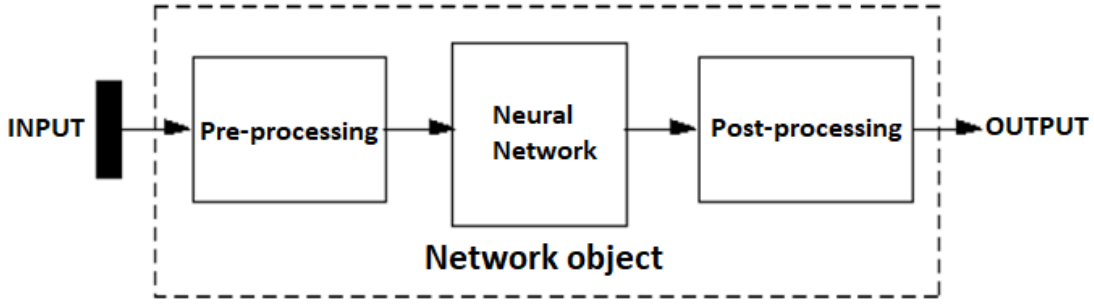

Figure 71 - Sequence's scheme of processing steps between input and output

Back-propagation algorithm

The configuration of a multi-layer perceptron neural network has to be made in order to obtain the output desired by exploiting a set of input data. The neural network is trained by managing input data according to some fitting rules, like the back-propagation learning rule.
The learning process of the ANN consists of a calculation of the errors of the neurons in the hidden layers by back-propagating the errors from the output layer.

The following formulas and equations are in accordance with [51].
The sum of squared errors of the output layers are obtained as following:

$$E^2 = \frac{1}{2} \sum_{i=1}^{N_o} (e_i)^2 \tag{3}$$

N_o is the total number of neurons in the output layer while e_i represents the error at the i-th neuron of the output layer. The error e_i can be assumed as the difference between the expected value of the output $\tilde{y}_i$ and the output at the i-th neuron y_i:

$$e_i = \tilde{y}_i - y_i \tag{4}$$

The weights *w* and the offsets ϑ are changed in order to minimize the sum of squared errors as following:

$$\Delta w_{ij} = -\gamma \frac{\partial E^2}{\partial w_{ij}} \qquad \Delta \vartheta_i = -\gamma \frac{\partial E^2}{\partial \vartheta_i} \tag{5}$$

Where γ is a constant. The derivatives of the sum of squared errors in respect to the weights and the offsets are calculated as:

$$\frac{\partial E^2}{\partial w_{ij}} = \frac{\partial E^2}{\partial i_i} \frac{\partial i_i}{\partial w_{ij}} \qquad \frac{\partial E^2}{\partial \vartheta_i} = \frac{\partial E^2}{\partial i_i} \frac{\partial i_i}{\partial \vartheta_i} \tag{6}$$

Where, according to (1):

$$\frac{\partial i_i}{\partial w_{ij}} = a_j \qquad \frac{\partial i_i}{\partial \vartheta_i} = 1 \tag{7}$$

It's possible to define:

$$\delta_i = -\frac{\partial E^2}{\partial i_i} \tag{8}$$

This training rule is based on the steepest descent along the gradient of the error surface (see [51] for further details). In the end the variation of the weight and offset results in the following:

$$\Delta w_{ij} = \gamma \, \delta_i a_j \qquad \Delta \vartheta_i = \gamma \, \delta_i \tag{9}$$

The term δ_i is iteratively calculated, this process is called back-propagating algorithm.

It's possible to rewrite the partial derivatives as:

$$\delta_i = -\frac{\partial E^2}{\partial i_i} = -\frac{\partial E^2}{\partial o_i}\frac{\partial o_i}{\partial i_i} \tag{10}$$

Considering (2):

$$F'(i_i) = \frac{\partial o_i}{\partial i_i} \tag{11}$$

The term $F^{'}(i_i)$ represents the derivative of the activation function of the i-th neuron with respect to the input i_i. In order to evaluate the term δ_i it's possible to take into account two different alternatives showed as following.

Assuming that the i-th neuron belongs to the output layer it's possible to write:

$$\frac{\partial E^2}{\partial o_i} = -(\tilde{y}_i - y_i) \tag{12}$$

Substituting in (10) and considering (11) the term δ_i results as:

$$\delta_i = (\tilde{y}_i - y_i)\, F_i^{'}(i_i) \tag{13}$$

Assuming that the i-th neuron belongs to a hidden layer:

$$\frac{\partial E^2}{\partial o_i} = \sum_{h=1}^{N_o}\frac{\partial E^2}{\partial i_h}\frac{\partial i_h}{\partial o_i} = \sum_{h=1}^{N_o}\frac{\partial E^2}{\partial i_h}\frac{\partial}{\partial o_i}\sum_{k=1}^{N_h} w_{hk}\, o_k = \sum_{h=1}^{N_o}\frac{\partial E^2}{\partial i_h} w_{hi} = -\sum_{h=1}^{N_o}\delta_h\, w_{hi} \tag{14}$$

In the expression above N_h is the total number of neurons which are linked to the h-neuron. Substituting in (10) and considering (11) it is possible to obtain:

$$\delta_i = F^{'}(i_i)\sum_{h=1}^{N_o}\delta_h\, w_{hi} \tag{15}$$

The expressions (13) and (15) allow to evaluate iteratively δ for every unit into the network.
In both the different situation analysed (i-th neuron belonging at the output layer or at the hidden layer), the expressions found permit to evaluate iteratively the term δ for each unit into the network. Thanks to this backward propagation, it is possible to calculate the error at the output and to distribute it to the layers back of the network.

During the training process, the weights of each connection are iteratively calculated once for each "*epoch*" in order to obtain progressively the lowest possible training error between the outputs simulated and the outputs fed to the network in order to train it.

In addition to the *training error*, the learning process of the network can be monitored also by the *generalization error*. Each of the two errors can be described by the two following curves (*Figure 72*), which are called *learning curves*:

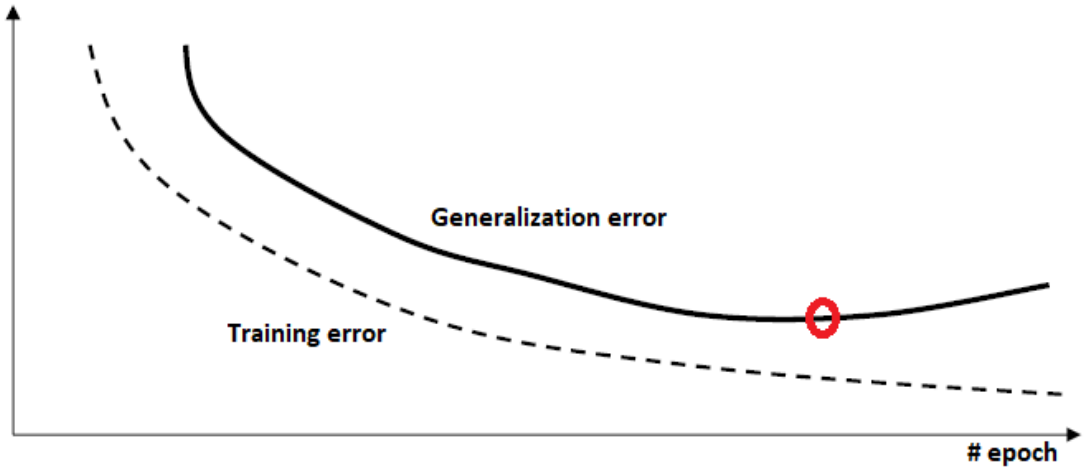

Figure 72 - At the red circle the generalization error starts increasing, this situation could bring to a data overfitting

The generalization error represents a measure of how efficient the neural network is generalizing its predictive function. Every neural network is trained with an input and output datasets, but it's important to remind that its main function is to predict outcome values referred to "new" inputs data, never used for the training process.
The generalization error has to be minimized in order to avoid *overfitting*. This occurs, as explained before, when the network has memorized the training examples, but it has not learned how to properly describe the general behaviour.

Looking at the two learning curves (*Figure 72*), the training error curve tends to decrease always, while the generalization error curve, after a variable number of iterations, starts increasing (which means a possible overfitting behaviour): it's good to stop the training process before the occurrence of such critical situation.
Usually, the overfitting is caused by a too high number of hidden layers and neurons, but also by a too limited training sample data sets [52][51].

In order to improve the network 's ability to generalize results, it is possible to use input and output data sets large enough to provide an efficient fit. The larger the training samples are, the better the network will be able to generalize the results with new input data [52].

As in the case of the current work, the input and output datasets are quite limited, so it's possible alternatively to use two different methods for improving generalization and avoiding the overfitting: *early stopping* and *regularization*.

Early stopping is a technique in which the whole available data are divided into three subsets: the *training set*, the *validation set* and the *test set*.
The *training set* is composed by samples dedicated to the computing of the gradient. Moreover, they are used to update the network weights and biases. The *validation set* is composed by samples that aren't used for the training process. They are instead used in order to calculate the error (between target and simulated outputs) which is monitored during the training process. Usually during the starting phase of the training process, the validation error keeps decreasing, as does the training set error. However, when the data start to be overfitted by the neural network, the error on the validation set typically begins to rise. At this specific iteration of the training process, the learning is interrupted and the network weights and biases are saved.

The third subset is called *test set*, it is composed by data not used during training, the test set error is instead used to compare different models. It is also useful to plot the test set error during the training process. It is possible to recognize a poor division of the data set, that happens in the moment in which the error on the test set reaches a minimum at a significantly different epoch than the one in which the validation set error has the lowest value.

The *regularization* is the second possible technique useful to avoid an overfitting behaviour and to improve generalization. The idea behind this technique is to modify the performance function, that usually, for training feedforward neural networks, is represented by the sum of squares of the network errors on the training set [57].

$$F = mse = \frac{1}{N}\sum_{i=1}^{N}(e_i)^2 = \frac{1}{N}\sum_{i=1}^{N}(t_i - \alpha_i)^2 \tag{16}$$

The network 's ability to generalize results can be improved adding a term consisting in the mean of the sum of squares of the network weights and biases:

$$msereg = \gamma * msw + (1-\gamma) * mse \tag{17}$$

In the expression above γ represents the performance ratio, while the term *msw* can be written as:

$$msw = \frac{1}{N}\sum_{j=1}^{N} {w_j}^2 \tag{18}$$

This performance function makes it possible to obtain a neural network configured with connections having smaller weights and biases. Thus, forcing the output response to be smoother and "*regularized*". So, it is possible to have a more generalized output with a less probability to overfit the data.
The regularization technique has as drawback the introduction of a new parameter γ. The choice of the optimal value for the performance ratio is not straight-forward: if γ is too large it's probable to have overfitting and thus nullifying the advantages of the regularization technique; vice versa a too small performance ratio doesn't allow the network to efficiently fit the training data.

Training algorithms

The following represent the two main used algorithms available in the Matlab software in order to obtain a reliable and efficient neural network:

- *trainlm*

The *trainlm* network training function basically updates weight and bias values according to Levenberg-Marquardt (LM) optimization which is a classical and popular approach for solving non-linear equations.

This training algorithm automatically stops when any of the following conditions occurs:

- The maximum number of iterations (decided by the designer) is reached.
- The maximum amount of time (default value) is exceeded.
- Performance is minimized to a specific default value.
- The performance gradient falls below a specific default value.
- The Marquardt adjustment parameter μ, which is changed iteratively during the training process according to the LM method, exceeds a specific threshold default value.
- Validation performance has increased more than a default number of times since the last time it decreased (when using validation set).

All the default values to which reference is made in the upper list, are automatically imposed by the training algorithm (see [58] for more details).

The last condition, among the ones just listed, is referred in particular to the early stopping technique previously described. Such condition imposes that the training is stopped automatically when the generalization error starts increasing, that is meaningful in an overfitting situation. This behaviour is notable for example thanks to the validation set error curve. It allows to understand and assess the risk of overfitting. The *trainlm* network training algorithm is typically fast, but it requires more computational memory than other algorithms.

- *trainbr*

The *trainbr* network training function is based on the Levenberg-Marquardt optimization as the previous network training, but in a different way which takes the name of *Bayesian regularization*.
The Bayesian regularization algorithm has the main focus on the regularization of the output signal in order to obtain a more generalized behaviour and avoid overfitting. This training algorithm usually requires more time than the previous one.

The *trainbr* training algorithm automatically stops when any of the following conditions occurs:

- The maximum number of iterations (decided by the designer) is reached.
- The maximum amount of time (default value) is exceeded.
- Performance is minimized to a specific default value.
- The performance gradient falls below a specific default value.

- The Marquardt adjustment parameter μ, which is changed iteratively during the training process according to the LM method, exceeds a specific threshold default value.

All the default values to which reference is made in the upper list, are automatically imposed by the training algorithm (see [59] for more details).

Looking at the stopping conditions of this training algorithm, it is notable that they are the same as in the previous algorithm, but without the last condition. This is because in the *trainbr* algorithm the validation data set in null by default. Therefore, all the information contained in the datasets is used for the training process.
Consequently, the Bayesian regularization permits to better manage problems in which the available datasets are noisy or small.
See [60] and [61] for a more detailed discussion of Bayesian regularization.

4.1.2 Driver model configuration and architecture

As described before, the required model with the aim of predicting the drivers' reactions referred to the scenario analysed, has been configured as an artificial neural network. Both the input and the output datasets have been introduced to the neural network in form of matrices. Each column represents a specific input or output, while each row is meaningful of the specific driver. The input and output datasets consist respectively of matrices made of 11 and 3 columns, the number of rows is the same for both the datasets, it is equal to the total number of drivers involved in the experiment analysed.

Input variables

Here are listed the eleven input variables taken into account in order to train the neural network:

- The current driving mode

1. Manual driving mode
2. Intentional car following driving mode
3. Adaptive cruise control driving mode
4. Traffic jam assist driving mode

- The information about the driver

5. Driver's age
6. Driver's gender
7. Driver's km/year travelled
8. Driver's years of license accumulated
9. Driver's experience regarding the use of adaptive cruise control

- The information about the state of the ego vehicle in respect to the TC

10. Time till intersection for the ego vehicle in the moment in which the TC gets into the intersection
11. Driver's perception time: the moment in which the driver notices the presence of the TC

These input variables are either continuous and discrete (Boolean). The discrete variables are the type of the driving mode adopted by the specific driver, the gender and the driver's experience of the use of the adaptive cruise control.
In particular, for what concern the values of the driving modes variables, they have been assigned in a quite simple way, typical of the Boolean variables: each driver input data contains four variables regarding the four possible driving modes, it has been imposed a value of 1 to the driving mode considered, while a value 0 to all the others. Since all the input data of the drivers have been placed together under the same columns, the neural network is able to distinguish which is the current driving mode used for each single participant. It hasn't been possible to consider only one variable including all the driving modes because of computational issues.

The gender variable is Boolean and can be either 0 for female or 1 for male. An analogue Boolean variable has been used in order to classify the drivers used to the adaptive cruise control in respect to the novices.

The continuous input variables are the driver's age, average mileage per year, years since driver's license acquired, time to intersection for the ego vehicle and driver's perception time.
The time till intersection corresponds to the moment in which the TC is getting into the intersection area. It has to be noted that this input variable actually includes two "hidden" variables: the speed of the ego car and its distance from the intersection. It has been chosen to utilize the time till intersection variable in order to keep the model as smart and compact as possible. However, it was noted that the situation wouldn't have been different if the speed and the distance had been considered as two separated variables.
The input variable regarding the moment in which the driver notices the TC represents an important information in order to properly model the driver's behaviour. As it will be discussed in the following paragraphs, it is possible to state that the braking reaction depends also on the moment in which the driver perceives something that could be dangerous. Because of this, the perception time has been treated as an input variable to the neural network.

Output variables

The output variables of the neural network represent the results of the model's prediction. As anticipated, the main drivers' reactions found in the analyses regarded the braking behaviour, because of this, there is no evidence of output variables concerning the steering of the vehicle.

Here the list of the three output variables:

1. Brake reaction time
2. Driver's mean force on the brake pedal
3. Maximum vehicle's deceleration

All the outputs of the neural network are continuous variables. As listed above, the main information that the model aims to predict are the moment in which the driver brakes, which is represented by the brake reaction time, the mean force that the driver has to impose to the brake pedal while braking and the maximum vehicle's deceleration.
Note that the first two output variables are directly related to the driver's reaction during a braking on a critical situation. The output regarding the maximum deceleration is rather a vehicle's dynamics attribute corresponding to the driver's braking action: this is the reason why the maximum deceleration has been included as output variable describing the driver's behaviour.

Model's architecture

The structure of the neural network model has been chosen based on the matter in question. The network has been configured with two hidden layers, because of this, the typology of the presented model could assume the name of "*deep neural network*" (a neural network with more than one hidden layer, see [62]).
The structure of the neural network can be described intuitively with the scheme below:

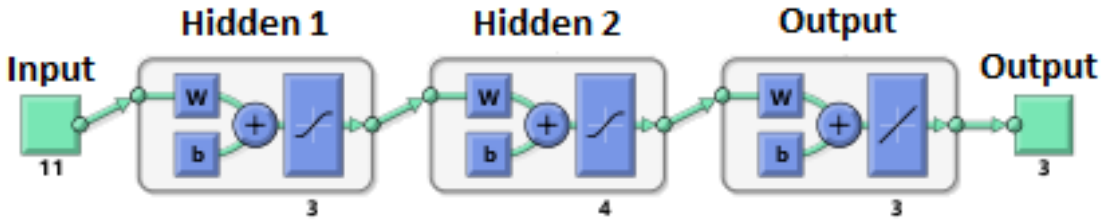

Figure 73 - Overview of the neural network

As previously showed, the signals coming from the eleven inputs are treated by two hidden layers; in the end the information flow crosses the output layer and gives as result the three final outputs required.

The choices regarding the number of hidden layers as well as the corresponding number of hidden neurons, were chosen based on heuristic testing (trial and error). In particular, the neural network was trained several times changing from time to time its features. This procedure was stopped after reaching a stable and satisfactory performance.
In this case, the choice to configure the neural network with two hidden layers guaranteed a better performance in respect to only one layer. The number of neurons included into the two hidden layers are respectively three and four. The number of hidden neurons was kept quite low to avoid a possible overfitting behaviour of the neural network. With such configuration, the output values assumed steadily reasonable results, in accordance to the input data fed to the network. Moreover, the training process resulted fast and accurate.

In matters of the neurons' transfer functions, it can be seen that the neurons regarding the two hidden layers have been configured with a tan-sigmoid transfer function in order to keep the values always between -1 and +1.

Configuring the hidden layers of the network with a non-linear transfer function, allows the network to learn non-linear relationships between the input and output datasets. The output layer is instead constituted with a linear transfer function, this permits to manage function fitting problems, as in the case of this model.
The *trainbr* learning algorithm has been utilized to train the network. The Bayesian regularization algorithm permits to train this specific network in a better way than with the *trainlm* algorithm. The reason for this is that the number of samples included into the input and output datasets is quite low. It has been noted that training the network with a *trainlm* algorithm creates worse results for the prediction and generalization.
Both the input and the output data were pre-processed before applying them for the training process. In particular they were normalized within a uniform range (-1 – +1). This treatment helped to prevent larger numbers from overriding smaller ones, with the consequence that the learning process resulted faster and efficient.
After the training, the output data were transformed back into the units of the original target data in order to be ready to be used.

The following scheme shows in a very clear way the structure of the designed neural network:

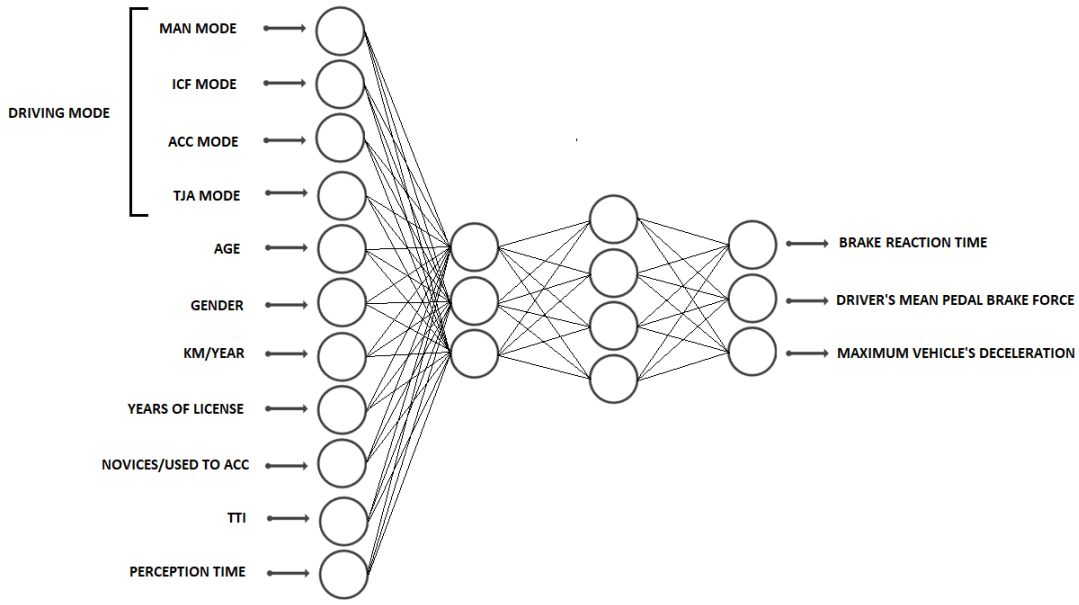

Figure 74 - Neural network's architecture

On the left it is possible to notice the eleven inputs of the model. Each neuron in the input layer communicates its information to each of the neurons contained in the first hidden layer. The first hidden layer transmits information to the second hidden layer resulting finally into the three outputs of the model.

Analysis of the inputs' influence, validation and application of the model

After having created the structure of the model, the effect of each input variable is studied in regards to the performance.
The goal of this analysis is to understand which variables are carrying the most information regarding the outputs of our model. It's easy to understand that the eleven input variables may don't assume the same importance on the final results.

For this reason, the neural network has been trained neglecting one input variable at a time and taking note about the changes of the network's performances.
The last phase regarding the design process of the neural network consists in the validation of the model.
This is useful in order to understand if the designed model is actually reliable and able to predict with a sufficient generalizing capability the outputs required. Feeding the network with new data allows us to understand if the model represents a generalized behaviour of the three outputs, without overfitting the data.
In presence of an overfitting, the model wouldn't be able to understand and manage the new input dataset, resulting in totally unreasonable outputs. This would happen if the numbers of hidden layers and neurons were too high in respect to the dimension of the datasets.
The validation phase has obviously been realized after the training process. A new input dataset (unused in the train phase) has been fed to the model. This new dataset is basically the same used for the training process but modified with the addition of random noise.

In particular, the values have been modified as following:

- Time to intersection = Time to intersection with the addition of a random noise value $\in$ [-0.5 , 0.5] s
- Perception time = Perception time with the addition of a random noise value $\in$ [-0.5 , 0.5] s
- Driver's age = driver's age with the addition of a random noise value $\in$ [-5 , 5] years
- Km/year=km/year with the addition of a random noise value $\in$ [-7000 , 7000] km/year
- Years of license = years of license with the addition of a random noise value $\in$ [-5 , 5] years
- Gender = random binary value (0,1)
- Experience with the ACC = random binary value (0,1)

Subsequently, the same validation test was repeated feeding the neural network with inputs affected by the same random noise values listed above, except for the variable referred to the time to intersection. For such input, the noise value added was changed as following:

- Time to intersection = Time to intersection with the addition of a random noise value $\in$ [-2 , 2] s

Since the time to intersection for ACC and TJA driving modes available to train the network was fixed to a specific and constant value, this further validation test was performed to verify the behaviour of the semi-automated driving modes with a wider variation of the time to intersection compared to the previous set of noise.

After the design and validation phases, the model was applied to simulate its possible concrete application. In particular, it involved the prediction of the reactions regarding a single specific driver, whose input characteristics could be easily imposed. In order to do this, the layout of the model interface was arranged so as to facilitate the insertion of the desired driver's information, in accordance with the requirements of the user.

4.2 Results

This section is dedicated to the results provided by the designed neural network. They aim to assess the quality and reliability of such model.
In particular, the following graphs describe the resulting performances in respect of both the capability of reproducing properly the data analysed, and the ability of predicting new outputs.
All the graphs and boxes shown in this paragraph were obtained by the use of Matlab.

The neural network is trained with the available datasets analysed in paragraph Results3.2, the results regarding the learning process are summarized in *Figure 75*:

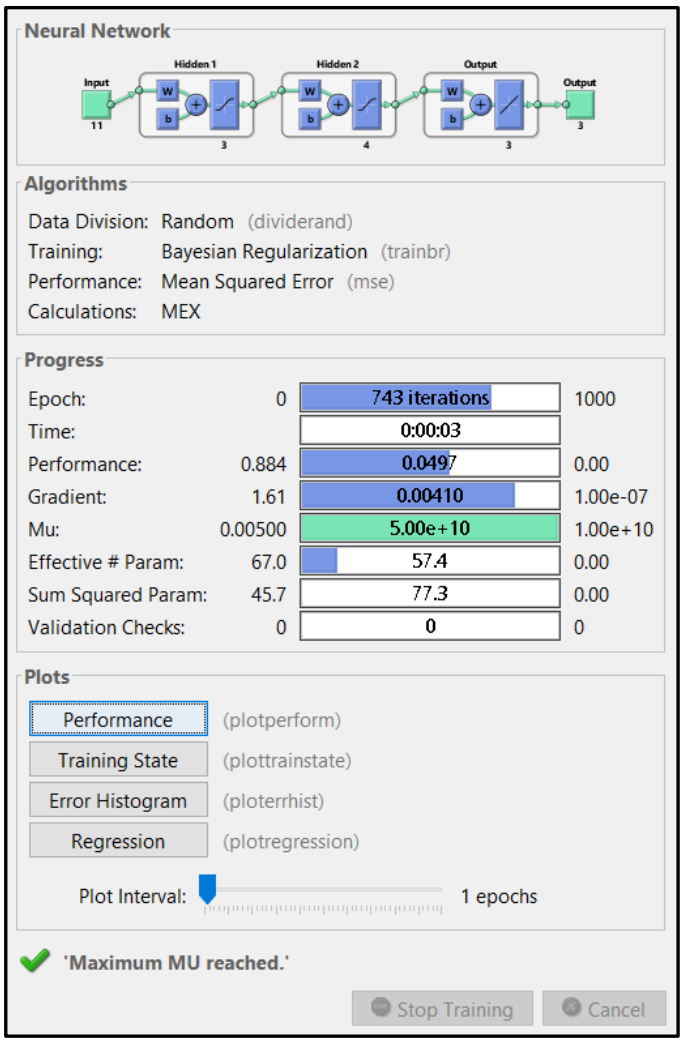

Figure 75 - Results of the training process

Since the results of the learning process can change every time a neural network is trained (due to the randomness of the training algorithm adopted). The graph represents an example describing one of the possible results. The neural network was trained several times to be sure of the reliability and robustness of the resultant behaviour.

In this case, the training process stopped when the maximum μ factor is reached. This is one of the stopping condition described in paragraph 4.1.1 regarding the *trainbr* training algorithm.

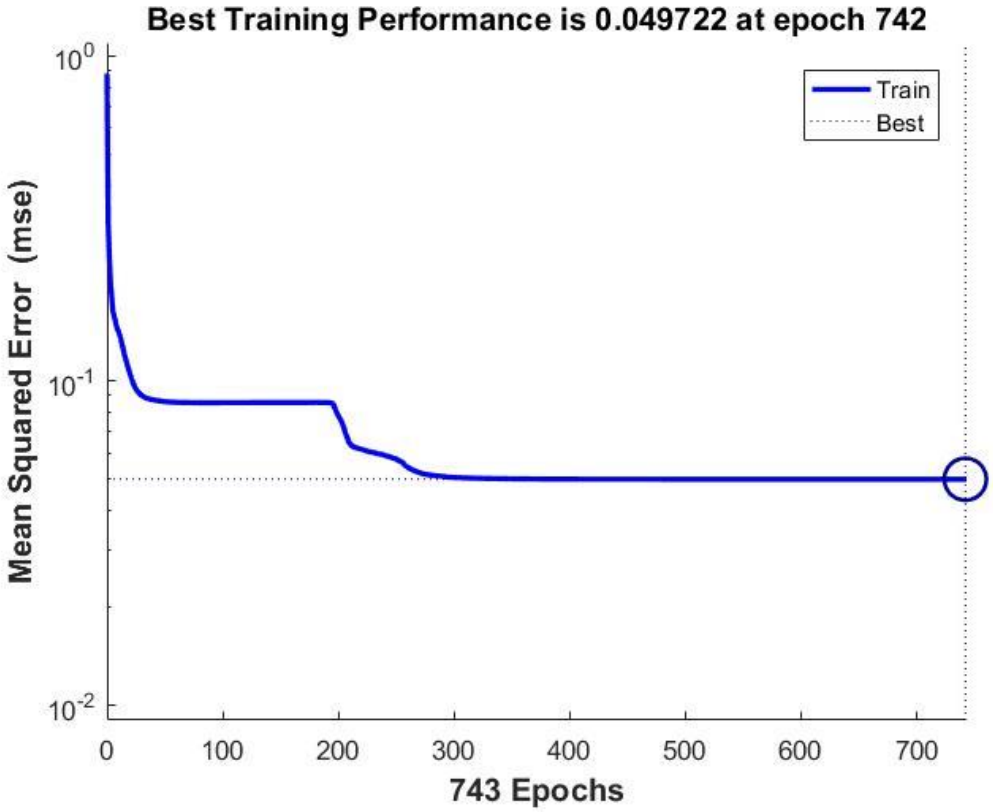

Figure 76 - Performance of the training process

As can be seen from *Figure 76*, the training process stops after 743 epochs (iterations). Since the training starts always with random values concerning the weights, the number of epochs is highly variable at every training of the network.

In this case, the minimum mean squared error obtained at the end of the training process, was 0,049722.

4.2.1 Capability of reproducing the results analysed

This paragraph shows the results about the model capability of reproducing the results obtained during the analysis of the scenario, starting from the same initial input data. This was made in order to verify if the neural network's training performed well.
The following graphs show the correlations using the R regression coefficient (see [63] for more information), which is a value that shows the linear regression correlation between the target network outputs (the data available from the analysis activity) and the simulated network outputs, obtained with the same inputs data. In this way it is possible to understand if the neural network is efficiently trained.

As discussed in paragraph 4.1, the aim of the training process was to obtain a neural network able to represent the general trend of the output, avoiding the overfitting and underfitting behaviours. Each of the three outputs of the model was analysed in the following figures, dividing between manual and semi-automated driving modes.

- Brake reaction time

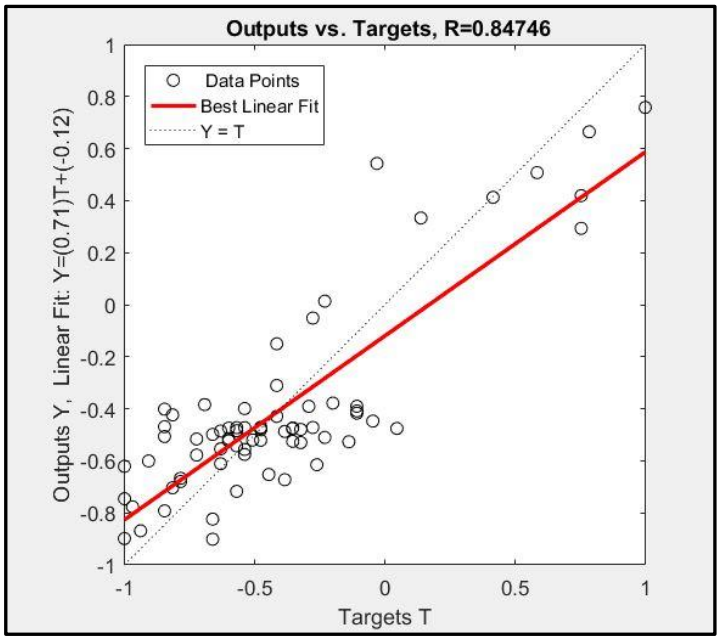

Figure 77 - Brake reaction time: comparison between simulated and target outputs

Figure 77 shows the linear regression line between the simulated and target outputs regarding the brake reaction times. The following graphs, *Figure 78-79*, describe the behaviour of the brake reaction times in respect to the time to intersection, at the moment in which the TC gets the intersection. The blue points are referred to the simulated outputs, while the red circles regard the target experimental outputs.

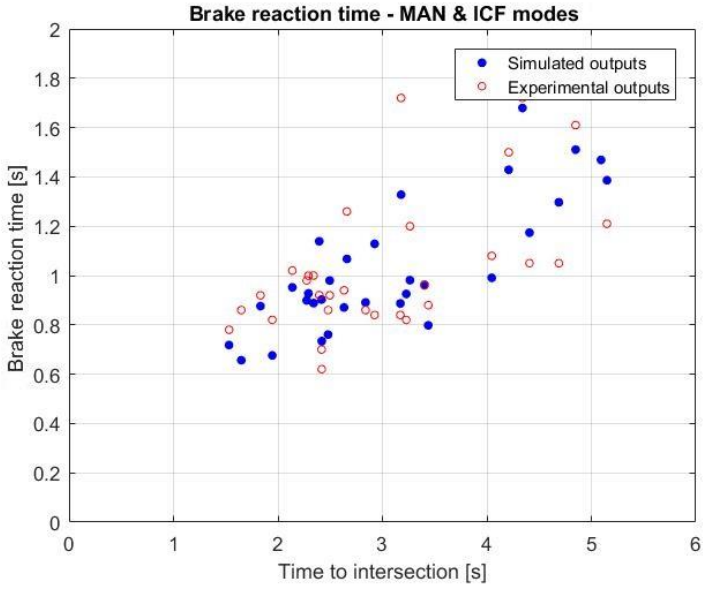

Figure 78 - Manual driving modes, brake reaction times in respect to TTI: simulated and target outputs

Figure 78 describes the relationship between brake reaction time and time to intersection regarding MAN and ICF driving modes. Starting from the original input data used for the training process, the model is able to reproduce the trend of the results found in the analyses: the simulated outputs are very close to the experimental ones which were used during the training process. Thus, the neural network was properly trained.

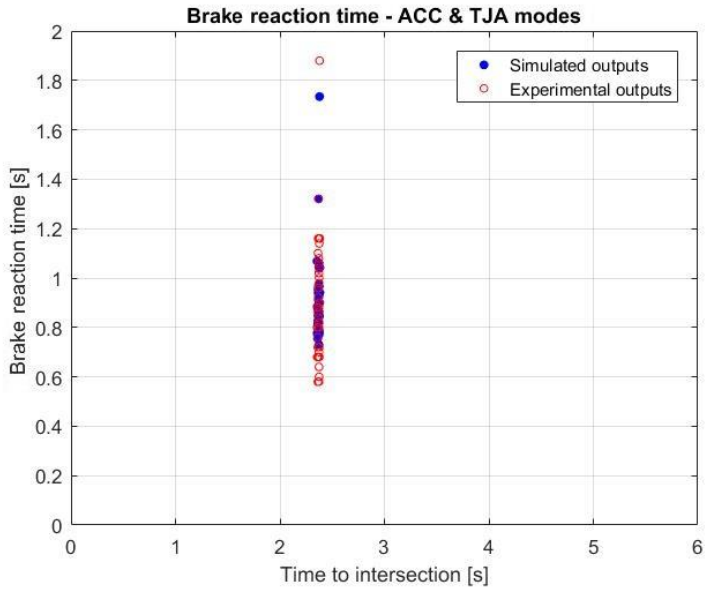

Figure 79 - Semi-automated driving modes, brake reaction time in respect to TTI: simulated and target outputs

As already described in paragraph 3.2, the semi-automated driving (ACC and TJA modes) were performed in a scenario designed with a fixed time to intersection. Consequently, this behaviour is reflected also by the simulation of the model: looking at *Figure 79*, all the points are referred to the same time to intersection. The neural network reproduces correctly the results previously found (simulated outputs points follow the trend of the experimental ones).

Since the brake reaction time has a correlation (albeit not high) with the perception time of the TC (3.2.9), it is possible to show the relationship between those two variables even with the outputs simulated by the model (*Figure 80-81)*.

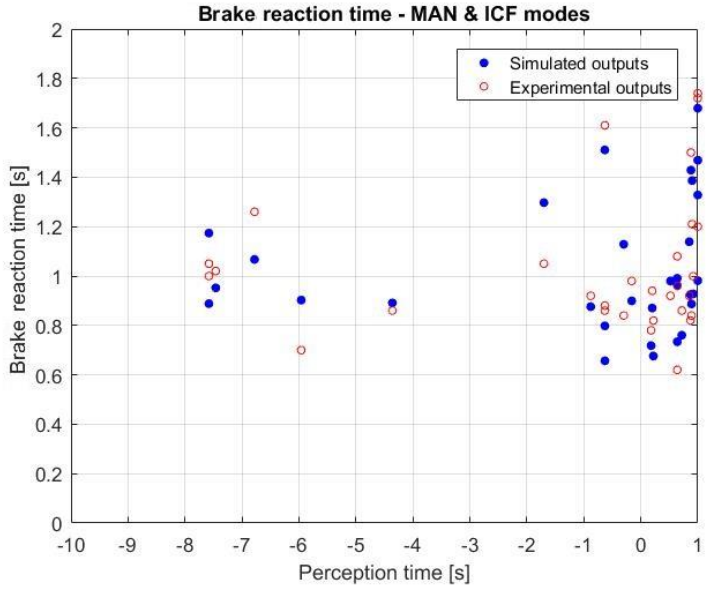

Figure 80 - Manual driving modes, brake reaction time in respect to the perception time: simulated and target outputs

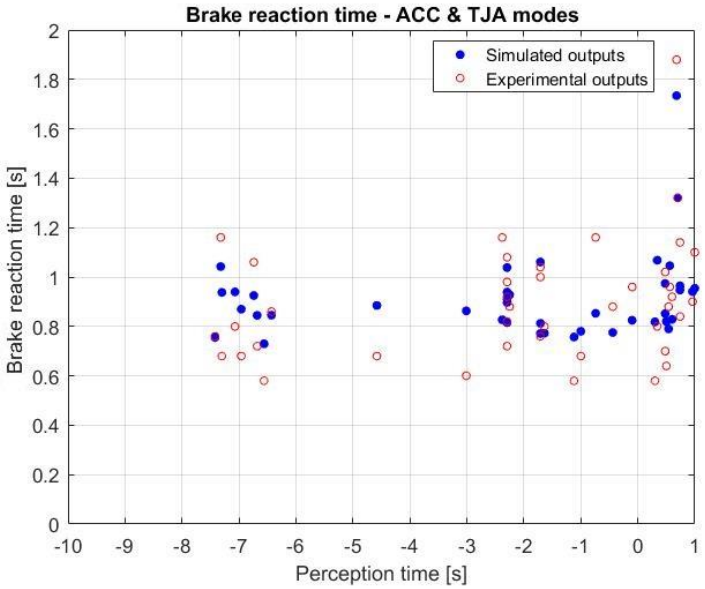

Figure 81 - Semi-automated driving modes, brake reaction time in respect to the perception time: simulated and target outputs

Even in these cases the neural network is able to reproduce correctly the results obtained in the analyses. As for all the other graphs shown, the presence of a slight discrepancy between the experimental and the simulated points is still indicative of a good training, without the presence of overfitting.

- Mean brake pedal force

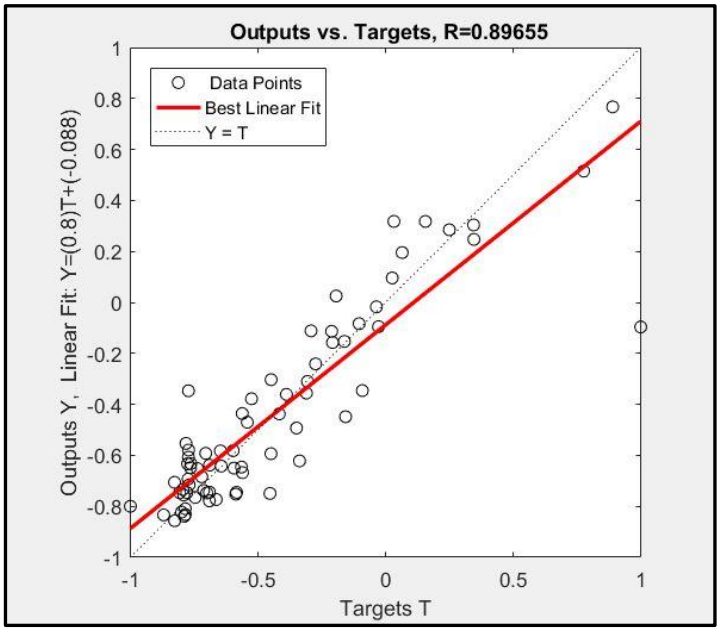

Figure 82 - Mean brake pedal force: comparison between simulated and target outputs

As regarding the mean brake pedal force, comparing the simulated outputs by the model with the target output data (*Figure 82*), it is possible to observe a good value of the R coefficient: the model is adequately trained also for this output variable.

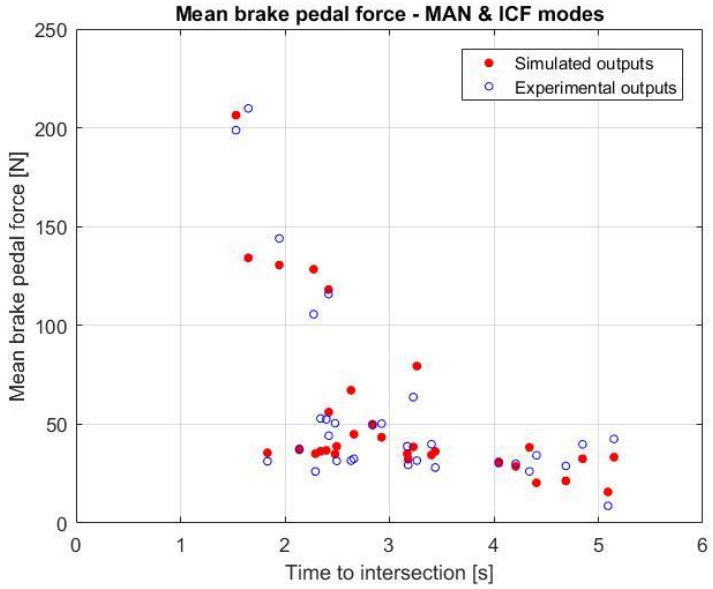

Figure 83 - Manual driving modes, mean brake pedal force in respect to TTI: simulated and target outputs

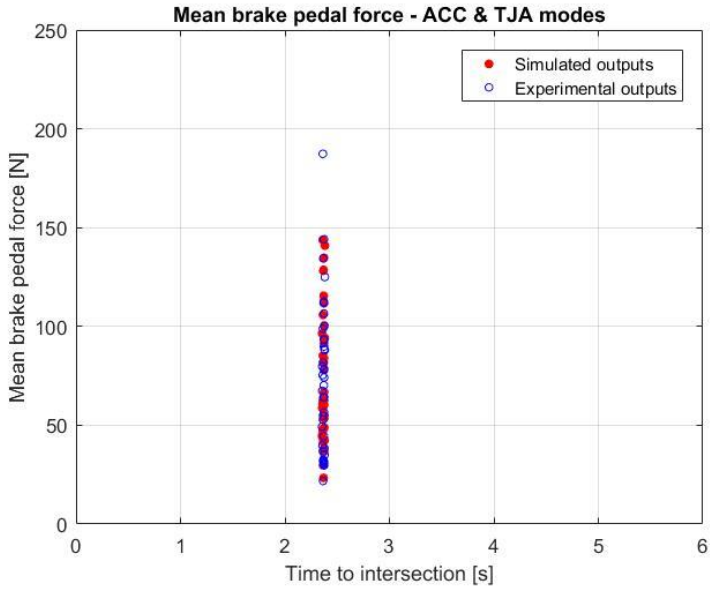

Figure 84 - Semi-automated driving modes, mean brake pedal force in respect to TTI: simulated and target outputs

The result showed by *Figure 82* is confirmed by the two previous graphs (*Figure 83-84*). The simulated outputs follow quite correctly the trend about the target experimental outputs. The neural network was successfully trained.

- Maximum vehicle's deceleration

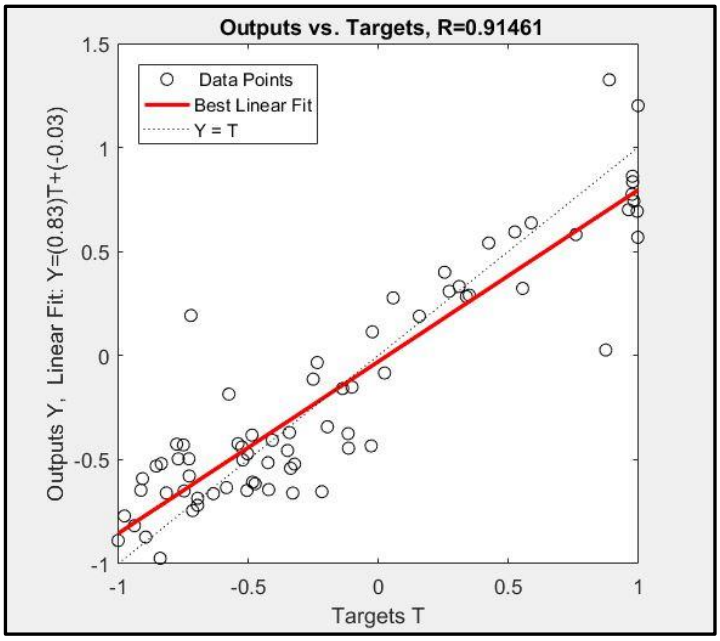

Figure 85 - Maximum vehicle's deceleration: comparison between simulated and target outputs

As shown by *Figure 85*, the neural network is capable of reproducing correctly also the results about the maximum deceleration. There is a high R coefficient between the simulated outputs after the training and the reference ones.

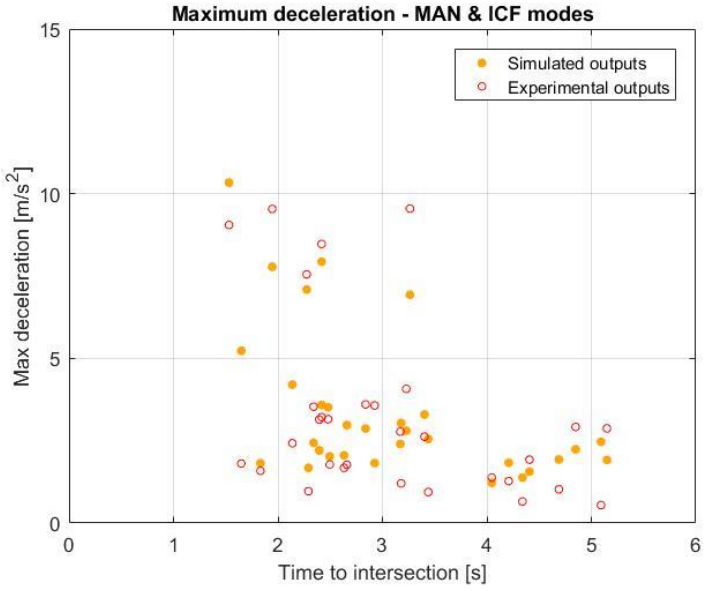

Figure 86 - Manual driving modes, maximum vehicle's deceleration in respect to TTI: simulated and target outputs

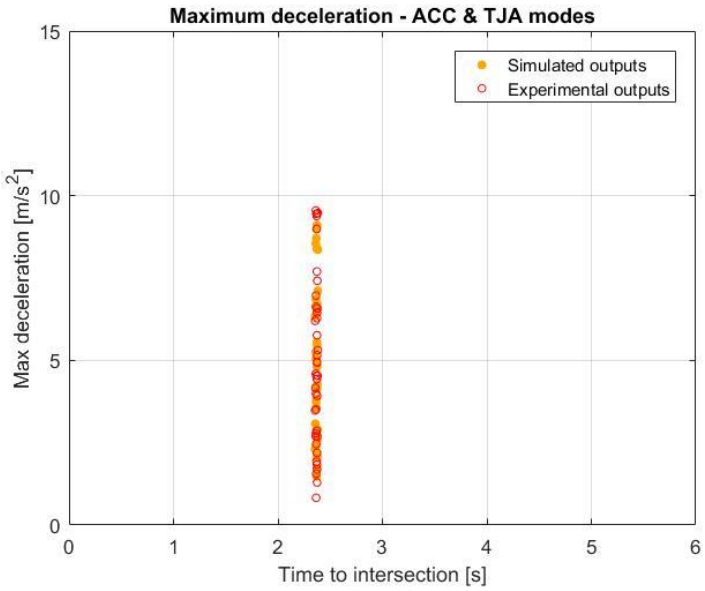

Figure 87 – Semi-automated driving modes, maximum vehicle's deceleration in respect to TTI: simulated and target outputs

The previous graphs confirm the result of the R coefficient showed in *Figure 85*. The simulated outputs (yellow points) follow with fidelity the trend of the experimental ones (red circles). This is valid regarding both the manual (*Figure 86*) and the semi-automated driving modes (*Figure 87*).

Summarizing the linear regression values between the simulated and target outputs, the resultant R coefficients are the following:

- Brake reaction times, simulated vs target outputs: R = 0,847
- Mean brake pedal force, simulated vs target outputs: R = 0,897
- Maximum vehicle's deceleration, simulated vs target outputs: R = 0,915

It is noted that the values of these correlations are good. As previously stated, they vary as a consequence of the randomness which affects the initial values of the weights during the training algorithm (see paragraph 4.1.1). However, for what concerns the R values of the outputs considered, they result stationary around similar high values: this was noticed after the running of many training processes. The matching between high values and a low variability of the R coefficients is meaningful of a good and robust training process. Further and detailed considerations about this will be discussed in paragraph 5.2.

The graphs showed in this section are grouped in manual and semi-automated driving modes. This is made so that it can be immediately clear the reproducing capability of the designed neural network. In order to have a complete overview of the model's efficiency, the previous graphs (regarding the relationship between the output variables and the input considered) were obtained also for all the four driving modes separately.

Consequently, the *Spearman* coefficient has been calculated for each combination, the results are summarized in *Table 20*.

Table 20 - Resultant Spearman coefficients, comparison between analysis and model results

	Analysis results				Model results			
	MAN	ICF	ACC	TJA	MAN	ICF	ACC	TJA
BRT vs TTI	0,632	0,541			0,782	0,697		
MBPF vs TTI	-0,336	-0,641			-0,421	-0,726		
MVD vs TTI	-0,332	-0,636			-0,371	-0,510		
BRT vs PT	0,343	0,251	0,278	0,452	0,505	0,05	0,185	0,338

The results obtained by the model are quite similar to those resulting by the analysis activity. As previously described, since the experimental scenario ideated for the semi-automated modes was characterized by a fixed time to intersection (referred to the entrance of the TC), in such cases, the calculation of the *Spearman* coefficient was omitted (in accordance to [63]).

4.2.2 Most influential inputs

The designed neural network is featured by eleven inputs, as described in paragraph 4.1.2. The following table shows the R coefficients regarding the linear regression between the target outputs and the simulated ones. These coefficients are obtained neglecting one input at a time.
The results of *Table 21* aim to highlight the input variables which have the major influence on the performances of the neural network.

Table 21 - Results of the input's influence on the performance of the neural network

Input neglected	**R coefficient between simulated and target outputs**		
	BRT	MPF	MLD
No one	0,847	0,897	0,915
Years of license	0,836	0,883	0,903
Age	0,824	0,873	0,855
Gender	0,701	0,835	0,894
Km/year	0,812	0,846	0,877
Novices/used to ACC	0,794	0,832	0,863
PT	0,787	0,884	0,796
Driving modes	0,695	0,662	0,758
TTI	0,603	0,723	0,691
TTI, PT	0,502	0,826	0,774
Driving modes, PT	0,354	0,506	0,523
Driving modes, TTI	0,002	0,304	0,287

It can be noticed that, as expected, the input variables that mostly affect the performances of the neural network are the ones referred to the driving modes selection and the time to intersection at the entrance of the TC. The perception time has a lower influence in respect to the previous two.

4.2.3 Validation of the model

The previous paragraph showed that the designed neural network is able to reproduce correctly the results obtained by the analysis of the drivers' data. However, as described in 4.1.1 the aim of this model is mainly to generalize and to extend this ability to new input data, not considered during the training process.

In order to do this, the model is validated by the use of new inputs, which derive from the "original" ones, but with an addition of random noise (see paragraph 4.1.2 for more details). The model validation is assessed showing graphs about relationships between input and output obtained feeding the model with input data never managed by the network during its training. The trends of these relationships are compared (by calculation of *Spearman* correlation coefficients) to the trends referred to the same relationships but obtained with the original input data used during the learning process (which can be considered as the reference ones). Each of the following relationships are described taking into account each driving mode separately. For each graph, the *Spearman* coefficient is calculated, the final results are summarized at the end of the paragraph.

All the following results represent meaningful examples of the outputs obtainable by this modelling activity: each graph, and as consequence each *Spearman* coefficient, can change every time due to two random factors: the training process and the random noise added to the input data. The robustness of the model, as well as the consistency of the results, are assessed after the processing of several network trainings and simulations.

- Brake reaction time in respect to the time to intersection when the TC gets the intersection

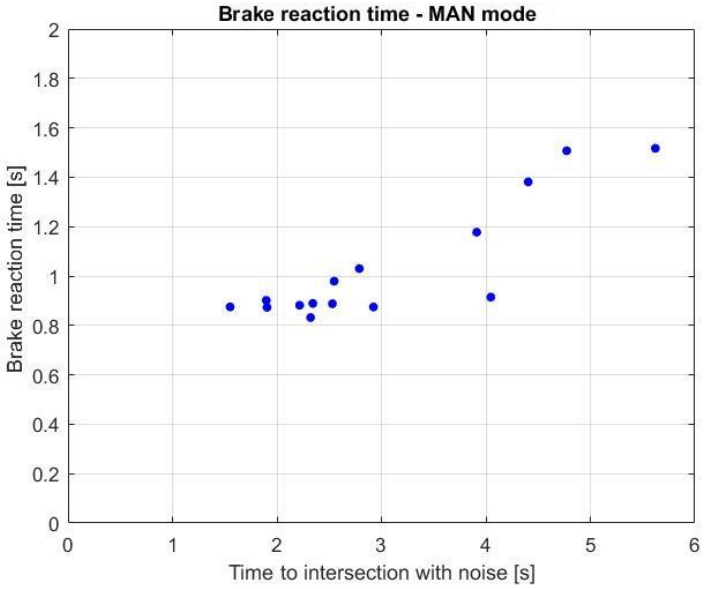

Figure 88 - Brake reaction time in respect to TTI with noise for MAN mode.
$\rho = 0{,}764$

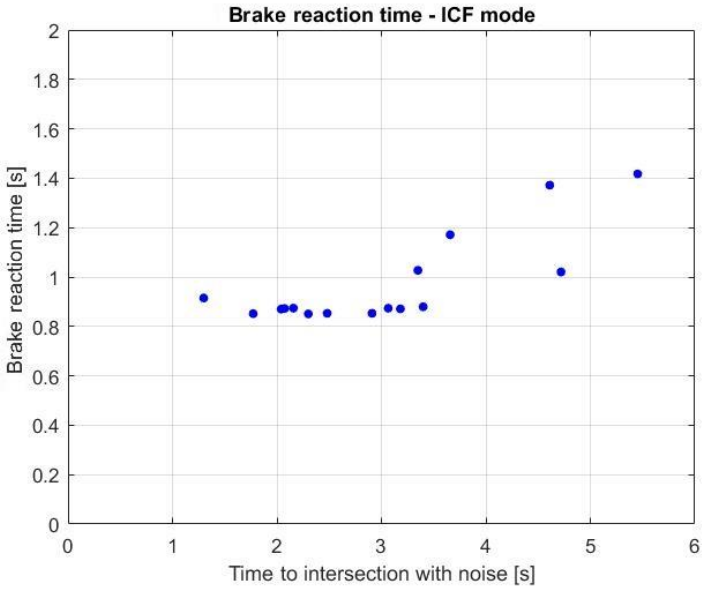

Figure 89 - Brake reaction time in respect to TTI with noise for ICF mode.
$\rho = 0{,}671$

Both for MAN (*Figure 88*) and ICF (*Figure 89*) mode the brake reaction time increases in a similar way with the time to intersection. The resulting *Spearman* coefficients are very similar to the ones found in the analysis (0). This means that, in this example, the model is able to predict well this relationship even with new input data. These results remain good and stable even after whichever simulation, thus this example represents meaningfully the general behaviour of the model regarding this relationship.

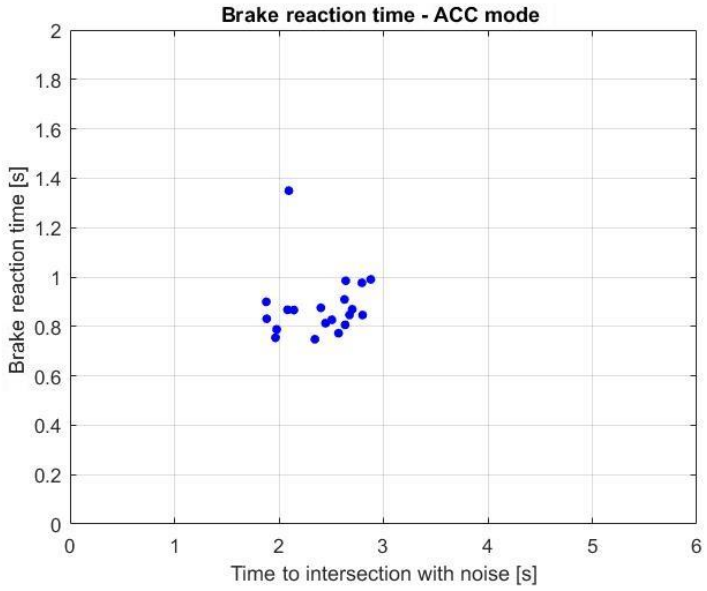

Figure 90 - Brake reaction time in respect to TTI with noise for ACC mode.
ρ = 0,298

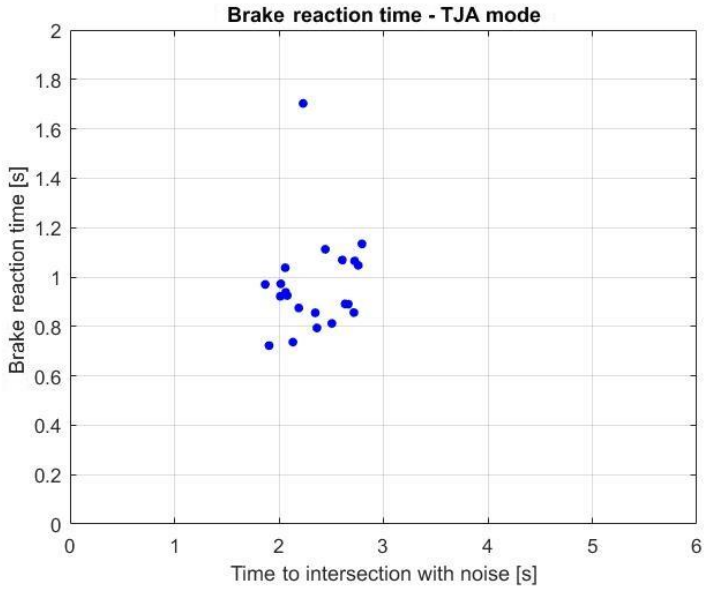

Figure 91 - Brake reaction time in respect to TTI with noise for TJA mode.
ρ = 0,244

Considering the semi-automated driving modes (*Figure 90-91*), they assume a similar behaviour. Since the random noise values added to the TTI are included in the range of ±0,5s, all the points are grouped in a narrow region, which is centred around the initial fixed time to intersection (2,37s). Despite this, the *Spearman* correlation coefficients are reasonable in respect to the analyses: the model is able to predict properly the results considering unseen input data. Even after several simulations, it was noted that these results, for what regards the semi-automated modes, are quite steady, but slightly less in respect to the ones obtained for the manual driving modes.
The mean brake reaction times seem to be comparable between all the four driving modes, which reflects the results of the analyses.

As stated in the previous paragraph 3.2.9 it is possible to investigate the relationship between brake reaction time and perception time.

- Brake reaction time in respect to the perception time with noise

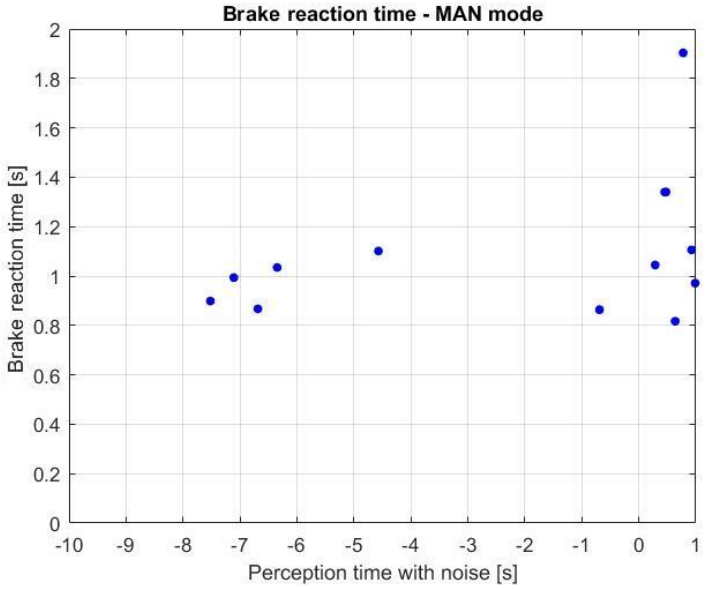

Figure 92 - Brake reaction time in respect to the perception time with noise for MAN mode.
$\rho = 0{,}550$

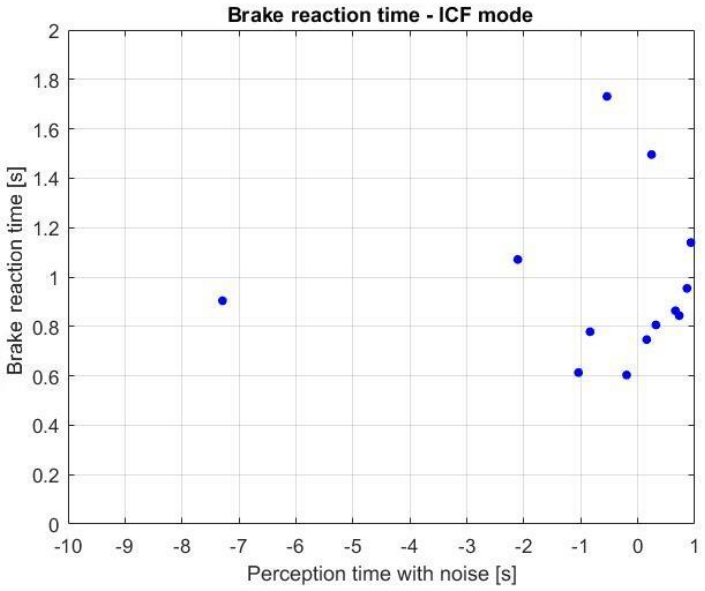

Figure 93 - Brake reaction time in respect to the perception time with noise for ICF mode.
$\rho = 0{,}250$

Figure 92 represents the relationship between brake reaction time and perception time considering the MAN driving mode. The points are more spread along the X axis in respect to the ICF mode, which is shown by *Figure 93*. This means that the neural network, even if fed with new data, is able to respect the trend found in the analyses: generally, the drivers in ICF mode perceive the TC later in respect to the same scenario in MAN driving mode. Moreover, it seems that in both the manual modes simulated, the brake reaction times tend slightly to increase when the TC is noted later by the driver. This is in accordance with 3.2.9 as well.

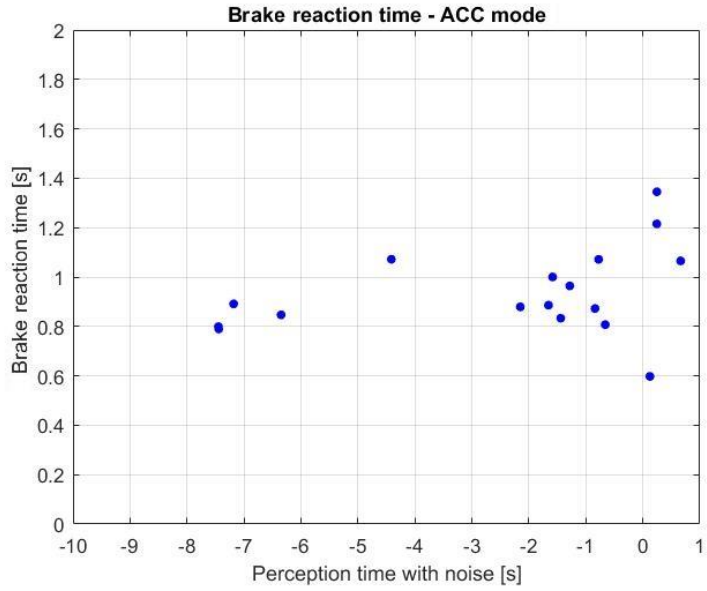

Figure 94 - Brake reaction time in respect to the perception time with noise for ACC mode.
$\rho = 0{,}550$

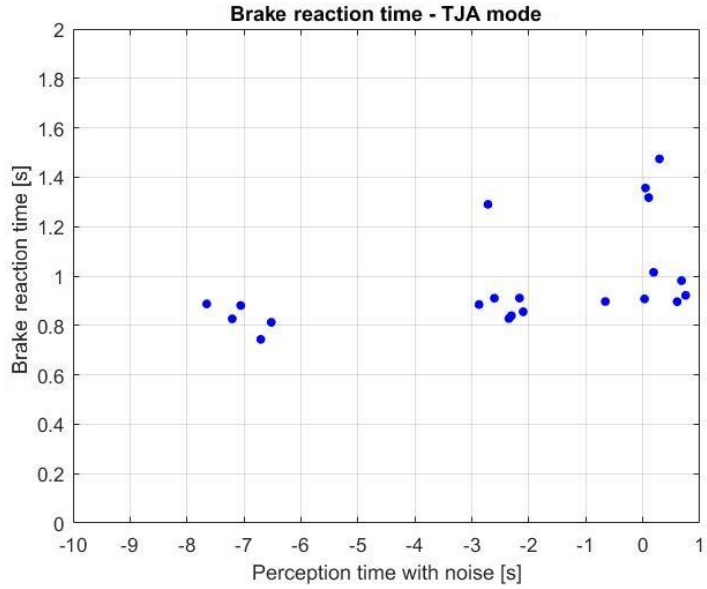

Figure 95 - Brake reaction time in respect to the perception time with noise for TJA mode.
$\rho = 0{,}657$

Figure 94-95 represent the brake reaction time in respect to the perception time for the semi-automated driving modes. In both the graphs the points are more spread with respect of *Figure 93*, this is in accordance with the results of the analyses. The *Spearman* coefficients are quite good: brake reaction time tends slightly to increase at later perception times. As observed during several simulations, the resulting brake reaction times never assumed unrealistic values, however the *Spearman* coefficients are quite variable depending on the random noise added to the inputs. It is possible to state that the prediction of this kind of relationship taking into account new input data is slightly less reliable in respect to the previous one (brake reaction time with respect to time to intersection).

- Mean brake pedal force in respect to the time to intersection

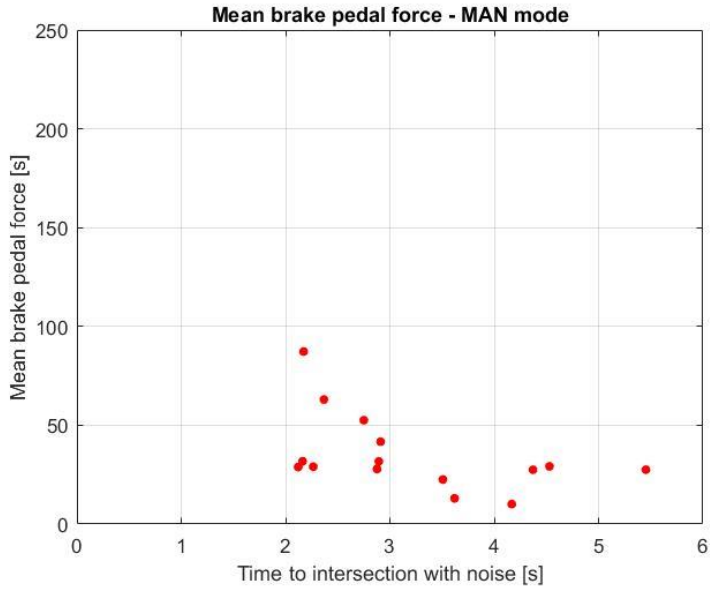

Figure 96 - Mean brake pedal force in respect to TTI with noise for MAN mode.
ρ = -0,568

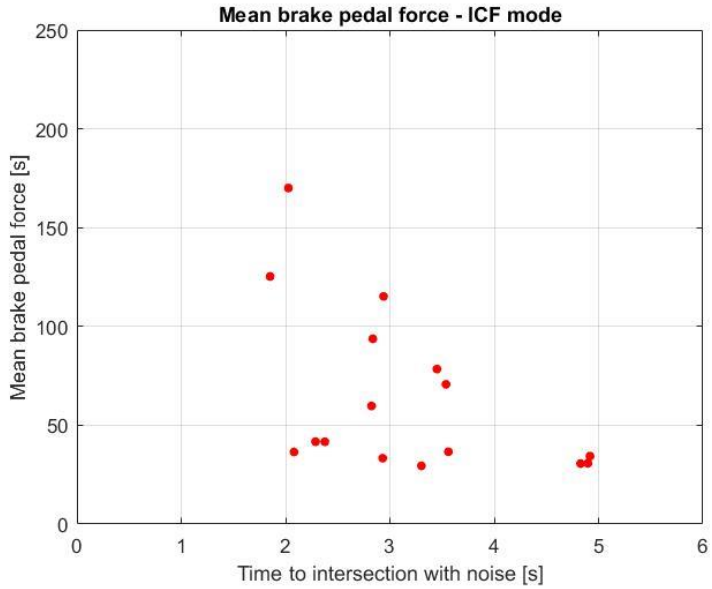

Figure 97 - Mean brake pedal force in respect to TTI with noise for ICF mode.
ρ = -0,553

Figure 96 represents the mean brake pedal force simulated (MAN mode) by the model in respect to a time to intersection different from the one considered during the training process. The trend seems good: the mean force pressed by the drivers decreases at high time to intersection (low risk). This behaviour is similar to the one referred to the ICF driving mode (*Figure 97*), which, however, seems to be more accentuated.
Even after several simulations, the trend of both the MAN and ICF modes always resulted as the ones showed in this example, whatever the random noise is: the model's generalization capability and robustness, in this case, is satisfactory.

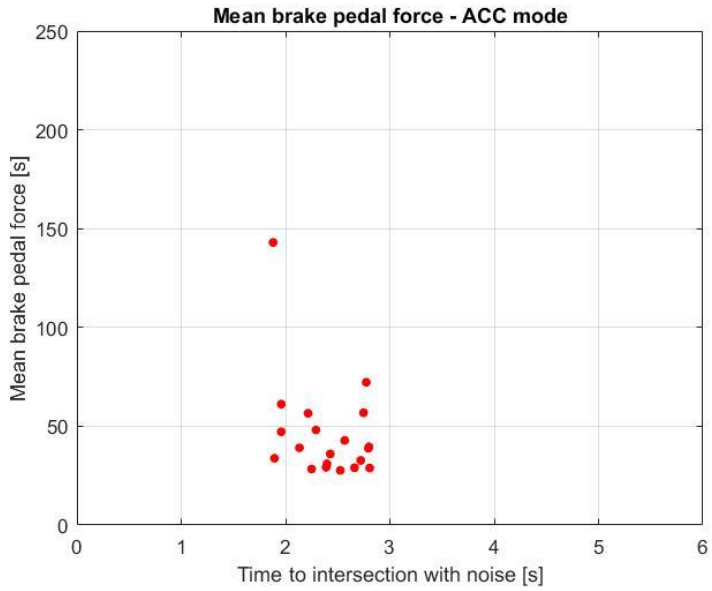

Figure 98 - Mean brake pedal force in respect to TTI with noise for ACC mode.
ρ = -0,242

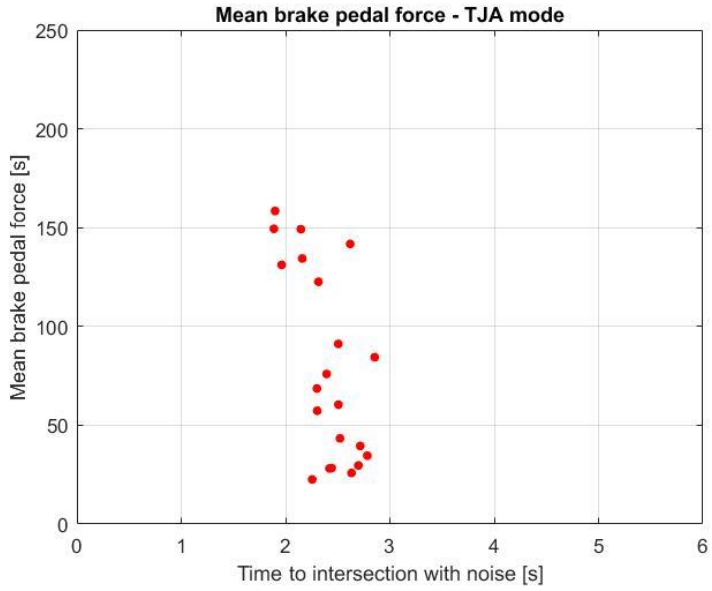

Figure 99 - Mean brake pedal force in respect to TTI with noise for TJA mode.
ρ = -0,518

Looking at the graphs of the semi-automated modes, it is possible to see that regarding the ACC mode (*Figure 98*), the model simulates, on average, lower mean forces than the ones referred to the TJA mode (*Figure 99*). This is in accordance with 3.2.7. In both ACC and TJA the points are grouped in a range of 1s referred to the time to intersection: this is due to the little amount of noise added (same situation of *Figure 90-91*). As for the manual driving modes, a quite good correlation is found, the model seems able to predict the values of mean brake pedal force in respect to new input values. However, for what concerns the semi-automated modes, these results didn't result so much steady after several simulations. Even if the values of mean brake pedal force calculated never assumed unrealistic values, the *Spearman* coefficients tend to vary slightly depending on the random values of noise added to the inputs.

- Maximum vehicle's deceleration in respect to the time to intersection

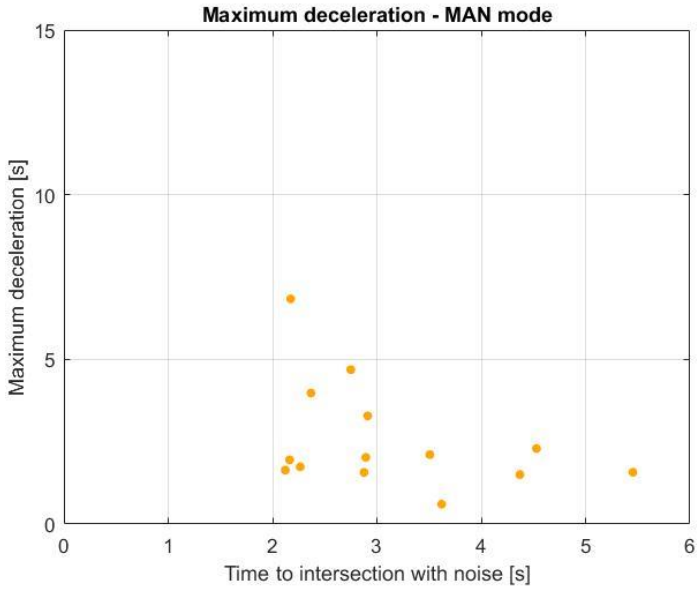

Figure 100 - Maximum vehicle's deceleration in respect to TTI with noise for MAN mode.
ρ = -0,379

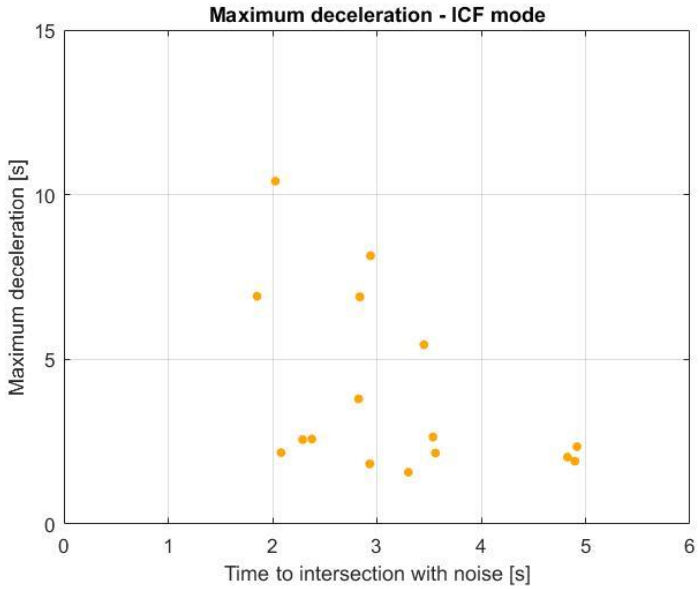

Figure 101 - Maximum vehicle's deceleration in respect to TTI with noise for ICF mode.
ρ = -0,491

The prediction of the maximum deceleration reached by the vehicle during braking, concerning both MAN (*Figure 100*) and ICF (*Figure 101*) driving modes, is in accordance with the results of the analyses 3.2.6. In fact, high values of deceleration correspond to small values of time to intersection (high risk). It is noted that this trend is slightly accentuated for the ICF driving modes. The model is able to manage properly new input data, different with respect to the ones used for the training process. These trends are stable even with the running several simulations: whichever random noise added to the input doesn't affect the performance of this prediction.

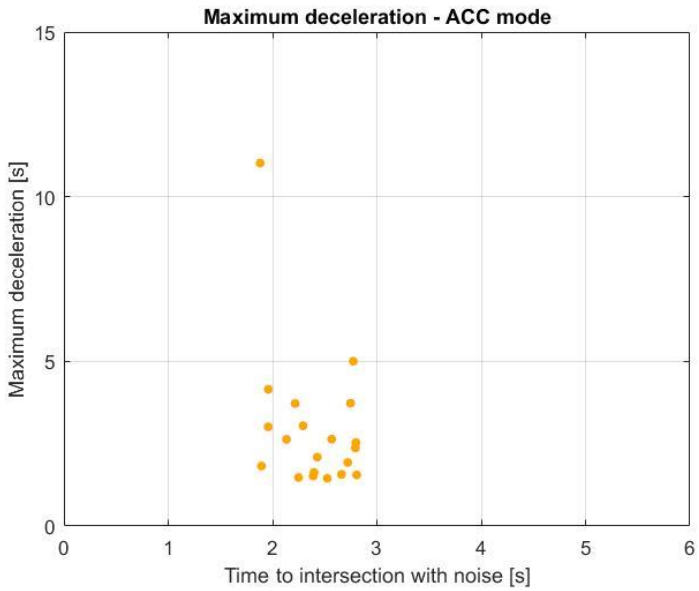

Figure 102 - Maximum vehicle's deceleration in respect to TTI with noise for ACC mode.
ρ = -0,220

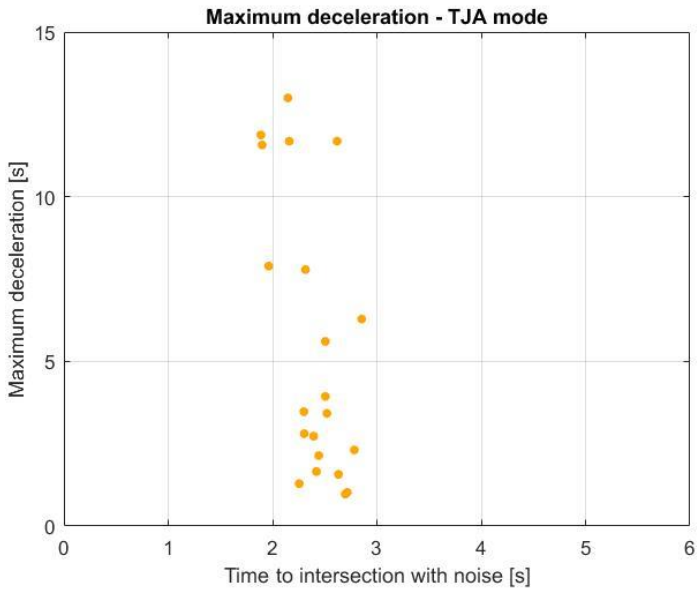

Figure 103 - Maximum vehicle's deceleration in respect to TTI with noise for TJA mode.
ρ = -0,543

As for the previous graphs regarding the outputs of semi-automated modes in respect to the time to intersection, the points in *Figure 102-103* are grouped in a narrow region due to the low amount of noise added to the input. However, the model seems able to perform a good prediction, the shape of the trends is steady even after several simulations. The points in ACC mode are more grouped at lower values of maximum deceleration in respect to the ones of TJA mode. This is in accordance with the results of the analyses (3.2.6).
With the running of several simulations, it was noted that the random noise values added to the inputs, seem to slightly vary the resultant *Spearman* coefficients. However, the maximum deceleration resulted from the model simulations assumed always reasonable values, in respect to the inputs.

The following table collects all the resultant *Spearman* coefficients showed in the previous graphs. It contains both the results regarding the performances of the model fed with the initial input data and the ones referred to the model fed with new inputs.

Table 22 - Spearman coefficients regarding the relationships modelled for the examples considered. Comparison between simulations run with original and noisy input data.

		MAN	ICF	ACC	TJA
Original input data	**BRT vs TTI**	0,782	0,697		
	MBPF vs TTI	-0,421	-0,726		
	MVD vs TTI	-0,371	-0,510		
	BRT vs PT	0,505	0,046	0,185	0,338
Input data with noise	**BRT vs TTI**	0,764	0,671	0,298	0,244
	MBPF vs TTI	-0,568	-0,553	-0,242	-0,518
	MVD vs TTI	-0,379	-0,491	-0,220	-0,543
	BRT vs PT	0,550	0,250	0,550	0,657

It is notable that, for the considered example's results, the neural network is able to predict the relationships desired, in a good way even with a new input data set, not used for the training process. These results are good in particular for the manual driving modes. As stated before, the model prediction of the outputs, regarding the semi-automated modes, sometimes could show a weak stability: it has been observed that, with the running of several simulations, the *Spearman* values slightly changed.
Considering all the relationships simulated, they respected the general trends found during the analyses: the values of brake reaction times, referred to all the four driving modes, on average, assumed similar values. Regarding both the mean brake pedal force and the maximum deceleration, the output values simulated for ACC and TJA modes assumed slightly higher values than the ones of MAN and ICF modes.
All the graphs regarding the TTI in semi-automated driving modes (*Figure 90, 91, 98, 99, 102, 103)* are characterized by outputs grouped in narrow regions, this is due to the fact that the random noise added to the initial fixed value of the time to intersection is quite little (noise range: ±0,5s): as a consequence, the range of TTI values investigated for what concern these driving modes is of only 1s.

In order to better assess the model behaviour concerning the prediction of the ACC and TJA modes outputs in a wider range, it is possible to add higher random noise values to the time to intersection.
It was chosen to increase the random noise (concerning only the TTI), with values included in a range of ±2s: in this way, the time to intersection referred to the entrance of the TC varies randomly in a range of 4s, delimited between +0,37s and +4,37s (initial fixed TTI value is 2,37s).

The following graphs show examples of results referred to the performances of the model, fed with the new input data, as just described.

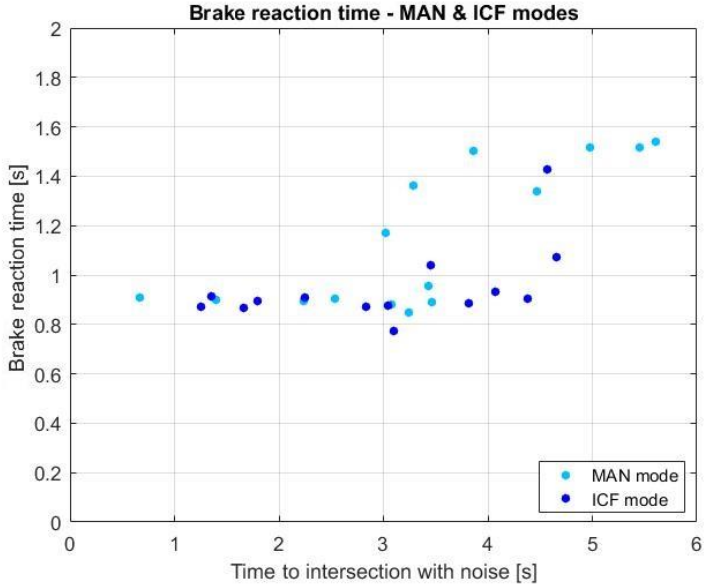

Figure 104 - Manual modes, brake reaction time in respect to TTI with ±2s of noise

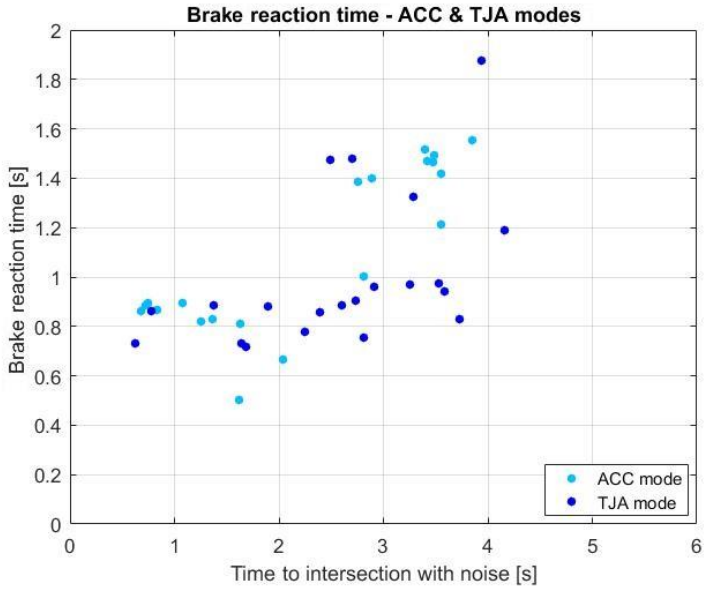

Figure 105 - Semi-automated modes, brake reaction time in respect to TTI with ±2s of noise

Even with a higher noise, the prediction of the brake reaction times in respect to the TTI is good, this is true in particular for the manual modes (*Figure 104*). Regarding the semi-automated modes (*Figure 105*), it is noted that the predicted values are more spread than the ones referred to the manual modes. No significant trend differences are found between MAN and ICF modes, as well as between ACC and TJA modes.
The higher random noise added to the TTI allows to investigate a wider range of values. The model seems able to extrapolate with a relevant reliability the desired results, starting from input data never managed during the training process. Even during the running of several simulations, the performance of the neural network remains stationary, the model is robust whatever random noise is added (in the range considered). This is true in particular for the manual driving modes.

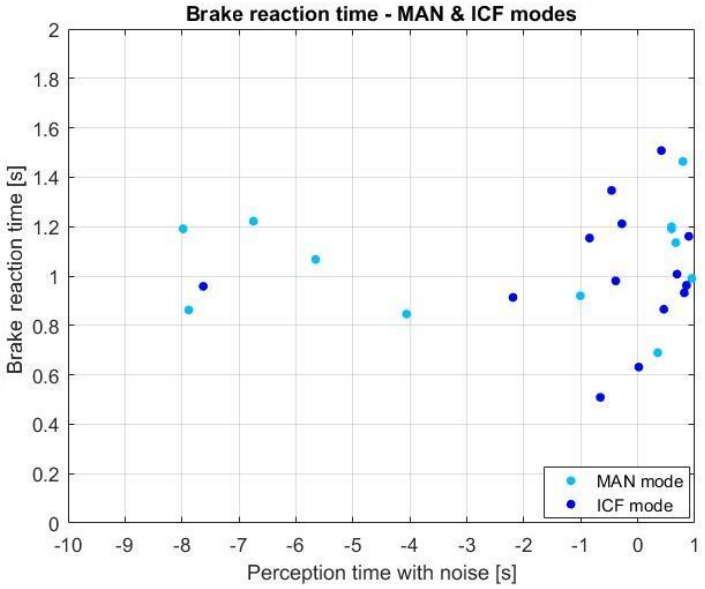

Figure 106 - Manual modes, brake reaction time in respect to the perception time with ±2s of TTI noise

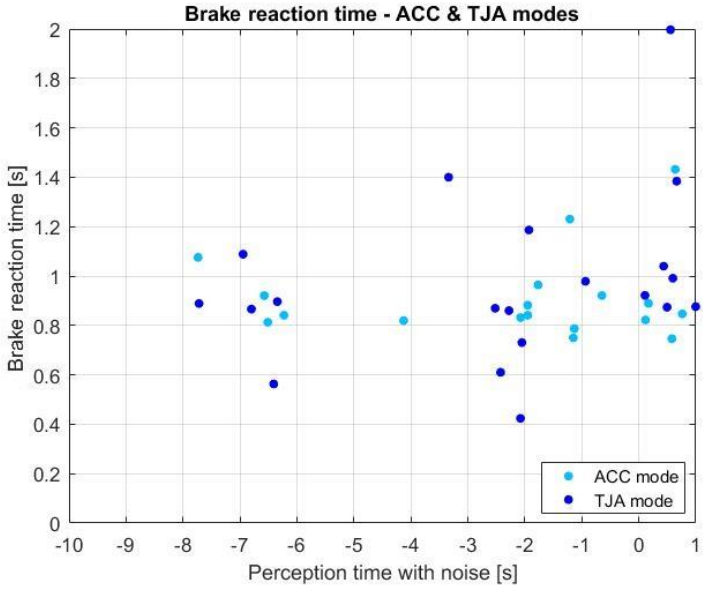

Figure 107 - Semi-automated modes, brake reaction time in respect to the perception time with ±2s of TTI noise

With a higher noise, the results about the relationship between brake reaction time and perception time are still good (*Figure 106-107*). In particular, looking at the manual modes (*Figure 106*), the model is able to maintain the characteristics regarding the ICF mode analysed in 3.2.9: the dark blue points are mostly placed at later perception times, as expected. The other driving modes are characterized by points more spread along the axis referred to the perception time. These trends resulted quite steady (sometimes the *Spearman* coefficients changes slightly) even during the running of several simulations. Therefore, whatever the higher noise is, the performance of the neural network, regarding such relationship, is only slightly affected.

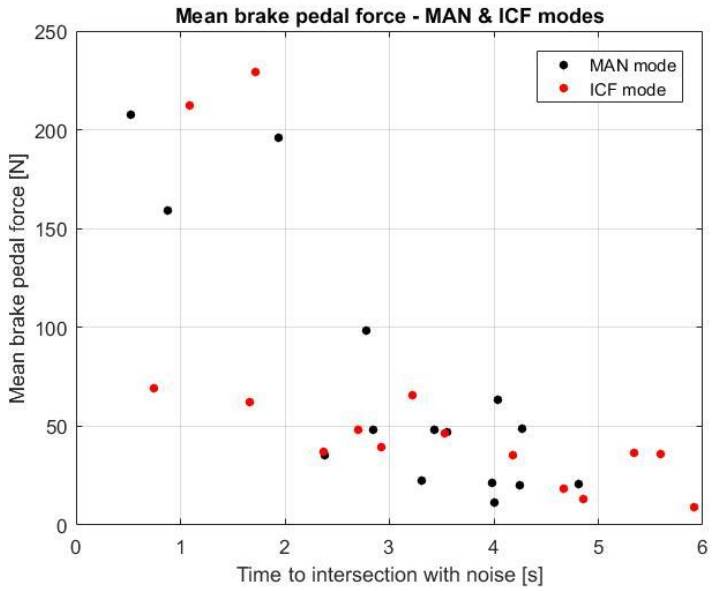

Figure 108 - Manual modes, mean brake pedal force in respect to TTI with ± 2s of noise

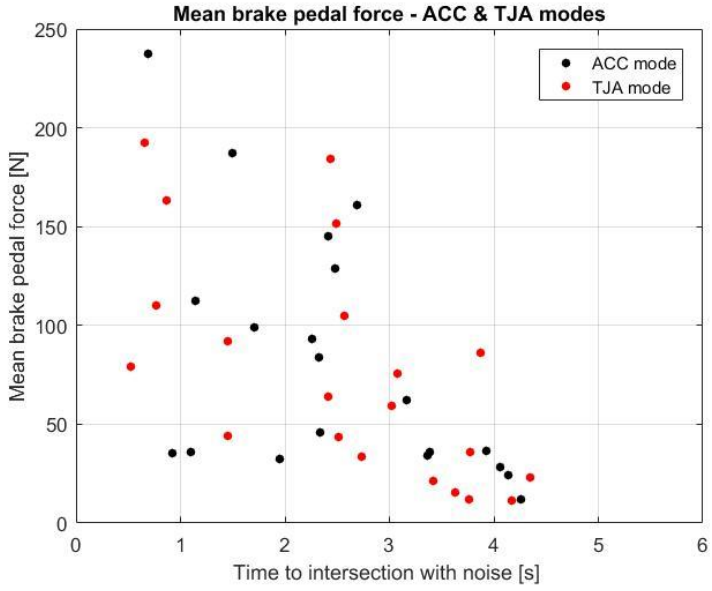

Figure 109 - Semi-automated modes, mean brake pedal force in respect to TTI with ±2s of noise

The correlation between mean brake pedal force and TTI is really good also with new input data: higher times to intersection correspond to lower mean brake pedal forces. This is true mainly for the manual modes (*Figure 108*). However, this trend is well confirmed also by the simulations of the semi-automated driving modes (*Figure 109*): even if, comparing with the manual modes, the points are more spread in the space, the model is able to extrapolate and to predict in a really good way the results. As regard to ACC and TJA modes, the high noise added to the TTI allows to explore a wide range of values, in this way the limitation imposed by the design of the experiment (TTI fixed) is by-passed. These results remain good (mainly for manual modes) even after several training processes and simulations, this is meaningful of the robustness of the model's capability of prediction.

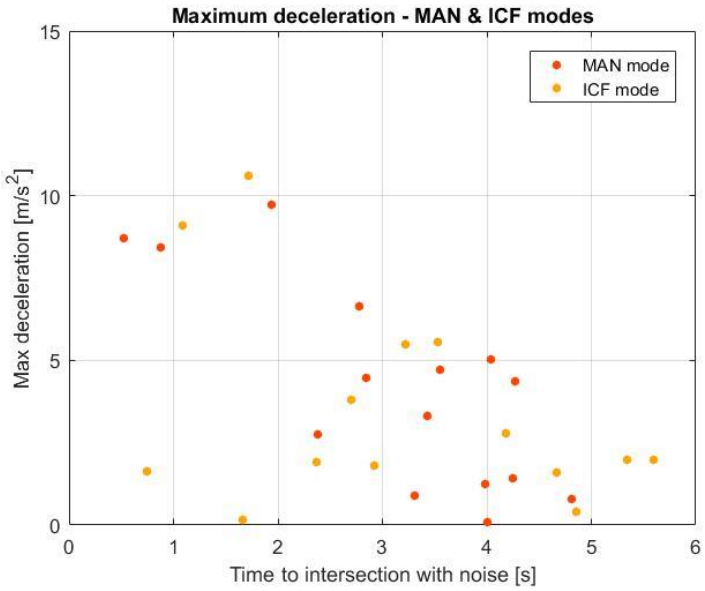

Figure 110 - Manual modes, maximum vehicle's deceleration in respect to TTI with ±2s of noise

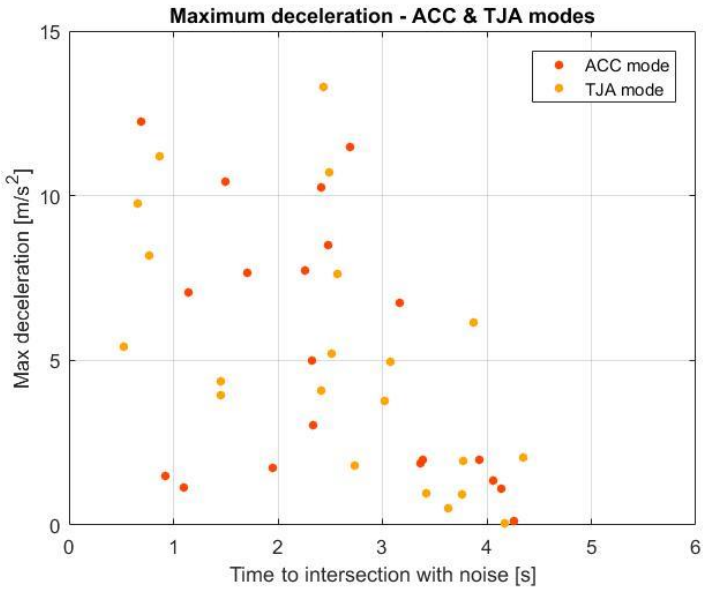

Figure 111 - Semi-automated modes, maximum vehicle's deceleration in respect to TTI with ±2s of noise

As regarding the maximum longitudinal deceleration (*Figure 110-111*), the neural network is capable of managing inputs very different in respect to the ones considered during the learning process. The trend of the maximum deceleration simulated is quite similar between manual and semi-automated modes. The values are always positive and reasonable, which means that the performance of the model is reliable and provides realistic results, whatever the random noise is applied. The running of several simulations assessed the same trends showed here: the model is able to predict such relationship in a quite steady way, this is true in particular for the manual driving modes.

As referred to the examples of outputs showed, the following *Table 23* summarizes the resultant *Spearman coefficients* of each driving mode.

These values are referred to the last situation considered, in which the model is fed with noisy input data, and in particular the time to intersection is modified adding random values included between a range of ±2s. The meaning of the coloured cells will be explained and discussed at paragraph 5.2.

Table 23 - Spearman coefficients obtained with new input data (TTI noise: ±2s)

	MAN	ICF	ACC	TJA
BRT vs TTI	0,675	0,715	0,713	0,613
MPF vs TTI	-0,646	-0,815	-0,508	-0,701
MLD vs TTI	-0,643	-0,238	-0,405	-0,651
BRT vs PT	0,429	0,188	0,144	0,357

Table 23 is now compared with the following one (*Table 24*), whose values have already been showed before inside *Table 22*. It is referred to the previous situation in which the time to intersection was modified adding random noise values included between a range of ±0,5s:

Table 24 - Spearman coefficients obtained with new input data (TTI noise: ±0,5s)

	MAN	ICF	ACC	TJA
BRT vs TTI	0,764	0,671	0,298	0,244
MPF vs TTI	-0,568	-0,553	-0,242	-0,518
MLD vs TTI	-0,379	-0,491	-0,220	-0,543
BRT vs PT	0,550	0,250	0,550	0,657

Observing the two tables, it is notable that the results found with higher TTI noise are still good. The model is able to predict the output values even with a very different new input data set. It has been noted that, except for an unavoidable variability, the performances of the model remain satisfactory also during the running of several training processes and simulations.
The increase of the TTI noise values allows to verify the model's generalization capability of the results also regarding the semi-automated modes. It couldn't have been properly assessed with a small variability of TTI values. Exploring a wider range of input TTI values, the trends of the outputs, regarding the semi-automated driving modes, seem good and reasonable.
These considerations are meaningful of an appropriate behaviour of the neural network. The results are, as expected, affected by an inevitable variability due to a low quantity of input data used for the training process, but the model shall keep a good capacity of prediction. It seems quite able to extrapolate the results even with a limited range of input data values used for the training process.
The model designed can compute the outputs regarding the driver's reactions during braking without falling in overfitting or underfitting situations.

4.2.4 Application

The last part of this section is dedicated to a practical application of the neural network described. As already said, this model aims to be a useful tool in order to predict the braking behaviour of a driver in a similar intersection scenario. In order to do this, it has to be able to take into account the initial conditions regarding whichever driver, including obviously the case of a single driver. It is precisely the latter a possible interesting and concrete model's usage.

After the training process, the neural network is ready to be used. It has been designed in order to facilitate the insertion of new input data. The following *Figure 112* is an input box example extracted from the Matlab script. It takes as input data the driving information described in 4.1.2 of a single driver. In particular, it is possible to select the driving mode considered, to insert the personal information of the driver, as well as the time to intersection and the perception time.

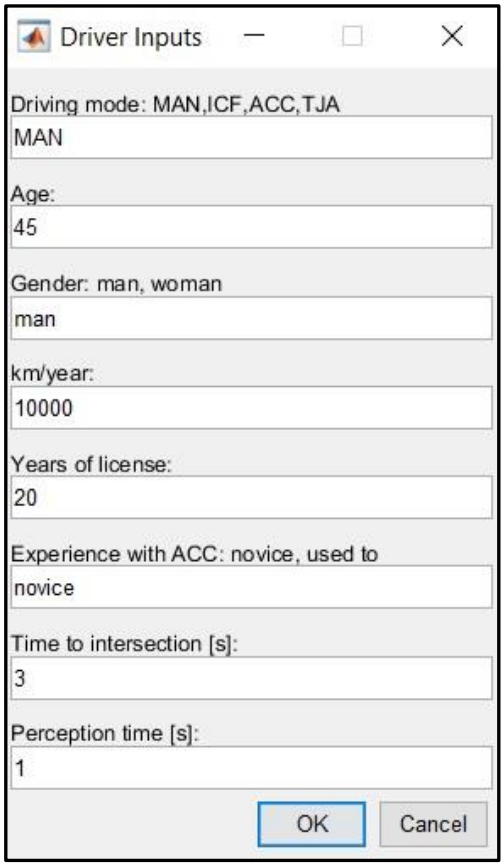

Figure 112 - Example of input box extracted from the Matlab code

The user can just easily fill in all the information required by the box, and after that, the model starts calculating the outputs referred to the driver considered. At the end of the process the following message box appears.

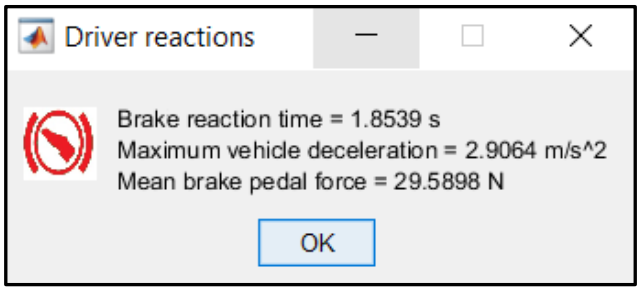

Figure 113 - Message box regarding the results of the model

Figure 113 shows the resulting outputs calculated by the model: the brake reaction time, the maximum vehicle deceleration and the mean brake pedal force. These values are referred to the specific driver and conditions selected.
The process just described is fast and easily repeatable for whichever case desired.

5 Discussion

This chapter is divided in two sections: First the discussion concerning the data analyses and second about the driver behaviour modelling. These parts represent the two main phases of the project.

5.1 Analyses

In these kinds of experiments, in which the boundary conditions are not always the same, the main issue is to define a feature in common. Something that can synchronize the different drivers' experiences and that can permit the comparison between them. In this project the entrance of the TC into the intersection was considered as the common stimulus that caused drivers' reactions between the simulations. However, as explained in chapter 2, this event did not occur always at the same driver's position for the two manual modes, but it did for the semi-automated ones. Indeed, the TC's entry was always defined by the lead vehicle's crossing. This implied that participants' position at this time was dependent on how close to the TC they were driving. As a matter of fact, this quantity in the two semi-automated modes was fixed by the system and so always constant.

As expected, braking was the most common action performed by the participants that had a reaction to the TC's movement. This is true for all the driving modes. In MAN mode, they were 75% of the total, in ICF 70%, in ACC 71%, in TJA 75%. Small oscillations regarding the steering wheel were found, in most of the cases linked with braking behaviour. However, looking at the amplitude and at the frequency of the steering wheel angle changes, it was not considered as an evasive steering manoeuvre but rather a corrective one. This behaviour can be attributed to the fact that there was only one lane per direction and many cars coming from the opposite way. In sight of this, it was impossible for the participants to avoid the TC by an evasive manoeuvre or by overtaking. Furthermore, this behaviour was confirmed by the graphs of the longitudinal and lateral accelerations, too. In particular, from the graph of the maximum lateral accelerations it can be seen that all the values except one were in the range of [-2, +2] m/s^2. If the participants had tried to avoid the TC, higher values of lateral accelerations would have been detected. Because of this, steering was not further analysed.

Concerning the two manual modes, it was found out that 25% of drivers in MAN mode and 26% in ICF mode released the throttle instead of braking. This behaviour can be attributed to the fact that drivers who just left the throttle had higher TTI in respect to those who decided to brake. Looking at the averages, it can be seen a difference in TTI of 0.75 seconds in MAN mode and of 3.14 seconds in ICF mode between these two kinds of actions. This means, it was enough to leave the gas pedal for all those participants that were driving at a lower speed and arrived at a higher distance from the intersection when the TC got into it.
In all driving modes, important results were obtained from the analyses of brake reaction times. Indeed, no significant differences were detected between the two manual modes and the semi-automated ones, even if the criticality was not always the same. This outcome is in contrast with the results of [27], in which higher reaction times were evident in the two semi-automated modes compared to the MAN and ICF mode. However, the scenario was different, being a cut-in scenario. As shown in *Figure 7*, the participant was driving on a 2+1 road when suddenly another vehicle

coming from the next lane cut its path. Anyway, the experiment was the same, so the participants considered were almost the same since the participants of the experiment drove through several different scenarios, among which the cut-in and the T-intersection. This result is interesting regarding the study of brake reactions with semi-automated systems. It indicates that same drivers can react in different ways giving more or less trust to the system according to the situation. Here, in the T-intersection, drivers reacted much sooner compared to the cut-in scenario. These fast reactions can be related to a lack of trust in the system or to the different type of scenario (T intersection vs. cut-in). As a matter of fact, in our T-intersection scenario the averages of the brake reaction times in the four driving modes are all between 0.85 sec and 1.05 sec. On the contrary, in the cut-in scenario the brake reaction times driving in manual modes were around 1.35 sec and in the two semi-automated modes were around 3-3.5 sec. Moreover, no significant differences were found in the T-intersection scenario between drivers used to ACC system and those ones novice to ACC. This is again in contrast with the results found in the cut-in scenario, in which it was detected that drivers used to ACC system were faster compared to the novices to ACC. The difference in time in [27] was about 0.5 sec between these two groups of drivers. On the contrary, here, the maximum difference is about 0.2 sec in TJA mode, whilst same averages were found out for ACC mode.

Concerning the brake reaction times of all drivers, as in [27], no significant differences were found between the MAN mode and the ICF mode. This means that following a lead car did not alter the alertness of drivers. No significant differences were found between the two semi-automated systems. This is in accordance with the results in [27]. Drivers reacted in the same way with TJA and ACC although the scenario was not completely longitudinal as the cut-in one, but involved vehicles coming from a perpendicular way.

In the manual modes, a medium direct correlation was found between brake reaction times and TTI in the moment in which the TC enters the intersection. For low TTI (more critical situation), lower reaction times were found. On the contrary, for high TTI (less critical situation), slightly higher reaction times were detected. So, as expected, drivers generally reacted faster in more critical situations. This connection was impossible to find in the two semi-automated modes, due to the fact that in these cases the TC entered always at the same time. As a matter of fact, the ego vehicle's speed and the distance from the car ahead were defined by the semi-automated systems.

The correlation found for the two manual modes between brake reaction times and TTI could be used also to explain such as fast and unexpected braking reactions in the semi-automated modes: lower values – about 0.6 – 0.7 smaller – of TTI can be noted in the semi-automated modes compared to the averages of the manual modes. This result can indicate that the scenario was more critical during driving with semi-automated systems compared to manual driving. Nevertheless, no significant differences in brake reaction times were found between the four driving modes. Moreover, even the small difference – about 0.1 – 0.2 sec. – between the manual and semi-automated modes wouldn't be present taking into account only the driving with similar criticality (TTI around 2.37 sec.).

Without any video of the simulations, it was not possible to clearly define the level of expectancy of the scenario analysed. Considering the situations described in [23] and argued in the introduction, this scenario could be placed between an "unexpected common" event and a "fully anticipated" one. It could be defined unexpected because the TC was used to get the intersection when the participant was almost in proximity

of that. But, at the same time it could be defined also anticipated, since the TC was visible by the participant's point of view. Taking into account also the reaction times related to these two event's categories, the T-intersection could directly find a place between them. Indeed in [23] it is stated that for "fully anticipated" events brake reaction times are around 0.70 – 0.75 sec, whilst for "unexpected common" events they are around 1.25 sec. As stated before, in this scenario values around 0.85 – 1.05 sec were detected.

Looking at the semi-automated modes, six participants did not have any reaction to the TC's entry both during driving with ACC and during driving with TJA. Also, no clear correlations were detected neither with participant's age, nor with the experience that they had with the ACC system. This outcome can be attributed to two different factors, either to an over reliance towards the semi-automated systems or to a learning effect due to the repetition of the scenario. Indeed, it was identified that for ten out of twelve participants, the T-intersection scenario with TJA or ACC happened as third or fourth repetition during experiment. So, it is possible that performing this scenario several times, some participants decided to do not try to avoid the TC.

Besides the reaction times, the analyses focused also on how the participants were braking. Significant higher brake jerks were identified in the two semi-automated modes. In particular, average values equal to 4.93 m/s^3 and 4.70 m/s^3 were detected in manual modes, whilst 6.81 m/s^3 and 6.98 m/s^3 in semi-automated modes. Moreover, in ACC and TJA mode, higher values were shown for all those drivers that were used to the ACC system. Taking into account that the average age of drivers used to ACC system is higher compared to the novice ones, this result can be directly linked to the age of the participants. Indeed, it has been shown, that drivers that braked harder were on average ten years older than the others. No analyses regarding the age of the drivers were performed for the two manual modes due to the fact that the boundary conditions were never the same: the TC was always entering at different times.
As stated previously, on average, the scenario in semi-automated modes can be considered more critical compared to the manual modes due to the simulation setup. So, the results for the brake jerk are in accordance with the findings in [23] where it is stated that the brake jerk and the maximum deceleration are directly proportional to the risk ($1/\tau_b$) in critical scenarios. However, in our analysis by driving mode, no relevant correlations were found between these two variables.
Regarding the maximum deceleration, a trend analogue to the brake jerk is present. Indeed, once again a significant difference was detected between manual and semi-automated modes. In particular, average values equal to 3.01 m/s^2 and 3.47 m/s^2 were detected for maximum decelerations in manual modes, whilst 4.58 m/s^2 and 5.54 m/s^2 in semi-automated modes. In the latter modes, older participants and experienced to the ACC system reached higher values. Furthermore, no significant correlations are present between the maximum decelerations and the risk of the scenario ($1/\tau_b$), except for the ICF mode. In this case, a medium direct correlation between the two variables was found. According to what was stated in [23], this result could bring out the presence of criticality in the scenario in ICF mode.
As expected, the mean brake pedal force analysis was consistent with the maximum deceleration.
So, summarizing the brake usage, it can be stated that the participants braked in a harder way driving in semi-automated modes compared to driving in MAN and ICF modes. Brake jerk and maximum deceleration values often showed the presence of emergency braking during driving with semi-automated systems. As a matter of fact,

similar values were detected in [23], in which car crashes and near crashes in real scenarios were taken into account. This outcomes' affinity is also an indication that drivers in this simulator study braked as in real situations. However, it has in previous studies been demonstrated that this is not always true [14]. Indeed, drivers' behaviour in simulator studies can distinguish itself from real situations depending on the scenario and on the sub-tasks [14]. Concerning the two manual modes, brake jerk and maximum deceleration values confirmed that emergency braking were less frequent in these cases. This can be explained by the circumstance of higher criticality in ACC and TJA scenarios. However, it can be attributed also to the fact that driving with semi-automated systems implies to have no throttle's control. So, drivers have one pedal less to control the deceleration of the vehicle. This factor can reduce driver's sensitivity on braking. Moreover, within the automated driving modes, it can be detected that drivers used to the ACC system, that are also older (on average), braked harder compared to the novices. This could mean that they were more scared about the TC and they could trust even less the system. Unfortunately, the latter statement did not find any confirmation in the brake reaction times' analyses.

The general trend of drivers' gaze behaviour seems to be similar through all driving modes. So, drivers looked at the same directions in the time window analysed, regardless of driving modes. On the contrary, the quantity of time spent to look in those directions (mostly straight and to the right) seems to be affected by the modality in which they were driving. Comparing the two manual modes, drivers in ICF mode looked less to the right than drivers in MAN mode as expected. So, drivers following another vehicle are more focalized on the lead vehicle which has been observed before [26].

Furthermore, comparing the semi-automated modes, it was found that drivers look more to the right driving with a TJA system. This can be related to the fact that drivers are more likely to engage in other tasks travelling with this system [31]. They could feel more confident to look to the sides, knowing to have not only a longitudinal support, but also a lateral one.

Concerning driver's perception of the TC, interesting results were detected. In the analysis of the gaze behavior, drivers' perception was intended as the first time they were presumably looking towards the TC while approaching the intersection (several consecutive glances in direction of the TC). As expected, drivers in ICF mode recognize the presence of the TC later than driving in MAN mode or with semi-automated systems. On average, in ICF mode they realized its presence 0.63 sec before its start, whilst in MAN mode 1.91 sec, in ACC 1.71 sec and in TJA 2.30 sec before. This result is once again in accordance with [26]. As a matter of fact, it confirms that driving following a car ahead can decrease the spread of search in the horizontal direction, increasing the concentration on the vehicle ahead. Furthermore, this kind of behaviour could lead drivers to be less aware of the threat, increasing in this way the criticality of the situation.

Finally, no strong correlations were found out between brake reactions and perception times. So, even if drivers realized the presence of the TC several seconds before its start, they had similar reactions to those ones that saw it only at the last moment. Hence, seeing it a lot before does not give any additional clue that it will suddenly enter. However, it has to be stated that perception times that are much before the TC's entry are less reliable than those ones close to the time zero. This is due to the fact that several seconds before, the participants are too distant from the intersection. As a matter of fact, the angles between them and the TC are smaller than 5 deg. So,

looking in the direction of the TC might not properly mean that the driver is really looking to that, but rather only straight. Insight of this, taking into account only perception times close to time zero (-1 s, +1 s), a direct correlation seems to be present between these two factors. This result would be reasonable: it would mean that a driver reacts faster, if notes before the TC's movement. So, focusing on TC when it is on the verge of getting the intersection would logically give the driver a reaction advantage.
In sight of the performed analysis, the outcomes could be used in order to develop an ADAS capable of changing its response times in function of the scenario's criticality. In this way, the system could alert the driver in time without causing any inconvenience.

5.2 Modelling

A neural network approach was chosen for this study, using training and validation datasets from simulator experiment. Since the correlations between input and output data found weren't clearly linear, the choice of adopting a machine learning technique that allowed for non-linear modelling, was appropriate.
As described in 4.1.1 this model type is a "black box" approach. It has the advantage that it can be used when there is a correlation between the input and the output data, without exactly knowing which kind of relationship is present. The main disadvantage is that it is not possible to clearly understand which are the hidden processes with which the data are elaborated [61–66]. However, for the goal and scope of this work, that disadvantage was not considered a main factor. The matter of this study was to build a tool capable of representing the driver's reactions during the scenario analysed, regardless on the way by which it computes the results. Although we chose an ANN approach, we do acknowledge that alternative modelling approaches may have performed equally good. Such methods include other machine learning techniques or different forms of regression.

Since each model's input affects the computation of the resulting outputs, defining which inputs among the possible available ones had to be taken into account were challenging. It is important to feed the model with relevant data that carries information in regards of the desired output [62, 65, 66]. A relationship between inputs and outputs (even though weak) has to exist, but it's not important which it is, since it is a job of the neural network to manage it [53, 62, 66, 67]. All the input data by which the model was trained were judged as relevant for the output results. These decisions were taken after a long study of the available variables, in respect to the scenario analysed. Obviously, although the output results of the network depend on each input variables, the latter ones don't all assume the same importance. For example, driver's information such as the gender, the age, or the years of license, could be considered as low affecting inputs. Other input variables such as the time to intersection or the selection of the driving mode between manual or semi-automated, assumed a much more relevant importance regarding the output results. After a proper setting, the neural network can attribute greater weights to the most important input variables. Vice versa it can weigh with a lower value the less important ones [1, 10, 67].

Observing the input variables, they don't belong to the same variable type: some are discrete, while others are continuous. Moreover, some inputs regard precisely driver personal information, some variables concern the whole driving "career history", and

other variables are more specifically referred to the actual driving condition. Generally, the TTI and the perception time, strongly depend on the behaviour of the driver before reaching the intersection scenario: the TTI (at the TC entrance) is related to the distance the driver keeps to the triggering lead vehicle, which was variable for MAN and ICF modes but was kept fixed (and so the TTI) for the semi-automated modes. This determined, as a consequence, a great difference regarding the modelling activity between manual and semi-automated modes. Since the TTI played a really important role and was able to greatly affect the results of the model, the difference explained above was determinant concerning the outputs driver's reactions modelled. As regarding the perception time, such input variable was shared in the same way between manual and semi-automated driving modes. Although such input showed weak linear correlation in respect to the brake reaction time, the choice of including the perception time was made in order to better define the driver behaviour before the occurrence of the criticality. In this way, the model takes into account an input variable regarding a visual aspect, even more specifically focused on the driver behaviour in respect to the TTI. The latter consideration can be extended also for what regard the gender, the age of the driver, the km/years, the years of license and the experience with the ACC system. Even all these input variables hadn't a clear correlation with the model's outputs, however they contributed to enlarge the point of view by which the driver's behaviour was studied and modelled. In this way, the driver's reactions were derived from inputs concerning aspects of different nature. Unfortunately, a general limitation of the neural network is that they perform better if the quantity, the variability and the range of input data used for the training process is high [62, 67]. A neural network needs to be prepared on a large variety of situations, which happens only after a proper training process. However, the data available included a limited number of drivers and the variety of inputs was rather narrow.
As a consequence, the designed neural network was fed by input data that were specific for the scenario analysed. Attempts have been made to make up for this tricky situation by utilizing a training algorithm featured by a Bayesian regularization. In this way, all the available data were used in order to perform a training process as much efficient as possible. In general, such decision improved largely the performances of the neural network, regarding the modelling of both the manual and the semi-automated driving modes.

The variables used for the model's validation consisted in the correlations analysed during the study of the collected data. These latter were used as benchmark in order to judge the results found applying the neural network. In this way it was possible to understand if the model was subjected to overfitting or underfitting behaviour, as well as it was able to generalize the results even when fed with new input data. The architecture of the neural network was designed in order to allow the model to perform in the best way possible, in respect to the matter in question. In particular, the number of hidden layers, the number of hidden neurons and the training algorithm were chosen with trial and error after several attempts. The number of hidden layers was imposed to two, featured by respectively three and four hidden neurons. Such decisions allowed the present neural network to avoid the overfitting behaviour, as well as the underfitting one. Moreover, the time demanding concerning the training and simulation processes didn't result excessive. A too higher number of hidden neurons would have overly enhanced the model's learning, worsening the neural network generalization capability. Vice versa an underfitting behaviour would have

occurred with a too low number of hidden neurons [62, 67]. The model's results were based on two strong assumptions:

- All the graphs and *Spearman* correlation coefficients showed are all referred to examples of output results. As described, the variability of such results depended on the randomness regarding both the noise added to the input data during the validation phase, and the training process itself. The examples showed are meaningful of the behaviour of the model regarding such predictions. The model was trained and applied several times, at the same conditions, in order to assess the reliability of the examples showed.
- For what concerns the semi-automated driving modes, the trends of the output variables in respect to the time to intersection were assumed as similar to those referred to the manual driving modes. This was made because, as already showed, the available data didn't allow to define these correlations (TTI at TC's entrance is fixed for ACC and TJA modes), but it makes sense to think that the situation was the same: the brake reaction time increased with the time to intersection, while the mean brake pedal force, as well as the maximum vehicle's deceleration increased with a decrease of the TTI.

However, not all the correlations calculated were characterized by the same "stability". The model seemed able to predict outputs with different levels of robustness. The coloured cells of *Table 23* aim to facilitate the discussion about the model's performances.
Such table showed the resultant *Spearman* coefficients regarding the relationships modelled with input data different from the ones used for the training process.

The *Spearman* coefficients contained in the green cells of *Table 23* represent the correlations between the output variables and the time to intersection, regarding the manual modes. It is possible to notice that those values are quite good in accordance with the results obtained during the analysis, which are the reference ones. Moreover, the repetition of several tests assessed that those results were stable. The model computed outputs regarding such relationships in a robust way and it was able to reliably predict the trend of the driver's reactions variables even with very different input data, in respect to the ones used for the training process. This stability can be motivated by the large variability of input data used during the learning process: the model was extensively trained, thus it was prepared to manage properly new unseen data. About that, as already stated, the time to intersection played a really important role since it was different and variable for the whole input data set.

The orange cells of *Table 23* show the same relationships as the ones just discussed, but they are referred to the semi-automated driving modes. With respect to the analysis' results, those values are good as well, but here a less stable model capacity of prediction was found; during several training and simulation processes, it was noticed that such correlations were subjected to a greater variability.

The performances of the neural network were validated adding a random noise. In particular, initially each TTI value was modified adding a random value contained in a range of 1s, included between ±0,5s. Concerning the semi-automated modes, this allowed the TTI to assume values between +1.87s and +2.87s (fixed original TTI value: 2,37s). The results showed that generally the correlation coefficients reflected the ones of the analysis, even if slightly lower; however, the consistency of such

values, verified after several training processes, wasn't so good. This disappointing performance regarding the semi-automated modes, could have been originated by two main causes, characterized by different natures. First of all, the reliability of a neural network's results is strongly dependent on the width of the range of values described by the input data by which it is trained. In particular, the model is able to manage reliably new input data whose values are included in the input data's range of values. Outside this range, the model theoretically isn't able to predict properly the results [53, 62, 67]. As a consequence, since the neural network was trained with only one value of TTI (referring to ACC and TJA), it was not prepared to manage in a stable way different new input TTI values. This imposed a strong limitation which affected the capability of modelling the driving reactions regarding the semi-automated driving modes.

The second possible cause focuses on a statistical point of view: it is known that as the samples under study become increasingly homogeneous on one or both variables, the absolute value of the correlation coefficient decreases [63]. This is exactly what happened in this case: for ACC and TJA driving modes, the time to intersection assumed values contained in a range of data of only 1s (high homogeneity of the TTI samples). Therefore, the resulting *Spearman* coefficients often assumed lower values in respect to the reference ones.

It is understandable that the problem referred to the first cause was unavoidable. It was intrinsic of the data in possession, which depended, in turn, on the way in which the VTI experiment's scenario, considering the semi-automated driving, was designed. The second cause, instead, resulted more "modifiable". In order to make up for that, a higher range of variation was attributed to the random noise regarding the TTI. In this latter situation, the random noise values added to the TTI changed randomly in a range of ±2s, delimitated, for ACC and TJA modes, between +0.37s and +4.37s. The consequence of this was noticeable looking at the model resulting graphs regarding the relationships between outputs and TTI: the points were more spread in the space in respect to the previous condition, thus, better *Spearman* coefficients were found. Since the group of samples regarding the TTI was less homogeneous, it was possible to observe a more reasonable trend of the relationships analysed. Furthermore, a less homogeneity brought benefits also regarding the stability and the robustness of such results: the training and simulation processes of new input data resulted in much more steady values.

It is possible to conclude that, even though the prediction capability, regarding the drivers' reactions trend during semi-automated modes, was made taking into account new input data unseen by the neural network, the results were still satisfactory. This is true also for the results concerning the manual modes, which data, however, weren't affected by the issues previously described.

Beside the relation with the time to intersection, the brake reaction time was the only input variable that, according to the results found in the data analyses, had a relationship with the perception time. The values of the *Spearman* coefficients, referred to this kind of correlation, are showed in the yellow cells of the *Table 23*. The perception time, as already discussed, allowed to define the driver profile also from a behavioural point of view, it was, in fact, derived from a deep analysis of the driver's gaze direction. Unfortunately, the strength of such relationship wasn't so relevant: as noted by the results of the analyses, the correlation between brake reaction time and perception time was weak. This was, inevitably, reflected also in the results obtained by the neural network. Looking at the resultant *Spearman* coefficients, they still

assumed, in the reported example, values that are quite reasonable. However, as assessed with several trainings of the network and simulations, the stability of such results wasn't so reliable (it happened that quite low values were obtained). Although this variability, for which the results were affected, wasn't so dramatic (the model never computed unrealistic brake reaction times), those correlation values slightly changed depending on the random noise added to the inputs.
Besides the *Spearman* coefficients, if the attention is focused on the graphs of the model resulting relationships (*Figures 92, 93, 94, 95, 106, 107*), it is possible to notice that they represented a trend always quite good (accordingly to the graphs obtained in the analysis results), even after several simulations. In the light of this, it is therefore possible to state that the model was still able to generalize properly, also taking into account new input data, the trend between perception time and brake reaction time. As regarding the variability of the *Spearman* coefficients, it was instead caused by the homogeneity of the resulting data [1], which could be more or less accentuated accordingly to the randomness of the noise added to the inputs. The homogeneity of the data is more evident observing the situation regarding the intentional car following driving mode (*Figure 93, 106*): even if the trend modelled by the neural network was correct, the higher density of brake reaction times at late perception times (which is typical of this driving mode), implied occasionally very low *Spearman* coefficients.

The possible application of the model is for the prediction of the braking reactions regarding a single driver. The layout interface of the neural network was designed in order to facilitate the user: it is allowed to define the desired input information regarding the driving situation that is aimed to be modelled. It is believed that this can be a very interesting future usage of such model because it allows taking into account the information regarding whichever driver, computing the corresponding output results. Since the computational time isn't excessive, the process is fast and it can be easily repeated. The limitation of such application is that its performances are obviously closely linked to the way in which the model was designed. In particular, this possible application is feasible only for the intersection scenario on which the study of this work was based. The resulting reactions obtained by the modelling of the driver's behaviour could be ideally utilized, besides a prediction for its own sake, even for the testing and the improvement of advanced driver assistance systems. Both in manual and semi-automated driving, the driver could be helped to take decisions concerning for example the time in which starting to brake, or the force to be applied to the brake pedal at the occurrence of a critical situation. Since the input information regarding the personal data of the driver vary depending on the driver, they could be difficulty implemented on a vehicle software control unit. The main information that a hypothetical ADAS, featured by such model, could take into account, could be the type of the current driving mode and the time to intersection. Generally, an hazardous cut-in movement of another car, could be detected by sensor units [68–72] before it starts jeopardising driving safety. In such moment, it would be hypothetically possible to calculate the time to intersection and, as consequence, computing a visible warning in order to alert the driver for the need of a braking. In case of semi-automated vehicles, the warning could be, if the driver is still not braking, followed by an automatic braking imposed by the system. Since the model computes also results concerning the mean brake pedal force, this warning could be ideally also helpful in order to notify the driver regarding the required force to press the brake pedal. If the pedal force imprinted is lower than the one calculated by the model, the driver should be urged to brake harder.

These ideas are just some possible examples of applications which could be realized by a model whose typology is the same as the one presented in this work. However, in order to bring such applications within reach, an enhancement of the performances regarding this model's prediction capability is required. There is certainly plenty of scope for improvement regarding the neural network designed: it is believed that a greater variety of data coming from new driving simulations or real measurements, could help to obtain more accurate training processes and, consequently, even better results.

6 Conclusions and future research

This study was dedicated to analyse and model driver's reactions in a critical T-intersection – where a turning car was suddenly entering the subject vehicle's path –, considering different levels of automation. The activity concerned the process and study of data collected during an experiment performed with the VTI driving simulator III. The participants underwent the critical scenario during manual driving, intentional car following driving and two semi-automated driving conditions regarding the use of the adaptive cruise control and the traffic jam assist. The results showed that, generally, the main drivers' response to the criticality was braking, which was often accompanied by steering corrective manoeuvres of small amplitudes, that couldn't be classified as evasive steering.
The brake reaction time resulted independent from the driving mode adopted, the drivers' experience with adaptive cruise control and the drivers' age. Drivers' braking was studied taking into account the mean force applied to the brake pedal, the jerk at brake onset and the maximum deceleration reached and results showed differences in respect to the driving mode configuration. In particular, drivers braked with a higher mean brake pedal force, higher jerk at brake onset and higher maximum deceleration during semi-automated driving compared to manual driving. Besides, findings showed that drivers experienced with adaptive cruise control, who were also the oldest, performed significant harder braking compared to the others. The different behaviour could be motivated by lack of trust in the system, due to the awareness of its limits.
The analysis also investigated the drivers' gaze direction before approaching the intersection and showed that, during intentional car following mode, drivers perceived the presence of the TC later compared to the other driving modes. This specific behaviour for ICF was attributed to the different task that characterized this driving configuration: driver focused attention mainly to the lead vehicle that had to follow.

The modelling activity resulted in the creation of a feedforward back-propagating neural network, whose design, configuration and architecture were based on the results obtained during the analysis. Such model was focused on the prediction of drivers' braking behaviour, represented by brake reaction time, mean brake pedal force and maximum deceleration reached. The considered inputs were the driving mode, the time to intersection, the perception time and driver's profile (gender, age, km/year travelled, years of license accumulated, experience with ACC system). The performance of the model allows to reproduce properly the reactions of the drivers analysed, moreover it is characterized by an appreciable generalization capability. Indeed, it is able to manage new input regarding a desired driver approaching the critical scenario under study, without overfitting the data. The model resulted fast, easy to use, flexible and quite accurate, especially as regards the prediction of drivers' reactions for manual driving modes. The model's outcome concerning the semi-automated driving resulted less reliable. In fact, the lack of variability of which, the available data, were affected, penalized the model's training process concerning such driving modes. Even if attempts were made to remedy this, it is believed that further measures are required.

Future research should be focused mainly on the expansion of the dataset, which could be beneficial for both the analysis and mainly the modelling of drivers' reactions. This could be achieved by further driving simulator studies and real experiments.

It is considered that a larger dataset could improve significantly the study of such critical scenario. Moreover, this could enhance the model predicting performances considerably, concerning both manual and semi-automated driving. In particular, regarding the latter, simulations designed with variable times to intersection are considered necessary in order to better assess drivers' reactions.
In order to further validate the model described in this thesis, its application could be extended also to critical scenarios different from the one under study. Such improvements could make the presented model even more accurate, aiming to be a useful tool to evaluate driver's behaviour and to develop advanced driver assistance systems focused on critical scenarios.

7 References

[1] A. Sharov, “T-intersection.” [Online]. Available: https://unsplash.com/photos/ejSsZ6uZ1ZA. [Accessed: 02-Mar-2018].

[2] Vision zero, “One million lives at stake.” [Online]. Available: http://www.visionzeroinitiative.com/one-million-lives-at-stake/.

[3] Michael Pines, “Top 25 Causes of Car Accidents.” [Online]. Available: https://seriousaccidents.com/legal-advice/top-causes-of-car-accidents/.

[4] J. A. Groeger, “Understanding driving: applying cognitive psychology to a complex everyday task,” 2000.

[5] W. J. Horrey, C. D. Wickens, and K. P. Consalus, “Modeling drivers’ visual attention allocation while interacting with in-vehicle technologies,” *J. Exp. Psychol. Appl.*, vol. 12, no. 2, pp. 67–78, 2006.

[6] Latherow Law Office, “Where do most car accidents happen?” [Online]. Available: http://latherowandduignanlaw.com/where-do-most-car-accidents-happen/.

[7] Istat, “Incidenti stradali,” vol. 2014, pp. 0–20, 2011.

[8] A. Pietro Bardelli, A. Bacchini, and F. Sassi, “Advances in Artificial Intelligence: From Theory to Practice,” vol. 10351, pp. 513–522, 2017.

[9] NHTSA, “The Long-Term Effect of ABS in Passenger Cars and LTVs,” *Natl. Tech. Inf. Serv.*, no. August, p. 89, 2009.

[10] Federal Transit Administration, “Transit Automation Research,” 2018. [Online]. Available: https://www.transit.dot.gov/automation-research.

[11] J. D. Lee, “Fifty Years of Driving Safety Research.,” *Hum. Factors*, vol. 50, no. 3, pp. 521–528, 2008.

[12] O. Benderius, G. Markkula, K. Wolff, and M. Wahde, “Driver behaviour in unexpected critical events and in repeated exposures – A comparison,” *Eur. Transp. Res. Rev.*, vol. 6, no. 1, pp. 51–60, 2013.

[13] Swedish National Road and Transport Research Institute, “VTI - RESEARCH, DEVELOPMENT, INVESTIGATION RELATED TO INFRASTRUCTURE, TRAFFIC AND TRANSPORT.” [Online]. Available: https://www.vti.se/en/.

[14] J. D. L. Donald L. Fisher, Matthew Rizzo, Jeff K. Caird, *Driving simulation for engineering, medicine, and psychology*. 2011.

[15] Society of Automotive Engineering, “Operational definitions of driving performance measures and statistics. Surface vehicle recommended practice J2944,” 2015.

[16] B. H. Barret, G.V. Kobayashi, M. Fox, “Feasibility of studying driver reaction to sudden pedestrian emergencies in an automobile simulator,” *Hum. Factors*, vol. 10, no. I, pp. 19–26, 1968.

[17] P. L. Olsonl, M. Sivak, and A. Arbor, “Perception-Response Time to Unexpected Roadway Hazards,” vol. 28, no. 1, pp. 91–96, 1986.

[18] D. B. Fambro, D. L. Picha, and K. Fitzpatrick, “Driver Perception – Brake Response in stopping sight distance situations,” 1998.

[19] J. D. Lee, D. V Mcgehee, T. L. Brown, and M. L. Reyes, “Collision Warning Timing , Driver Distraction , and Driver Response to Imminent Rear-End Collisions in a High-Fidelity Driving Simulator,” vol. 44, no. 2, pp. 314–334, 2002.

[20] R. Jurecki and T. L. Stańczyk, “Driver model for the analysis of pre-accident situations,” *Veh. Syst. Dyn.*, vol. 47, no. 5, pp. 589–612, 2009.

[21] G. M. Fitch, M. Blanco, J. F. Morgan, A. E. Wharton, and V. Tech, “Driver Braking Performance to Surprise and Expected Events,” pp. 2076–2080, 2010.

[22] M. Ljung, J. Engström, and M. Viström, “Effects of forward collision warning and repeated event exposure on emergency braking,” *Transp. Res. Part F Psychol. Behav.*, vol. 18, pp. 34–46, 2013.
[23] G. Markkula, J. Engström, J. Lodin, J. Bärgman, and T. Victor, “A farewell to brake reaction times? Kinematics-dependent brake response in naturalistic rear-end emergencies,” *Accid. Anal. Prev.*, vol. 95, pp. 209–226, 2016.
[24] H. Summala, “Brake Reaction Times and Driver Behavior Analysis,” no. September 2000, pp. 2014–2018, 2000.
[25] J. Engström, M. L. Aust, and M. Viström, “Effects of working memory load and repeated scenario exposure on emergency braking performance,” *Hum. Factors*, vol. 52, no. 5, pp. 551–559, 2010.
[26] D. Crundall, C. Shenton, and G. Underwood, “Eye movements during intentional car following,” *Perception*, vol. 33, no. 8, pp. 975–986, 2004.
[27] A. F. L. Larsson, K. Kircher, and J. A. Hultgren, “Learning from experience: Familiarity with ACC and responding to a cut-in situation in automated driving,” *Transp. Res. Part F Traffic Psychol. Behav.*, vol. 27, no. PB, pp. 229–237, 2014.
[28] K. Kircher, A. Larsson, and J. A. Hultgren, “Tactical Driving Behavior With Different Levels of Automation,” *Ieee Trans. Intell. Transp. Syst.*, vol. 15, no. 1, pp. 158–167, 2014.
[29] K. A. Brookhuis, D. de Waard, and W. H. Janssen, “Behavioural impacts of advanced driver assistance systems–an overview,” *Eur. J. Transp. Infrastruct. Res.*, vol. 1, no. 3, pp. 245–253, 2001.
[30] R. Parasuraman and V. Riley, “Humans and Automation: Use, Misuse, Disuse, Abuse,” *Hum. Factors J. Hum. Factors Ergon. Soc.*, vol. 39, no. 2, pp. 230–253, 1997.
[31] O. Carsten, F. C. H. Lai, Y. Barnard, A. H. Jamson, and N. Merat, “Control task substitution in semiautomated driving: Does it matter what aspects are automated?,” *Hum. Factors*, vol. 54, no. 5, pp. 747–761, 2012.
[32] H. T. Neville A. Stanton, Mark S. Young, Guy H. Walker and and S. Randle, “Automating the Driver’s Control Tasks,” *Notes*, 2001.
[33] Volvo Cars, “Adaptive Cruise Control – limitations.” [Online]. Available: https://support.volvocars.com/en-ca/cars/pages/owners-manual.aspx?mc=V423&my=2017&sw=16w46&article=e0b0e108aa3fc629c0a801e801071006. [Accessed: 28-Feb-2018].
[34] C. Paper and N. S. Ministerie, “A comprehensive driver behavior model for the evaluation of intelligent intersections . Paper No .,” no. 1305, 2006.
[35] N. Merat and J. D. Lee, “Preface to the special section on human factors and automation in vehicles: Designing highly automated vehicles with the driver in mind,” *Hum. Factors*, vol. 54, no. 5, pp. 681–686, 2012.
[36] Kim J. Vicente, *The human factor: revolutionizing the way people live with technology*. New York, 2006.
[37] G. Markkula, “A Review of Near-Collision Driver Behavior Models A review of near-collision driver behavior models,” no. September, 2016.
[38] G. Marti, A. H. P. Morice, and G. Montagne, “Drivers’ decision-making when attempting to cross an intersection results from choice between affordances,” *Front. Hum. Neurosci.*, vol. 8, no. January, pp. 1–12, 2015.
[39] M. Svärd, G. Markkula, J. Engström, F. Granum, and J. Bärgman, “A quantitative driver model of pre-crash brake onset and control,” pp. 339–343, 2017.

[40] G. Markkula, “Answering questions about consciousness by modeling perception as covert behavior,” *Front. Psychol.*, vol. 6, no. June, pp. 1–18, 2015.
[41] S. Chen, S. Zhang, J. Shang, B. Chen, and N. Zheng, “Brain Inspired Cognitive Model with Attention for Self-Driving Cars,” no. February, 2017.
[42] Y. Lin, P. Tang, W. J. Zhang, and Q. Yu, “Artificial neural network modelling of driver handling behaviour in a driver ± vehicle ± environment system,” *Int. J. Veh. Des.*, vol. 0, no. 0, pp. 1–22, 2004.
[43] S. B. Amsalu and A. Homaifar, “Driver behavior modeling near intersections using Hidden Markov Model based on genetic algorithm,” *2016 IEEE Int. Conf. Intell. Transp. Eng.*, no. October, pp. 193–200, 2016.
[44] J. Morton, T. A. Wheeler, and M. J. Kochenderfer, “Analysis of Recurrent Neural Networks for Probabilistic Modeling of Driver Behavior,” *IEEE Trans. Intell. Transp. Syst.*, vol. PP, no. 99, pp. 1–10, 2016.
[45] VTI, “Driving simulators technical specifications.” [Online]. Available: https://www.vti.se/en/research-areas/vtis-driving-simulators/.
[46] F. O. Flemisch, J. Kelsch, C. Loper, A. Schieben, J. Schindler, and H. Matthias, “Cooperative Control and Active Interfaces for Vehicle Assistance and Automation,” *FISITA World Automot. Congr.*, no. 2, pp. 301–310, 2008.
[47] M. Zaki, T. Sayed, and K. Shaaban, “Use of Drivers’ Jerk Profiles in Computer Vision-Based Traffic Safety Evaluations,” *Transp. Res. Rec. J. Transp. Res. Board*, vol. 2434, no. November, pp. 103–112, 2014.
[48] R. G. Mortimer, “Foot Brake Pedal Force Capability of Drivers,” *Ergonomics*, vol. 17, no. 4, pp. 509–513, 1974.
[49] M. Argyle, *Sequences of social behaviour as a function of the situation*. 1979.
[50] Charles Zaiontz, “Real Statistics Using Excel.” [Online]. Available: http://www.real-statistics.com/.
[51] G. (Giampiero) Mastinu, M. (Massimiliano) Gobbi, and C. (Carlo) Miano, *Optimal design of complex mechanical systems : with applications to vehicle engineering*. Springer, 2006.
[52] I. . Basheer and M. Hajmeer, “Artificial neural networks: fundamentals, computing, design, and application,” *J. Microbiol. Methods*, vol. 43, no. 1, pp. 3–31, Dec. 2000.
[53] M. I. S. Ismail, Y. Okamoto, and A. Okada, “Neural Network Modeling for Prediction of Weld Bead Geometry in Laser Microwelding,” *Adv. Opt. Technol.*, vol. 2013, pp. 1–7, 2013.
[54] G. E. Hinton, S. Osindero, and Y.-W. Teh, “A Fast Learning Algorithm for Deep Belief Nets.”
[55] K. Hornik, “Approximation Capabilities of Muitilayer Feedforward Networks,” *Neural Networks*, vol. 4, pp. 251–257, 1991.
[56] G. Cybenko, *Approximations by superpositions of sigmoidal functions*. 1989.
[57] MathWorks, “Improve Neural Network Generalization and Avoid Overfitting - MATLAB & Simulink - MathWorks Nordic.” [Online]. Available: https://se.mathworks.com/help/nnet/ug/improve-neural-network-generalization-and-avoid-overfitting.html. [Accessed: 13-Mar-2018].
[58] “Levenberg-Marquardt backpropagation - MATLAB trainlm - MathWorks Nordic.” [Online]. Available: https://se.mathworks.com/help/nnet/ref/trainlm.html. [Accessed: 02-Feb-2018].
[59] “Bayesian regularization backpropagation - MATLAB trainbr - MathWorks Nordic.” [Online]. Available: https://se.mathworks.com/help/nnet/ref/trainbr.html. [Accessed: 02-Feb-2018].

[60] D. J. C. MacKay, “Bayesian Interpolation,” *Neural Comput.*, vol. 4, no. 3, pp. 415–447, May 1992.
[61] F. Dan Foresee and M. T. Hagan, “Gauss-Newton approximation to Bayesian learning,” in *Proceedings of International Conference on Neural Networks (ICNN’97)*, vol. 3, pp. 1930–1935.
[62] M. A. Nielsen, “Neural Networks and Deep Learning.” Determination Press, 2015.
[63] D. E. Hinkle, W. Wiersma, and S. G. Jurs, *Applied statistics for the behavioral sciences*. Houghton Mifflin, 2003.
[64] H. Summula, “Towards Understanding Motivational and Emotional Factors in Driver Behaviour: Comfort Through Satisficing,” in *Modelling driver behaviour in automotive environments*, 2007, pp. 189–207.
[65] J. V. Tu, “Advantages and disadvantages of using artificial neural networks versus logistic regression for predicting medical outcomes,” *J. Clin. Epidemiol.*, vol. 49, no. 11, pp. 1225–1231, Nov. 1996.
[66] D. Svozil, V. Kvasnicka, and J. Pospichal, “Introduction to multi-layer feed-forward neural networks,” *Chemom. Intell. Lab. Syst.*, vol. 39, no. 1, pp. 43–62, Nov. 1997.
[67] P. J. (Petrus J. . Braspenning, Thuijsman F., and A. J. M. M. Weijters, *Artificial neural networks : an introduction to ANN theory and practice*. Springer, 1995.
[68] C. Dumitru and V. Maria, “Advantages and Disadvantages of Using Neural Networks for Predictions,” *Ovidius Univ. Ann. Econ. Sci. Ser.*, vol. XIII, no. 1, pp. 444–449, 2013.
[69] Maad M. Mijwel, “Artificial Neural Networks Advantages and Disadvantages | Maad M. Mijwel | Pulse | LinkedIn,” 2018. .
[70] M. Heinert, “Artificial neural networks – how to open the black boxes?,” *Proceedings*, pp. 42–62, 2008.
[71] Hagan; Beale; Demuth;, “Neural Network Toolbox - User’s guide.” 2017.
[72] C. Intel, “Advanced Driver Assistant System,” 2015.
[73] O. Gietelink *et al.*, “Development of advanced driver assistance systems with vehicle hardware-in-the-loop simulations * Development of advanced driver assistance systems with vehicle hardware-in-the-loop simulations,” *Syst. Dyn. Mon.*, vol. 44, no. 200, pp. 569–590, 2006.
[74] Jack Browne, “Integrated Radar Sensors Steer the Way for ADAS - Innovation Destination: Automotive,” 2017. .
[75] U. V. Gert Rudolph, “Three Sensor Types Drive Autonomous Vehicles | Sensors Magazine.” .
[76] Seunghyuk Choi, Florian Thalmayr, Dominik Wee, and Florian Weig, “Advanced driver-assistance systems: Challenges and opportunities ahead | McKinsey & Company.” .